ABSTRACT

Title of dissertation: MECHANISMS INVOLVED IN SYMPTOM
MODULATION BY TURNIP CRINKLE VIRUS
AND ITS ASSOCIATED SUBVIRAL RNAS

Fengli Zhang, Doctor of Philosophy, 2006

Dissertation directed by: Professor Anne E. Simon
Department of Cell Biology and Molecular Genetics

Turnip crinkle virus (TCV*) (family *Tombusviridae*, genus *Carmovirus*) is a positive-strand RNA virus. SatC, a satellite RNA associated with TCV, intensifies symptoms of TCV on all symptomatic hosts. *Arabidopsis* protoplast assays indicated that TCV virion levels are substantially reduced by the presence of satC or when two amino acids are inserted at the N-terminus of the coat protein (CP), resulting in similarly enhanced symptoms. Since the TCV CP is an RNA silencing suppressor, increased levels of the resultant free CP could augment silencing suppression resulting in enhanced colonization of the plant.

Cloning and sequencing of virus-derived small RNAs (vsRNAs) accumulating in *Arabidopsis* plants infected with TCV with or without satC showed that the majority of

vsRNAs are ~21-nt, purine-rich sequences. One TCV vsRNA species, TvsRNA5, is complementary to 3' UTR sequences in transcripts of 12 *Arabidopsis* genes. Transcript levels of 3 of these genes were reduced 2.4- to 4-fold by TCV infection, but restored to normal levels when infected with TCV containing a deletion in the TvsRNA5 sequence. This deletion did not affect levels of virus, but resulted in symptom attenuation in infected plants. These results suggest that at least some vsRNAs are specifically altering expression of host genes leading to phenotypic changes in host plants.

In addition, a technique has been established for detection of viral RNAs in whole plants, which makes use of the binding of the CP of MS2 bacteriophage (CP_{MS2}) to a 19 base hairpin (hp). Protoplast co-transfection of TCV containing the hairpin and a fusion protein construct consisting of CP_{MS2}, GFP and a nuclear localization signal (NLS) relocated GFP from the nucleus to the cytoplasm, indicating the presence of virus. TCV movement was also tracked by observing cytoplasmic GFP fluorescence in infected transgenic plants expressing the fusion protein. This technique should be amenable for detection of any virus with a transformable host.

MECHANISMS INVOLVED IN SYMPTOM MODULATION BY TURNIP CRINKLE
VIRUS AND ITS ASSOCIATED SUBVIRAL RNAS

by

Fengli Zhang

Dissertation submitted to the Faculty of the Graduate School of the
University of Maryland, College Park in partial fulfillment
of the requirements for the degree of
Doctor of Philosophy
2006

Advisory Committee:

Professor Anne E. Simon, Chair
Professor George H. Lorimer
Associate Professor James N. Culver
Research Chemist Robert A. Owens
Assistant Professor Shunyuan Xiao
Professor Stephen M. Wolniak
Associate Professor Zhongchi Liu

ACKNOWLEDGEMENTS

I would like to thank all people who helped me during completion of my dissertation. First of all, I want to thank my supervisor Dr. Anne Simon for providing me with this great opportunity to work in her lab. In the past six years, her enthusiasm and dedication to science and her encouragement inspired me and will continue to influence me. Anne also gave me enormous help in improving my spoken and written English as well as presentation skills. I also appreciate that she supported me to attend several national virology conferences, which gave me excellent opportunities to communicate with other scientists. I am also deeply indebted to my committee members, Dr. George H. Lorimer, Dr. James N. Culver, Dr. Robert A. Owens, Dr. Shunyuan Xiao, Dr. Stephen M. Wolniak, and Dr. Zhongchi Liu for their valuable support and advice.

I would like to thank my colleagues Dr. Guohua Zhang, Dr. Sohrab Bodaghi, Dr. Vera Stupina, Dr. Jiuchun Zhang, John C. McCormack, and Rong Guo for their valuable discussion and friendship. I want to thank Catherine P. Gretschel and Nancee Soni for their help in managing lab business. I also want to thank Dr. Chi-Kuang Wen, Xiyan Li for answering many scientific questions.

I am grateful to my husband Xiaoping Sun for his love and encouragement. I would like to thank my son Qinwei Sun, whose interest in science always encourages me. I also want to thank my parents for their care, love, encouragement, and support.

TABLE OF CONTENTS

LIST OF TABLES

LIST OF FIGURES

LIST OF ABREVIATIONS

2, 4-D: 2, 4-dichlorophenoxyacetic acid

3' UTR: 3' untranslated region

3'-idT: 3' inverted deoxy-thymidine

5'-RACE: rapid amplification of cDNA ends

AGO: ARGONAUTE

BMV: Brome mosaic virus

BYV: Beet yellows virus

CaMV: Cauliflower mosaic virus

CCFV: Cardamine chlorotic fleck virus

CMV: Cucumber mosaic virus

CP: coat protein

CP_{MS2}: CP of MS2 bacteriophage

CvsRNA: satC vsRNA

CymRSV: Cymbidium ringspot virus

DCL: Dicer-like enzymes

DdRp: DNA-dependent RNA polymerases

diG: defective interfering RNA G

dpi: days postinoculation

dsRNAs: double-stranded RNAs

DTT: dithiothreitol

GFP: green fluorescent protein

GRAV: Groundnut rosette assistor virus

GRV: Groundnut rosette virus

HcPro: helper component proteinase

HEN1: HUA ENHANCER 1

HpRNAs: hairpin RNAs

hpi: hours postinoculation

HST: HASTY

HYL1: HYPONASTIC LEAVES 1

I: deoxyinosine residues

LB: L-broth

LssRNAs: larger single-stranded small RNAs

miRNA: microRNA

MS: Murashige-Skoog salts

NLS: nuclear localization signal

nt: nucleotide

OH: hydroxyl groups

ORF: open reading frame

PAZ: Piwi/Argonaute/Zwille

PBS: phosphate buffered saline

PCM: protoplast culture medium

PEG: polyethylene glycol

PIM: protoplast isolation medium

PPV: Plum pox virus

PSTVd: Potato spindle tuber viroid

PTGS: Post-transcriptional gene silencing

PVX: Potato virus X

PVY: Potato virus Y

R proteins: disease resistance proteins

RCNMV: Red clover necrotic mosaic virus

RdRp: RNA-dependent RNA polymerase

RISC: RNA-induced silencing complex

RITS: RNA-induced initiation of transcriptional silencing

satC: satellite RNA C

satD: satellite RNA D

satRNA: satellite RNA

satY: satellite RNA Y

SDE3: SILENCING-DEFECTIVE GENE 3

SELEX: Sytematic Evolution of Ligands by Exponential Enrichment

SGS3: SUPPRESSOR OF GENE SILENCING 3

siRNA: small interfering RNA

ssRNA: single-stranded RNA

TCV: Turnip crinkle virus

T-DNA: transfer-DNA

TE: translational enhancer

TEV: Tobacco etch virus

TGS: Transcriptional gene silencing

TIP: TCV-interacting protein

Tm: melting temperature

TMV: Tobacco mosaic virus

TomBRV: Tomato black ring nepovirus

TRV: Tobacco rattle virus

TuMV: Turnip mosaic virus

TvsRNA: TCV vsRNA

TYMV: Turnip yellow mosaic virus

VIGS: virus-induced gene silencing

vsRNAs: virus-derived small RNAs

wt: wild-type

CHAPTER I

THE ROLES OF RNA SILENCING IN VIRUS-PLANT

INTERACTION: AN OVERVIEW

Introduction

RNA silencing is an ancient, evolutionarily conserved process in eukaryotic organisms including plants, animals, and fungi, which suppresses or silences gene expression in nucleotide sequence-specific manner. RNA silencing is triggered by long double-stranded RNAs (dsRNAs) or single-stranded hairpin RNAs (hpRNAs), which are cleaved by cellular RNaseIII-like enzymes, termed Dicers, to generate 21–24 nucleotide (nt) small RNA duplexes (Bernstein et al., 2001; Fire et al., 1998; Hannon, 2002). One selected strand of the small RNA duplex is then incorporated into an effector endonuclease complex to direct sequence-specific degradation or inhibition of complementary DNA or RNA at transcriptional or post-transcriptional levels (Hammond et al., 2000; Liu et al., 2004a; Verdel et al., 2004). Through its involvement in regulating gene expression, RNA silencing plays important roles in diverse biological activities including development and chromatin remodeling (Carrington and Ambros, 2003; Kidner and Martienssen, 2005).

RNA silencing can also be triggered by viruses invading host cells, which are processed by Dicers into ~ 21 nt small RNAs, termed virus-derived small RNAs (vsRNAs). vsRNAs are loaded into effector endonuclease complexes and direct nuclease

cleavage of complementary viral RNAs. The vsRNAs may also direct degradation of complementary cellular mRNAs, thereby interfering with host gene expression. In the past 15 years, advances in studying RNA silencing have led to breakthroughs in our understanding of the interaction between viruses and their hosts. For example, protein 2b encoded by *Cucumber mosaic virus* (CMV) was originally identified as a pathogenicity factor, required for long-distance movement of the virus (Ding et al., 1995). However, further studies indicated that this requirement may be the result of the role of 2b in suppressing RNA silencing, thereby helping virus to spread in plants (Brigneti et al., 1998). In this chapter, I will present the status of our knowledge of RNA silencing with an emphasis on how it is involved in the interaction between plant viruses and their hosts.

RNA silencing pathways revealed in plants

Since the original discovery of RNA silencing in petunia in 1990 (Napoli et al., 1990), RNA silencing has been extensively studied in plants, especially in the model plant *Arabidopsis thaliana*. Using various biochemical and genetic approaches, increasing evidence indicates that RNA silencing in plants operates through a group of interconnected pathways (Baulcombe, 2004; Herr, 2005; Qi and Hannon, 2005). As described below, RNA silencing pathways share the same basic reactions and are generally triggered by dsRNAs or hpRNAs derived from different sources. Furthermore, they may play different roles in plant developmental regulation.

Post-transcriptional gene silencing (PTGS) pathway

In 1990, Napoli et al. introduced a chimeric chalcone synthase gene into petunia in an attempt to generate more vibrant leaf color. Unexpectedly, the opposite effect was achieved, where forty-two percent of the transgenic plants generated white flowers and/or flowers with white sectors on a wild type pigmented background (Napoli et al., 1990). This phenomenon was originally termed co-suppression of the introduced transgene and homologous host gene copies, and was also found later in other transgenic plants (de Carvalho-Niebel et al., 1995b; Dorlhac de Borne et al., 1994; Hart et al., 1992; Smith et al., 1990; Van der Krol et al., 1990; Vaucheret et al., 1995). Co-suppression significantly decreased the steady-state levels of both host and transgene mRNAs. The transgenes were transcribed normally in the nucleus, indicating that this co-suppression was operating at post-transcriptional levels to silence gene expression, thereby termed post-transcriptional gene silencing (PTGS) (de Carvalho-Niebel et al., 1995a; Vaucheret et al., 1997).

Further chemical and genetic studies of PTGS determined that it is triggered by the long dsRNA derived from transgenic inverted repeats (Fire et al., 1998; Figure 1.1A). The dsRNA is processed by Dicer into ~21 nt RNA duplexes, termed small interfering RNAs (siRNA). One selected strand of the siRNA, which has the 5' phosphate at the less stable end of the duplex, is loaded into an endonuclease complex termed RNA-induced silencing complex (RISC). This single-stranded siRNA can base pair with complementary mRNAs transcribed from transgenes or host genes to guide mRNA cleavage or degradation by RISC (Baumberger and Baulcombe, 2005).

Figure 1.1 RNA silencing pathways revealed in plants (see the text for details). (A) The PTGS pathway. The dsRNA are encoded by transgenes present as inverted repeats. (B) The miRNA pathway. The miRNAs originate from the RNA polymerase II transcripts from endogenous non-coding miRNA genes. (C) The *trans*-acting siRNA pathway. The dsRNAs are synthesized by cellular RdRp-mediated primer extension on mRNA templates using complementary siRNAs (primary siRNAs) as primers or de novo transcription from RNA fragments generated in the miRNA pathway. (D) The TGS pathway. The dsRNA are derived from transgenes present as inverted repeats. M, methylation of DNA that suppresses gene transcription.
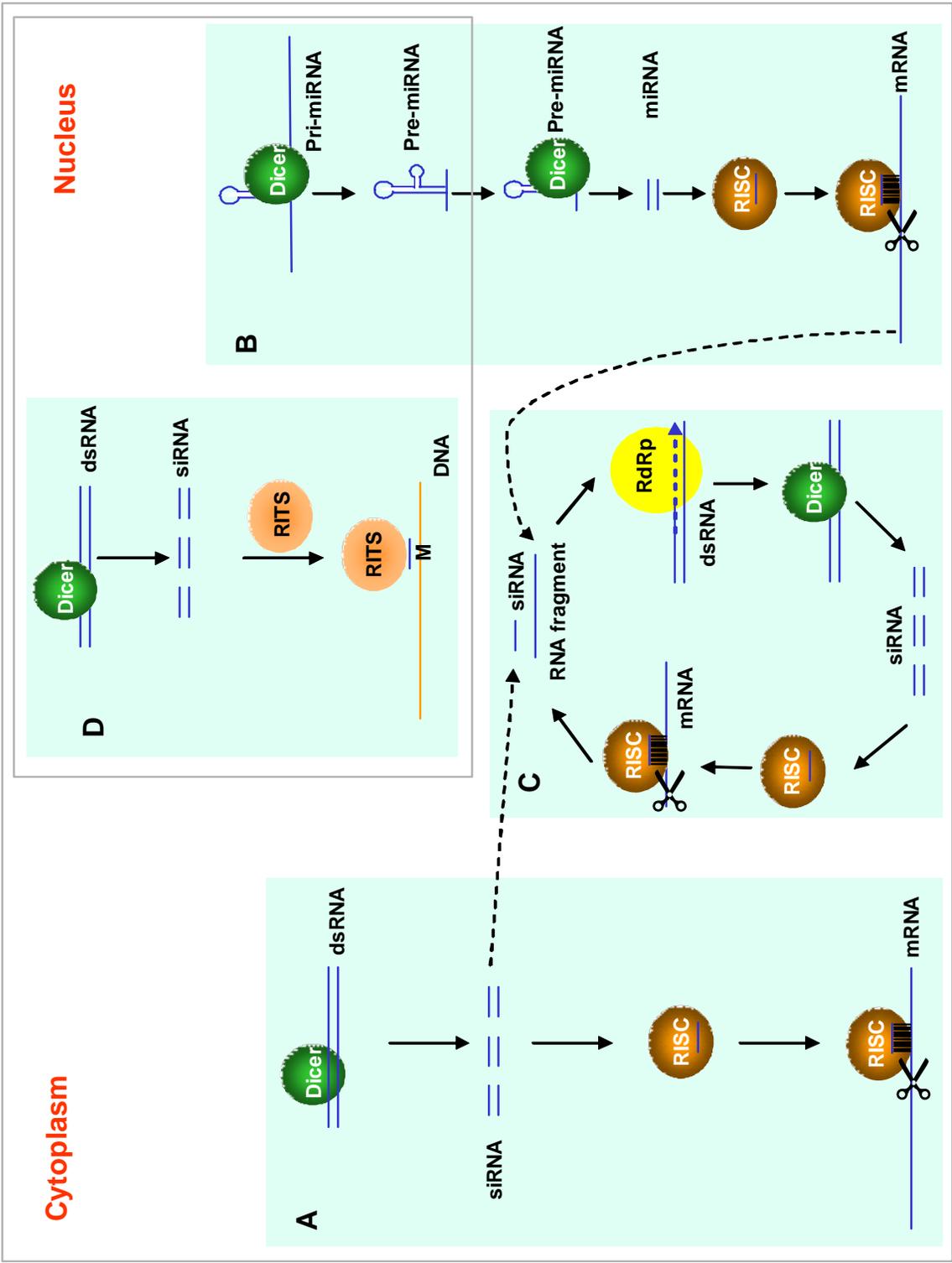
Endogenous microRNA (miRNA) pathway

During cloning of siRNAs, it was found that eukaryotes generate another type of small RNA, termed microRNAs (miRNAs) (Bartel, 2004; Jones-Rhoades and Bartel, 2004). Further studies revealed that miRNAs originate from RNA polymerase II transcription of endogenous non-coding miRNA genes (Bartel, 2004; Chen, 2005; Kim, 2005; Figure 1.1B). miRNAs, which are similar in size (~21 nt) and structure to siRNAs, are generally contained within hairpin stems in transcripts that are capped, spliced, and polyadenylated. The miRNA gene transcripts (pri-miRNAs) are cleaved by Dicers in the nucleus to generate 60- to 70-nt intermediates, termed pre-miRNAs (Denli et al., 2004; Han et al., 2004; Lee et al., 2003; Zeng et al., 2005). The pre-miRNAs are then recognized and exported by an ortholog of exportin-5 in plants to the cytoplasm (Lund et al., 2004), where they are further processed by cytoplasmic Dicers into ~21-nt miRNAs (Chendrimada et al., 2005; Forstemann et al., 2005). One strand of the duplex (the miRNA) is incorporated into RISC and guides cleavage of complementary mRNAs transcribed from host genes (Bartel, 2004; Kidner and Martienssen, 2005). Through directing silencing of cellular mRNAs, the miRNAs negatively regulate genes expression required for various plant development processes including organ polarity, leaf growth, stem cell identity, and developmental transitions (Ambros, 2001; Pasquinelli and Ruvkun, 2002).

Trans-acting siRNA pathway

Genetic analyses of *Arabidopsis* siRNAs recently revealed one silencing pathway in plants, whose operation requires cellular RNA-dependent RNA polymerase (RdRp) (Yoshikawa et al., 2005). In this pathway, the long dsRNAs cleaved by Dicers are synthesized by cellular RdRp-mediated primer extension on mRNA using complementary siRNAs (primary siRNAs) as primers (Herr, 2005; Figure 1.1C) or de novo transcription from RNA fragments generated in the miRNA pathway (Yoshikawa et al., 2005). The siRNAs generated in this pathway incorporate into RISC and target mRNA sequences that may have no complementarities with the primary siRNAs or miRNAs. Therefore, these siRNAs are termed *trans*-acting siRNAs (Allen et al., 2005; Yoshikawa et al., 2005). In addition to RdRp, other proteins are also required for the *trans*-acting siRNA pathway. For example, a coiled-coil protein (SUPPRESSOR OF GENE SILENCING3, SGS3) in *Arabidopsis* functions to protect the single-stranded RNA fragments produced in the miRNA pathway from degradation by nucleases (Yoshikawa et al., 2005). The *trans*-acting siRNAs are involved in regulation of plant development because RdRp and SGS3-defective *Arabidopsis* mutants display defects in development such as altered leaf curvature and narrowed petioles (Peragine et al., 2004).

Transcriptional gene silencing (TGS) pathway

The three pathways described above involve RNA-RNA interactions between small RNAs and their complementary mRNAs. RNA silencing can also operate at the level of transcription (TGS). TGS was first discovered in plants infected with *Potato spindle tuber viroid* (PSTVd). PSTVd, a short pathogenic circular RNA, guides de novo DNA

methylation of DNA copies transgenetically integrated into the plant genome (Wassenegger et al., 1994). Further studies indicated that in this pathway, Dicer cleavage of the transgenic inverted RNA transcript in the nucleus generates 24-nt siRNAs, which are longer than siRNAs produced by other pathways (Figure 1.1D). The 24-nt siRNAs load into a nuclear effecter complex, termed RNA-induced initiation of transcriptional silencing (RITS) complex, to guide DNA methylation (cytosine-5) and histone modifications, thereby suppressing gene transcription (Verdel and Moazed, 2005; Verdel et al., 2004). TGS may also function to protect the DNA genome against damage caused by transposons (Baucombe, 2004).

RNA silencing-related cellular proteins in plants

As described above, a number of different cellular proteins or protein complexes are involved in RNA silencing, including Dicers, RISC, and RdRps. The cellular proteins functioning in RNA silencing may vary among plant species, which provides tremendous flexibility in the initiation and execution of RNA silencing. For example, it has been found that *Arabidopsis*, poplar, and rice contain four, five, and six Dicer genes, respectively (reviewed by Watson et al., 2005). Since our knowledge of RNA silencing in plants mostly comes from studies of the pathways in *Arabidopsis*, proteins in *Arabidopsis* that play key roles in RNA silencing (Table 1.1) are discussed below.

Table 1.1 *Arabidopsis* proteins involved in RNA silencing

Code	Protein name	Function	References
DCL1	DICER-LIKE1	Generation of miRNAs	Park et al., 2002; Reinhart et al., 2002
DCL2	DICER-LIKE2	Generation of vsRNAs in VIGS and 24-nt endogenous siRNAs	Borsani et al., 2005; Xie et al., 2004
DCL3	DICER-LIKE3	Generation of 24-nt siRNAs in the TGS	Xie et al., 2004
DCL4	DICER-LIKE4	Generation of trans-acting siRNAs in PTGS	Dunoyer et al., 2005; Gasciolli et al., 2005; Yoshikawa et al., 2005
AGO1	ARGONAUTE1	mRNA cleavage	Baumberger and Baulcombe, 2005; Fagard et al., 2000; Qi et al., 2005; Vaucheret et al., 2004
AGO4	ARGONAUTE4	chromatin modification	Zilberman et al., 2004
AGO7	ARGONAUTE7	mRNA cleavage	Adenot et al., 2006
RDR1	RNA-DEPENDENT RNA POLYMERASE1	Required in the PTGS and *trans*-acting siRNA pathways	Yu et al., 2003
RDR2	RNA-DEPENDENT RNA POLYMERASE2	Involved in the TGS pathway occurring in the nuclear	Herr et al., 2005; Xie et al., 2004
RDR6	RNA-DEPENDENT RNA POLYMERASE6	Required for operation of the *trans*-acting siRNA pathway	Dalmay et al., 2000; Mourrain et al., 2000
SDE3	SILENCING-DEFECTIVE GENE3	RNA helicase	Dalmay et al., 2001; Himber et al., 2003
SGS3	SUPPRESSOR OF GENE SILENCING3	RNA stabilizer	Mourrain et al., 2000; Yoshikawa et al., 2005
HST	HASTY	Putative exportin	Park et al., 2005
HEN1	HUA ENHANCER1	RNA methylase	Li et al., 2005; Yu et al., 2005
HYL1	HYPONASTIC LEAVES1	dsRNA-binding protein	Hiraguri et al., 2005; Lu and Federoff, 2000

Dicers

Using biochemical and genetic methods, four Dicer-like enzymes (DCLs) have been identified in *Arabidopsis*, which are responsible for generation of the different classes of small RNAs (Aravin and Tushl, 2005; Wang and Metzlaff, 2005). DCL1 functions in the miRNA pathway to process polymerase II transcripts into miRNAs (Kurihara and Watanabe, 2004; Park et al., 2002; Reinhart et al., 2002). DCL2 is involved in generation of vsRNAs (Xie et al., 2004) and some endogenous siRNAs (Borsani et al., 2005). DCL3 is required for processing long dsRNA precursors into 24-nt siRNAs in the TGS pathway (Qi et al., 2005; Xie et al., 2004). DCL4 is required for generation of siRNAs involved in the PTGS pathway (Dunoyer et al., 2005) and the *trans*-acting siRNA pathway (Gasciolli et al., 2005).

These findings indicate that different Dicers are responsible for production of different small RNAs. However, complete blockage of siRNA biogenesis in the *trans*-acting siRNA pathway requires mutation of both DCL3 and DCL4, suggesting that Dicers are functionally redundant to some degree (Gasciolli et al., 2005). Functional redundancy in siRNA production and DNA methylation of DCL2, DCL3 and DCL4 was further demonstrated by using transfer-DNA (T-DNA) insertional mutagenesis, which generated all possible double mutants as well as dcl2/dcl3/ dcl4 triple mutant (Henderson et al., 2006). When a specific Dicer is not available, other Dicers can substitute for it and switch silencing to another pathway (Herr, 2005).

Among the four DCLs in *Arabidopsis*, DCL1, DCL2, and DCL3 contain a RNA-binding PAZ (Piwi/Argonaute/Zwille) domain that is structurally homologous with the active center of RNase H. Mutations within the PAZ domain result in decreased cleavage

efficiency, suggesting that the PAZ domain is important for the function of DCLs in RNA silencing (Zhang, 2004). However, DCL4 is unusual because it lacks a PAZ domain. It may utilize adaptor molecules to interact with the RNA templates in its silencing pathway.

RISC

As mentioned above, siRNAs and miRNAs are incorporated into RISC to guide cleavage or degradation of their complementary mRNAs (Hutvagner, 2005; Schwarz et al., 2003). RISC is a cellular multisubunit protein complex, with its key component, an ARGONAUTE (AGO) protein, containing a PAZ RNA-binding domain and a PiWi RNase H-like domain (Jones-Rhoades et al., 2006; Liu, et al., 2004a; Song, et al., 2004). Among the proteins involved in RNA silencing, the PAZ domain is found only in Dicers and AGO proteins. Ten AGO homologues, termed AGO1-10, have been identified in *Arabidopsis* (Bohmert et al., 1998; Fagard et al., 2000; Hunter et al., 2003; Zilberman et al., 2003). AGO1 selectively recruits miRNAs, *trans*-acting siRNAs, and transgene-derived siRNAs through its PAZ domain, but not the 24-nt siRNAs generated in the TGS pathway (Baumberger and Baulcombe, 2005; Qi et al., 2005; Vaucheret et al., 2004). AGO1 cleaves miRNA-targeted RNAs in vitro though its PiWi domain that is proposed to constitute an RNase catalytic center (Baumberger and Baulcombe, 2005). Mutation of *Arabisopsis* AGO4 substantially decreased maintenance of DNA methylation triggered by transgenes in the TGS pathway, without blocking DNA methylation initiation, suggesting that AGO4 may function in the 24-nt siRNA-directed chromatin modifications (Zilberman et al., 2003). In addition, some *trans*-acting siRNAs control leaf development

through the action of AGO7 (Adenot et al. 2006). Functions of other AGO proteins in *Arabidopsis* are currently not known. However, sequence similarities among AGO proteins suggest that they might have similar activities but recruit different subsets of small RNAs.

RdRps

Arabidopsis has six cellular RdRps (RDR1-6), which synthesize dsRNAs that are processed by Dicers into siRNAs. These RdRps share common amino acid sequences that are distantly related to the catalytic domain of DNA-dependent RNA polymerases (DdRp) (Iyer et al., 2003). RDR1 is required in the PTGS and *trans*-acting siRNA pathways (Dalmay et al. 2000; Mourrain et al. 2000; Yu et al., 2003). RDR2 mutants are defective for production of endogenous 24-nt siRNAs, suggesting that RDR2 is involved in the TGS pathway occurring in the nucleus (Herr et al., 2005; Xie et al., 2004). RDR6 is required for operation of the *trans*-acting siRNA pathway as described above. Function of other RdRps in *Arabidopsis* is not yet clear. It is proposed that combination of various RdRps, Dicers, and AGO proteins contribute to functional diversification of silencing pathways.

RdRp synthesize dsRNAs by primer-dependent or primer-independent (de novo) mechanisms. For primer-dependent mechanisms, primary siRNAs are needed to serve as primers in RdRp-directed primer extension on single-stranded RNA (ssRNA) templates to generate dsRNA (Sijen et al., 2001; Vaistij et al., 2002; Voinnet et al., 1998). For primer-independent mechanisms, ssRNAs are converted to dsRNAs by RdRp-mediated de novo transcription. Consistent with this mechanism, it was found that tomato cellular

RdRp can catalyze de novo synthesis of complementary RNAs from ssRNA templates in vitro (Schiebel et al., 1993). In wheat germ extracts, ssRNAs can be converted into dsRNAs by putative cellular RdRp activity (Tang et al., 2002). It is not known how RdRp correctly differentiate the silenced transgene RNAs from the non-silenced endogenous RNAs. One possibility is that the silenced RNAs lack 5' cap and/or 3' poly(A) tails and therefore appear aberrant compared with "normal" non-silenced RNAs, which may make them accessible for RdRps.

HEN1, HST, HYL1, SGS3, and SDE3

In addition to the four dicers, ten AGO proteins, and six RdRps, an increasing number of additional proteins have been recently identified in *Arabidopsis* that help to generate the different classes of small RNAs (Herr, 2005; Hutvagner, 2005; Kidner and Martienssen, 2005; Wang and Metzlaff, 2005). For example, HUA ENHANCER 1 (HEN1) is a methyltransferase that methylates the 3' terminal nucleoside of miRNA duplexes (Yu et al., 2005). HASTY (HST) is an ortholog of exportin-5 in *Arabidopsis*, which is necessary for export of pre-miRNAs into the cytoplasm from the nucleus (Park et al., 2005). HYPONASTIC LEAVES 1 (HYL1) is a dsRNA-binding protein that interacts with DCL1 for miRNA biogenesis (Hiraguri et al., 2005; Lu and Federoff, 2000). SGS3 is a coiled-coil protein stabilizing the single-stranded RNA fragments cleaved in the miRNA pathway from degradation by nucleases as described above (Mourrain et al., 2000; Yoshikawa et al., 2005). SILENCING-DEFECTIVE GENE 3 (SDE3) is an RNA helicase that may act to resolve secondary structures present in RdRp templates (Dalmay et al., 2001; Himber et al., 2003).

13

The antiviral defense role of VIGS in plants

Most plant viruses contain positive-strand RNA genomes that encode genetic information required for viral infection in hosts. Studies of plants infected by such positive-strand RNA virus as *Tobacco etch virus* (TEV), *Potato virus X* (PVX), and *Potato virus Y* (PVY) indicate that viral infection can be restricted or blocked by transgenic expression of portions of the viral genomic RNA (English et al., 1996; Goodwin et al., 1996; Lindbo and Dougherty, 1992; Mueller et al., 1995; Tanzer et al., 1997). Further studies of this phenomena indicated that the overexpression of viral RNA fragments induces a PTGS-like silencing activity that targets viral RNAs, termed virus-induced gene silencing (VIGS) (Kumagai et al., 1995; Ruiz, et al., 1998).

VIGS was originally considered to be PTGS because it was thought to be triggered by long dsRNAs generated in the process of viral replication. However, there is no direct evidence supporting the existence of dsRNA intermediates during replication of the vast majority of RNA viruses. Direct evidence that VIGS is not triggered by the dsRNA comes from sequencing of the vsRNAs cloned from plants infected with *Cymbidium ringspot virus* (CymRSV). The CymRSV-derived vsRNAs are not randomly distributed throughout the viral RNAs, which would be expected if they were generated by digestion of a long dsRNA like that in the PTGS pathway, but rather they are primarily derived from discrete "hotspot" regions (Molnar et al., 2005). Furthermore, the vsRNAs are mainly derived from plus-strands, which are present at levels 10-100 fold higher than those complementary minus-strands generated during virus replication (Molnar et al., 2005). These results suggest that VIGS is triggered by the hairpin structures present in

14

the single-stranded viral RNA molecules, a mechanism similar to biogenesis of endogenous miRNAs (Rhoades et al., 2002; Szittya et al., 2002; Voinnet, 2005; Figure 1.2A). The contribution of such intra-molecular base-pairing to vsRNA generation is strongly supported by the fact that inverted transgenic repeats, when inserted into recombinant virus, trigger more efficient VIGS than inserted linear RNA fragments (Lacomme et al., 2003). vsRNAs generated in PSTVd-infected plants are also mainly derived from intramolecular pairing region of their circular RNA genome (Denti et al., 2004; Itaya et al., 2001; Papaefthimiou et al., 2001).

vsRNAs incorporate into RISC and guide cleavage of viral RNAs, thereby preventing accumulation of virus in plants. The antiviral role of VIGS is indicated by the "recovery" phenomena in nontransgenic plants. For example, the severe symptoms initially displayed by upper leaves of *Nicotiana clevelandii* infected with *Tomato black ring nepovirus* (TomBRV) were significantly attenuated after systemic spread of the virus (Ratcliff et al., 1997). Northern blot results indicated that virus content in recovered leaves was reduced significantly. Furthermore, the recovered leaves were resistant to secondary inoculation of TomBRV (Ratcliff et al., 1997). VIGS can also explain the phenomenon of cross-protection in which infection of a plant by a mild strain of a plant virus elicits resistance to a related severe strain (Ratcliff et al., 1999). This is caused by the VIGS induced by infection of the low-pathogenic virus, which targets homologous, high-pathogenic challenge viruses. The contribution of RNA silencing to plant resistance was also supported by finding that mutations in genes that encode proteins involved in RNA silencing pathways resulted in enhanced susceptibility to virus infection (Table 1.2). For example, loss-of-function mutation of RDR1 in *Arabidopsis thaliana* increases plant

Figure 1.2 RNA silencing induced by viruses in plants (see the text for details). (A) VIGS. (B) Secondary VIGS. (C) RISC cleavage of host mRNA directed by the vsRNA.
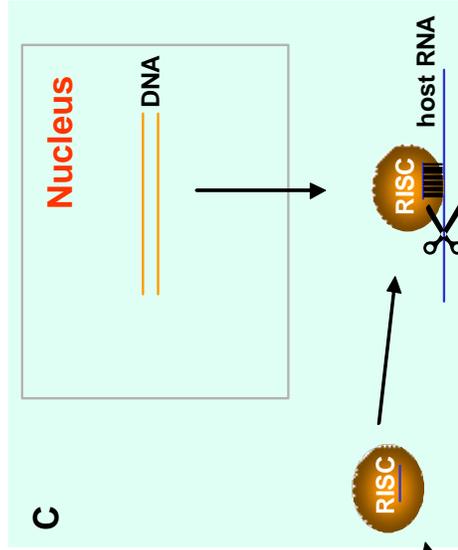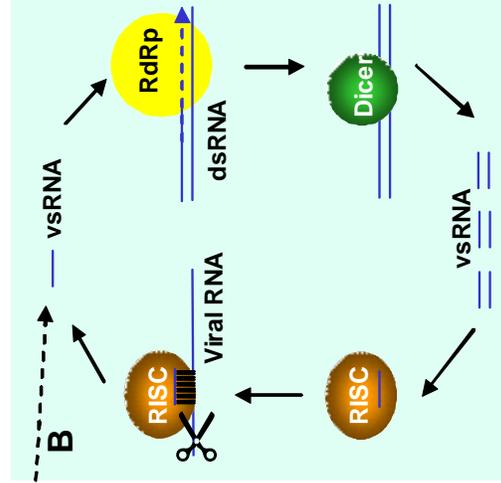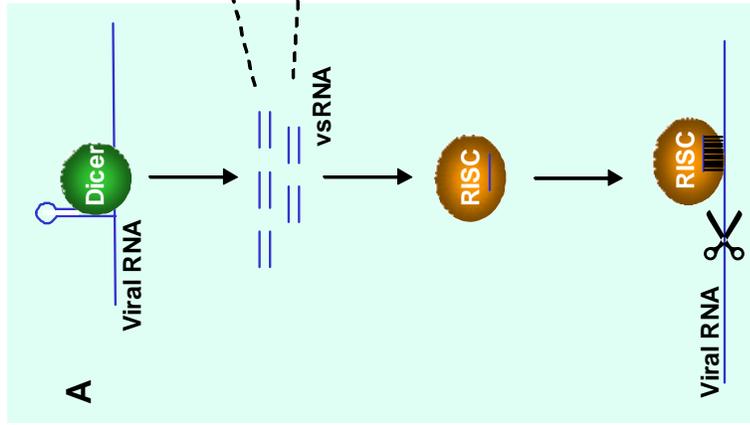
Table 1.2 Effects of host protein defects on plant susceptibility to viruses

Plant	Gene	Mutant	Enhanced plant susceptibility to viruses	No effect on plant susceptibility to viruses	References
Tobacco	RDR1	rdr1	Tobacco mosaic virus		Yu et al., 2003
Arabidosis	RDR1	rdr1	Tobamoviruses, Tobra viruses, Potexviruses	Cucumber mosaic virus	Yang et al., 2004; Yu et al., 2003
Arabidosis	RDR6	rdr6	Cucumber mosaic virus	Tobacco rattle virus Tobacco mosaic virus	Dalmay et al., 2001; Mourrain et al., 2000
Arabidosis	DCL2	dcl2	Turnip crinkle virus		Xie et al., 2004
Arabidosis	AGO1	ago1	Cucumber mosaic virus		Boutet et al., 2003
Arabidosis	SGS3	sgs3	Cucumber mosaic virus		Dalmay et al., 2001
Arabidosis	SDE3	sde3	Cucumber mosaic virus		Dalmay et al., 2001

susceptibility to Tobamoviruses, Tobraviruses and Potexviruses, but not to CMV (Yang et al., 2004; Yu et al., 2003). The differential effects on plant susceptibility to different viruses might be caused by specialization of components of silencing pathways.

The antiviral effects of VIGS can be further amplified by the action of cellular RdRps involved in RNA silencing. Amplification occurs via at least two mechanisms. The first mechanism requires the presence of primary vsRNAs, which are proposed to prime cellular RdRp-mediated extension on viral RNA templates to synthesize new dsRNA. The dsRNAs are then recognized by Dicers to trigger further rounds of VIGS, termed secondary VIGS (Figure 1.2B). Occurrence of this process is supported by finding that VIGS initiated by a vsRNA that was complementary to one location of a targeted mRNA resulted in accumulation of secondary vsRNAs that corresponded to adjacent regions (Vaistij et al., 2002). In *Arabidopsis*, synthesis of secondary vsRNAs and operation of secondary VIGS requires activities of RDR6, AGO1, SGS3, and SDE3, the key components involved in the *trans*-acting siRNA pathway (Himber et al., 2003; Mourrain et al., 2000; Vaistij et al., 2002; Yoshikawa et al., 2005). These proteins might also be involved in a second mechanism in which these proteins are thought to recognize aberrant RNAs produced by viruses and transcribe them *de novo* into dsRNAs (Mourrain et al., 2000). *Arabidopsis thaliana* mutants lacking functional AGO1, RDR6, or SGS3 were hypersusceptible to CMV, but not *Tobacco rattle virus* (TRV) and *Tobacco mosaic virus* (TMV) (Table 1.2) (Boutet et al., 2003; Dalmay et al., 2001; Muangsan et al., 2004), suggesting that there is some specialization in components of secondary VIGS.

Because of the specific and adaptive features as described above, RNA silencing is considered an antiviral defense mechanism in plants (Ahlquist, 2002; Gitlin and Andino, 2003). This mechanism is primarily mediated by the RNA-RNA interaction between vsRNAs and their complementary viral RNAs. It differs from the protein-based native immune system in plants, which is dependent on expression of membrane-bound or cytosolic disease resistance proteins (R proteins). The R proteins interact with specific viral proteins, termed elicitors (Dangl and Jones, 2001), to trigger a cascade of salicylic acid-dependent resistance reactions that result in programmed cell death, known as the hypersensitive response. In compatible plant-virus interactions, the viral elicitor escapes recognition of R protein, leading to disease development.

Counterdefense strategies of viruses to VIGS

As described above, when a virus enters a host cell, it induces RNA silencing that prevents its accumulation in plants. To successfully infect plants, viruses need to evolve strategies to overcome this antiviral mechanism. Viruses encode specific proteins, termed suppressors, which suppress silencing. Alternatively, viruses may evade silencing by replicating in nuclease-inaccessible sites. Studies of these strategies will help us understand regulation of RNA silencing. These strategies also provide us with examples of co-evolution between hosts and parasites.

Suppression of RNA silencing

Over the past several years, a large number of plant viruses have been found to encode silencing suppressors (Table 1.3). One of the best-characterized examples is the helper component proteinase (HcPro) of Potyviruses, which contains a proteinase domain catalyzing the autoproteolytic cleavage between HcPro and the adjacent protein within the large viral polyprotein. HcPro is a multifunctional protein, required for viral genome amplification, long-distance movement, and pathogenicity (Kasschau et al., 1997; Pruss et al., 1997). HcPro was the first silencing suppressor to be identified with early reports indicating that it suppresses VIGS, resulting in recovery of potyvirus-infected leaves (Anandalakshmi et al., 1998; Brigneti et al., 1998; Kasschau and Carrington, 1998). Overexpression of HcPro in tobacco dramatically reduced the levels of transgene-triggered siRNAs, suggesting that HcPro may suppress RNA silencing by interfering with the biogenesis of siRNAs (Johansen and Carrington, 2001; Mallory et al., 2002; Figure 1.2A). It was recently found that HcPro inhibits RNA silencing by binding to siRNAs in *Drosophila* embryo extracts, which requires a cellular factor that increases the affinity of HcPro binding to siRNA duplexes (Lakatos et al., 2006). Although the cellular factor is detectable in *Arabidopsis* extracts, it is currently not known whether it is required for efficient silencing suppression in plants (Lakatos et al., 2006). HcPro also interacts with the miRNA pathway by facilitating accumulation of miRNAs in transgenic *Arabisopsis* and tabacco plants (Dunoyer et al., 2004; Mallory et al., 2002) and reducing HEN1-mediated 3' terminal nucleoside methylation (Ebhardt et al., 2005).

The 2b protein of cucumoviruses, a small protein of about 100 amino acids encoded by an overlapping viral open reading frame, has also been identified as a silencing

Table 1.3 RNA silencing suppressors encoded by plant viruses

	Viral genus	Virus	Suppr-essors	Other functions	References
(+)-strand RNA viruses	Carmovirus	Turnip crinkle virus	p38	Coat protein	Qu et al, 2003; Thomas et al., 2003
	Cucumovirus	Cucumber mosaic virus; Tomato aspermy virus	2b	Host-specific movement	Brigneti et al., 1998
	Closterovirus	Beet yellows virus	p21	Replication enhancer	Reed et al., 2003
		Citrus tristeza virus	p20	Replication enhancer	Lu et al., 2004
			p23	Nucleic-acid binding	
			CP	CP Coat protein	
	Comovirus	Cowpea mosaic virus	S	Small coat protein	Liu et al., 2004b
	Hordeivirus	Barley yellow mosaic virus	γb	Movement; Pathogenicity determinant; Replication enhancer; Seed transmission	Yelina et al., 2002
	Pecluvirus	Peanut clump virus	p15	Movement	Dunoyer et al., 2002
	Polerovirus	Beet western yellows virus;	p0	Pathogenicity determinant	Pfeffer et al., 2002
	Potexvirus	Potato virus X	p25	Movement	Voinnet et al., 2000
	Potyvirus	Potato virus Y; Tobacco etch virus; Turnip mosaic virus	HcPro	Aphid transmission; Movement; Pathogenicity determinant; Polyprotein processing	Anandalakshmi et al., 1998; Brigneti et al, 1998; Kasschau and Carrington, 1998
	Sobemovirus	Rice yellow mottle virus	p1	Movement; Pathogenicity determinant	Voinnet et al., 1999
	Tombusvirus	Carnation Italian ringspot virus; Cymbidium ringspot virus; Tomato bushy stunt virus	p19	Movement; Pathogenicity determinant	Voinnet et al., 1999
	Tobamovirus	Tobacco mosaic virus; Tomato mosaic virus	p30	Replication	Kubota et al., 2003
	Tymovirus	Turnip yellow mosaic virus	p69	Movement; Pathogenicity determinant	Chen et al., 2004
(-)-strand RNA viruses	Tospovirus	Tomato spotted wilt virus	NSs	Pathogenicity determinant	Bucher et al., 2003
	Tenuivirus	Rice hoja blanca virus	NS3	Unknown	
DNA viruses	Geminivirus	African cassava mosaic virus	AC2	Transcriptional activator	van Wezel et al., 2002; Voinnet et al., 1999
		Mungbean yellow mosaic virus	C2		
		Tomato yellow leaf curl virus	C2		

suppressor. Initial evidence indicated that expression of CMV 2b from PVX vector in tobacco plants prevented initiation of VIGS (Brigneti et al., 1998). Unlike HcPro, 2b does not reverse silencing that is already established in plants, suggesting that 2b may target steps different from that of HcPro (Brigneti et al., 1998). Transgenic expression and grafting experiments provide strong evidence that 2b blocks the movement of the systemic silencing signal (Guo and Ding, 2002; Figure 1.2D). CMV 2b suppression of silencing is triggered by multiple inducers including siRNAs, dsRNAs, or DNA plasmids expressing dsRNAs in single cells, indicating that 2b may also function by inhibiting siRNA-directed mRNA degradation (Qi et al., 2004).

The p19 protein of tombusviruses, which is essential for systemic spread of the virus and symptom development in host plants (Russo et al., 1994), is also a silencing suppressor (Voinnet et al., 1999). In vitro binding assays indicated that p19 binds to 21-nt siRNAs in an RNA size-selective manner (Silhavy et al., 2002; Vargason et al., 2003; Ye et al., 2003). Further studies indicated that the affinity of p19 binding to siRNA correlates with viral infection severity, suggesting that p19 may suppress silencing by binding to siRNAs, therefore preventing their incorporation into the RISC (Chapman et al., 2004; Dunoyer et al., 2004; Lakatos et al., 2004, Silhavy et al., 2002; Figure 1.2A).

In addition to the suppressors described above, proteins encoded by other viruses, such as p25 of PVX, p69 of *Turnip yellow mosaic virus* (TYMV), and p21 of *Beet yellows virus* (BYV) have also been identified as silencing suppressors (Chen et al., 2004; Reed et al., 2003; Voinnet et al., 2000). As described above, the identified suppressors are diverse in sequence and structures and function to interfere with different

steps of RNA silencing, indicating that they might have evolved independently in different virus groups.

Escape from RNA silencing

The susceptibility of individual viruses to RNA silencing strongly depends on the vsRNA-targeted sequences contained in the viral genome. Viruses may escape from silencing by imbedding the silencing-targeted sequences into high-order structures. This hypothesis is supported by the fact that viruses containing transgenes or other non-viral sequences are usually strongly targeted by VIGS (Mueller et al., 1995; Tanzer et al., 1997), since the non-viral sequences have not evolved structural features to inhibit targeting of silencing. Viruses may also escape silencing by mutating vsRNA-targeted sequences. For example, insertion of host miRNA-targeted sequence into *Plum pox virus* (PPV) genome reduced virus replication, but the virus readily escaped silencing through mutations within the miRNA-targeted region (Simon-Mateo and Garcia, 2006).

Some viruses may resist cellular nucleases by replicating in nuclease-inaccessible sites. For example, it has been found that *Brome mosaic virus* (BMV) replication protein 1a forms vesicles budding into the endoplasmic reticulum membrane (Sullivan and Ahlquist, 1999). The RNA templates and the replication protein 2a containing a central RdRp domain are then recruited into the vesicles, which therefore become sites of replication (Ahlquist, 2006; Chen et al., 2001; Sullivan and Ahlquist, 1999; Wang et al., 2005). Replication occurring in membrane-bound vesicles is proposed to reduce the exposure of viral RNAs to the RNA silencing-mediated host defense mechanism. Additionally, other features of viruses, such as packaging of viral RNAs into capsids or

replication of dsRNA viruses within their capsids, can also be considered as strategies for resisting RNA silencing.

Modulation of host gene expression by VIGS

Plants infected by viruses often display discernible symptoms such as discoloration, stunting, necrosis, and even death, which are caused by virus-triggered abnormal alterations of the developmental processes. As described above, some silencing pathways, such as the miRNA pathway, are involved in regulation of plant development. Since silencing pathways in plants are interconnected, mechanisms of viruses to suppress VIGS may also alter endogenous silencing pathways, affecting plant development and therefore contributing to symptom development.

Silencing suppressors interfere with the regulatory roles of miRNAs in plant development

Some viral suppressors are involved in endogenous silencing pathways. For example, infection of *Turnip mosaic virus* (TuMV) resulted in severe developmental defects on vegetative and reproductive organ, which can be reproduced by overexpression of TuMV-encoded HcPro in transgenic plants or a loss-of-function mutation of DCL1 (Jacobsen et al., 1999; Kasschau et al, 2003; Robinson-Beers et al., 1992). These results suggest that TuMV infection may cause symptoms by expressing HcPro, thus interfering with the regulatory role of miRNAs in plant development, since DCL1 is required for generation of miRNAs. This hypothesis is directly supported by

evidence that HcPro repressed the activity of miR171, an *Arabidopsis* miRNA that guides cleavage of at least eight mRNAs encoding *Scarecrow-like* transcription factors (Chapman et al., 2004; Kasschau et al, 2003). However, this hypothesis is not supported by findings that ectopic overexpression of DCL1 in HcPro transgenic *Arabidopsis* plants rescued phenotypic anomalies but not biogenesis of miRNAs and miRNA-directed mRNA cleavage (Mlotshwa et al., 2005). This result suggests that HcPro might interfere with an additional DCL1 activity that plays roles in plant developmental regulation but is independent of generation of miRNAs (Mlotshwa et al., 2005).

Studies of other RNA silencing suppressors indicated that overexpression of BYV p21 or TYMV p19 in transgenic *Arabidopsis* plants leads to significant increases in levels of three studied mRNAs (*ARF8*, *ARF10*, and *SCL6-IV*) (Reed et al. 2003; Silhavy et al. 2002; Voinnet et al. 1999). These three *Arabidopsis* mRNAs are down-regulated by three endogenous miRNAs (miR167, miR160, and miR171), respectively, in normal developmental processes (Chapman et al., 2004). Co-immunoprecipitation of p21 and p19 with miRNA duplexes from transgenic *Arabidopsis* inflorescence suggested that p21 and p19 might bind to the miRNA duplex, thereby inhibiting their incorporation into RISC during RNA silencing (Chapman et al., 2004). In general, the findings that proteins encoded by evolutionarily distinct viruses can affect the endogenous miRNA pathway indicate that it may be a general feature of silencing suppressors to contribute to symptom development.

vsRNAs may guide cleavage or degradation of homologous host mRNAs

As described above, endogenous siRNAs and miRNAs in plants regulate plant development by down-regulating levels of cellular mRNAs. Therefore, it is possible that vsRNAs contribute to symptom development by base pairing with complementary host mRNA transcripts to direct cleavage of host mRNAs (Figure 1.2C). This hypothesis is supported by evidence achieved from studies of non-coding CMV satellite RNA Y (satY) and PSTVd (Wang et al., 2004): (i) symptoms caused by CMV satY were significantly attenuated when silencing was suppressed by ectopic expression of HcPro; and (ii) transgenic expression of a short PSTVd hairpin RNA in tomato plants induced viroid-like symptoms. These results suggest that the vsRNAs derived from CMV satY and PSTVd, but not unprocessed subviral RNAs, may cause disease symptoms by directing silencing of cellular mRNAs transcribed from physiologically important genes.

The RISC-mediated mRNA degradation requires a minimum base pairing of ~19 nt between the small RNAs and their target RNAs (Vanitharani et al., 2003; Zamore, 2001). BLAST searches (Altschul et al., 1997) with full-length PSTVd revealed numerous genes from several plant species that contain 19- to 20-nt identities with the PSTVd sequence (Wang et al., 2004). Some of these plant genes, which encode transcription factors or chromodomain helicase DNA-binding proteins, contain sequence identities with the virulence modulation region of PSTVd. Therefore, it is possible that small RNAs derived from PSTVd direct silencing of these physiologically important host genes, resulting in symptoms (Wang et al., 2004). In addition to the evidence described above, miRNAs derived from animal DNA viruses, the herpesviruses, has also been proposed to modulate host gene expression by incorporating into RISC to guide host mRNA cleavage or

translational inhibition, although no host target genes have yet been identified (Cai et al., 2005; 2006; Grey et al., 2005; Neilson and Sharp, 2005; Pfeffer et al., 2004; 2005; Sullivan and Ganem, 2005).

vsRNAs may compete with endogenous small RNAs for interaction with silencing-related proteins

Efficient amplification of viruses in plants produces high levels of viral RNAs, which are cleaved by Dicers to produce a large number of diverse vsRNAs in host cells. The majority of the vsRNAs may not be complementary with host mRNAs and therefore are not capable of directing RISC to cleave host mRNAs. However, it is possible that vsRNAs function as suppressors of RNA silencing by competing with host endogenous siRNAs and miRNAs for binding to silencing-related proteins, since vsRNAs are structurally similar to miRNAs and siRNAs (Dunoyer and Voinnet, 2005). This non-specific protein-consumption strategy might contribute to symptom development, although supportive evidence from plant viruses is currently lacking. In addition to vsRNAs, larger viral or subviral RNAs associated with viruses are also potential competitors. For example, it was recently found that two non-coding RNAs associated with Adenovirus bind to exportin 5, which is required for export of the miRNA precursors from the nucleus to the cytoplasm (Andersson et al., 2005; Sano et al., 2006).

TCV as a useful system for studying virus-plant interaction

Turnip crinkle virus (TCV) (family *Tombusviridae*, genus *Carmovirus*) is a positive-sense RNA virus with a 4054-nt single-stranded genome, which encodes five proteins (Figure 1.3A; Hacker et al., 1992). p28 and p88, a translational readthrough product of p28 that contains the GDD (Glycine/Aspartic acid/Aspartic acid) polymerase active site consensus sequence, are translated from the genomic RNA. These two proteins, which comprise the viral RdRp, are both required for replication of TCV and its associated RNAs. p8 and p9, two movement proteins required for cell-to-cell viral movement, are translated from the 1.7 kb subgenomic RNA (Hacker et al., 1992; Li et al., 1998). The coat protein (CP), which is translated from the 1.45 kb subgenomic RNA, packages TCV-associated RNAs into 180-subunit, T=3 icosahedral virions (Heaton et al., 1991; Wang and Simon, 1999).

To infect a plant, under natural conditions, TCV must enter an initial cell aided by its vector (flea beetle). In the lab, TCV can be inoculated into plants by rubbing leaves. Genomic RNAs released from dissociated virions in the cytoplasm serve as templates for translation of viral RdRp using the cellular translation machinery. The RdRp, possibly together with other viral proteins and/or host factors, comprises a replicase complex that is responsible for viral replication (Lai, 1998). During viral replication, the genomic RNA serves as template to transcribe complementary minus-strand RNAs and the newly synthesized minus strands are then used as templates for synthesis of large quantities of progeny plus strands. In host cells, the amounts of plus strands are usually 10-100 fold higher than those of minus strands (Buck, 1996).
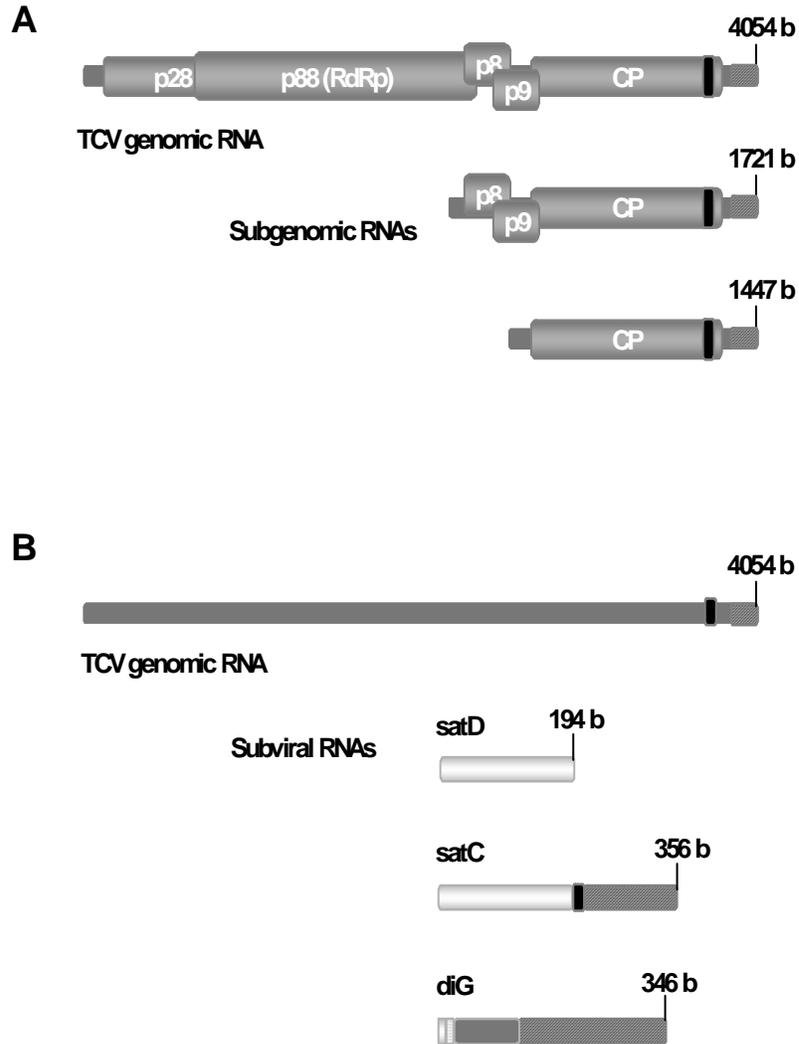
Figure 1.3 Genomic and subviral RNAs in the TCV system. (A) Genomic organization of TCV. p28 and p88 are expressed from the genomic RNA. p8 and p9 are expressed from the 1.7 kb subgenomic RNA. CP is translated from the 1.45 kb subgenomic RNA. (B) satC and satD are two satellite RNAs associated with TCV. satC is a chimeric RNA composed of satD and TCV sequences. diG is a defective inference RNA associated with TCV. Similar regions are shaded alike.

To be systemically infectious, TCV must move out of the initially infected cell, enter neighboring cells, and spread throughout plants. Virus movement involves two different steps: (i) cell-to-cell movement through plasmodesmata, which generally needs virus-encoded movement proteins to modify plasmodesmal size to allow viral transportation (Ghoshroy et al., 1997; Lazarowitz and Beachy, 1999; McLean et al., 1997); (ii) long-distance (vascular) movement through the phloem sieve tube network, which may require the presence of viral movement protein, CP, and some specific host factors (Carrington et al., 1996; Cronin et al., 1995; Scholthof et al., 1993; Seron and Haenni, 1996). The detailed mechanisms of p8 and p9 functioning in TCV movement is currently not known, although the approximately 30 kDa movement proteins of TMV and *Red clover necrotic mosaic virus* (RCNMV) are proposed to function by binding to viral RNAs and targeting them to the plasmodesmata (Citovsky et al., 1990; Deom et al., 1987; Giesman-Cookmeyer et al., 1995). TCV CP is required for virus systemic movement, but not cell-to-cell movement, in *Arabidopsis thaliana* and *Brassica campestris*, and systemic and cell-to-cell movement in other hosts such as *Nicotiana benthamiana* (Hacker et al., 1992).

Virion formation is essential for long-distance movement of some viruses such as TMV and CMV (Saito et al., 1990; Schmitz and Rao, 1998). However, it appears to be dispensable for viruses that are proposed to transport as the form of a ribonucleocomplex comprising viral RNAs and virus-encoded proteins (Dalmay et al., 1992; Dolja et al., 1994; Kaplan et al., 1998; Schneider et al., 1997; Wang and Simon, 1999). Mutations in TCV CP prevented virion accumulation, but not viral systemic spread, suggesting that

virion formation is not required for TCV movement and it may move as a ribonucleocomplex (Wang and Simon, 1999).

TCV has a wide host range among crucifers and is highly pathogenic on nearly all ecotypes of *Arabidopsis thaliana* tested except for ecotype Dijon (Simon et al., 1992). The hypersensitive response in Dijon is elicited by the interaction between the N-terminal 25 amino acids of TCV CP and a cellular transcription factor, termed TCV-interacting protein (TIP) (Kachroo et al., 2000; Ren et al., 2000). Infection of the susceptible *Arabidopsis thaliana* ecotype Columbia with TCV results in visible symptoms including stunting and delayed bolting leaves (Figure 1.4).

As described above, viruses are triggers and targets of VIGS. Therefore, to successfully establish an infection in plants, TCV must have evolved mechanisms to suppress VIGS in addition to failing to eliciting the plant's hypersensitive resistance. Investigation of all five TCV-encoded proteins for their ability to suppress silencing triggered by transient expressed GFP gene in *Nicotiana benthamiana* plants indicated that only the CP suppresses silencing (Thomas et al., 2003). The silencing suppressor role of CP was also independently identified by another research group (Qu et al., 2003). Both groups found that the TCV CP is a very weak or ineffective suppressor when generated from the TCV genome whereas it is as strong as other suppressors (e.g. tombusviral p19 and potyviral HcPro) when transiently expressed (Qu et al, 2003; Thomas et al., 2003). Further studies indicated that CP mRNAs transcribed from transient expression vectors accumulate earlier than those generated from infectious virus, suggesting that CP may be only effective when produced at an early step of RNA silencing.

Further studies of the suppressor role of TCV CP indicated that ectopic CP expression

Mock **TCV** **(+D)** **(+G)** **(+C)**
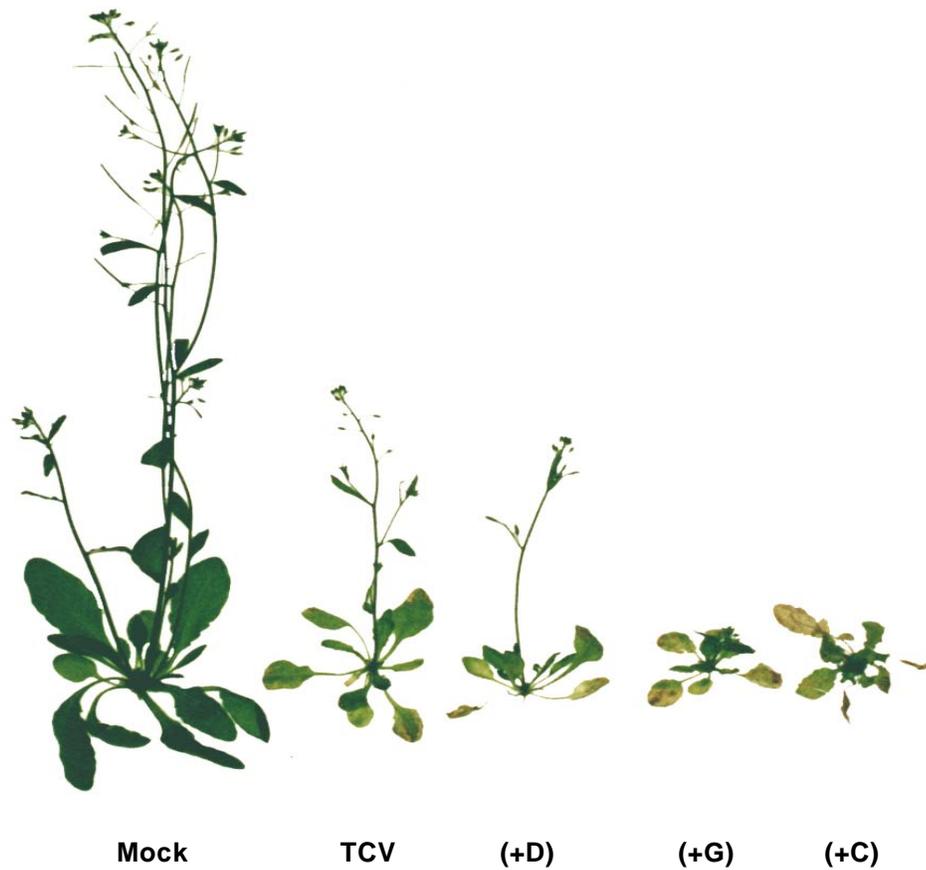
Figure 1.4 Comparison of effects of subviral RNAs on symptom expression. Col-0 seedlings at the six- to eight-leaf stage were inoculated on the oldest leaf pair with transcripts of TCV in the presence or absence of subviral RNAs. Plants were inoculated with buffer only (mock); TCV alone (TCV); TCV+satD (+D); TCV+diG (+G); TCV+satC (+C).

substantially reduced levels of 21- and 24-nt siRNAs while enhancing at least one miRNA (Chapman et al., 2004; Dunoyer et al., 2004). The non-interference of CP with dsRNA processing suggests that it might interfere with a process downstream of dicer activity (Dunoyer et al., 2004). Alternatively, CP could interact with small RNAs directly, which may cause vsRNA instability. Recent gel mobility shift assays indicated that the TCV CP binds to siRNA duplexes in an RNA size-independent manner (Merai et al., 2006), which is in contrast to the size-dependent manner of tombusviral p19 (Silhavy et al., 2002; Vargason et al., 2003; Ye et al., 2003). While resulting in a substantial reduction in host siRNAs, expression of TCV CP in *Arabidopsis* had little (Chapman et al., 2004) or no effect on host morphology (Dunoyer et al., 2004).

Since TCV CP contributes to symptom development by functioning in multiple viral processes, symptoms of TCV expressing various levels of wild-type (wt) or mutant CP have been studied. A single-base U-to-C change in the initiation codon of the CP gene (construct CPm) produced CP containing two additional amino acids (glutamic acid and threonine) at its N terminus due to translation initiating at an upstream non-canonical CUG codon (Figure 1.5; Wang and Simon, 1999). CPm translates the defective CP to about 10% of wt levels with decreased accumulation of the genomic and subgenomic RNAs and undetectable levels of virions (Figure 1.6A; Wang and Simon, 1999). Symptoms of *Arabidopsis* plants infected with CPm were only slightly delayed and were similar, but not identical to the symptoms associated with wt TCV (Figure 1.6B) (Wang and Simon, 1999). When *Arabidopsis* was inoculated with TCV engineered to express wt levels of the defective CPm CP (the construct CPm3 with nucleotides specifying the two

```
T C V       A C A  C U G  G A A  A U G  G A A  A A U  G A U  C C U  A G A
                            M      E      N      D      P      R

C P m       A C A  C U G  G A A  A C G  G A A  A A U  G A U  C C U  A G A
                     M     [E]    [T]     E      N      D      P      R

C P m 2     A C A  C U G  G A A  A U G  A C U  G A A  A A U  G A U  C C U  A G A
                            M     [T]     E      N      D      P      R

C P m 3     A C A  C U G  G A A  A U G  G A A  A C U  G A A  A A U  G A U  C C U  A G A
                            M     [E]    [T]     E      N      D      P      R
```

Figure 1.5 Sequences surrounding the translation initiation site for the CP in wt TCV and mutants derived from TCV. Bases altered or inserted in TCV are underlined. Changes in N-terminal amino acids in the TCV CP are boxed.

Figure 1.6 The effects of CP on symptom expression. (A) RNA gel blot of total RNA and protein gel blots of total protein and virions accumulating in protoplasts inoculated with TCV or CPm at 40 hours post inoculation. CPm produced about 10% of wt levels of CP and no detectable virions. (B) Symptoms of Col-0 plants inoculated with TCV or CPm with or without satC.

A
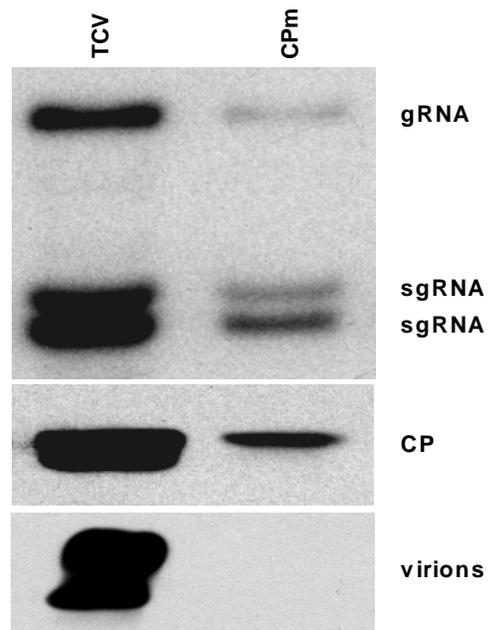
B
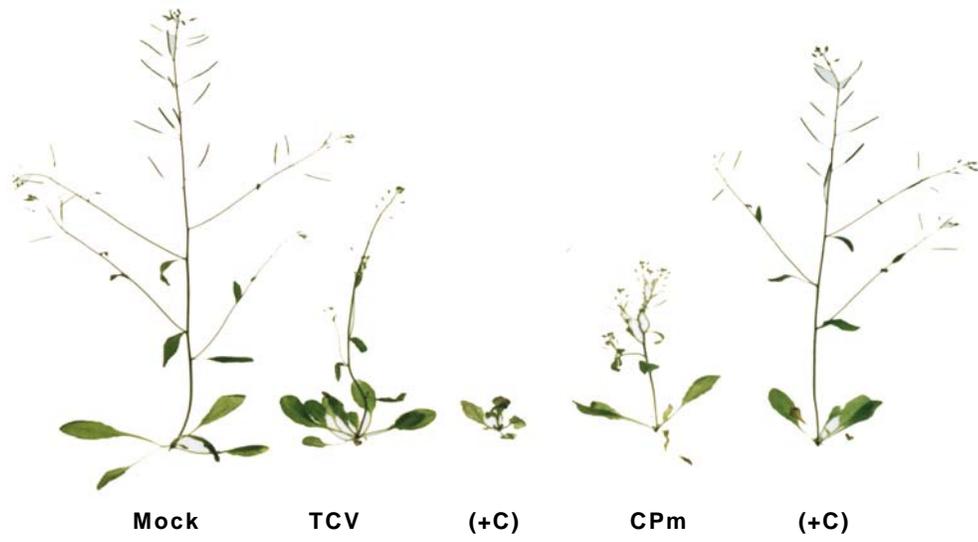
additional amino acids inserted after the translation initiation site; Figure 1.5), symptoms were greatly enhanced over wt TCV-induced symptoms (Wang and Simon, 1999). These results suggest that the symptom modulation is related to both the levels of CP and the two additional amino acids inserted at the N terminus (Wang and Simon, 1999). Both CPm and CPm3 can systemically infect the TCV-resistant Arabidopsis ecotype Di-0, suggesting that the N-terminal amino acid insertions prevent the interaction between CP and TIP, which would otherwise elicit hypersensitive resistance in plants (Kachroo et al., 2000; Ren et al., 2002).

Viral symptoms can also be modulated by the presence of unrelated, or partially related subviral RNAs, which require helper virus-encoded products for replication and systemic spread (Roossinck et al., 1992). TCV is naturally associated with several subviral RNAs including satellite RNA C (satC) (356 bases), satD (194 bases), and defective interfering RNA G (diG) (346 bases) (Figure 1.3B). satD, which appears to have originated from numerous short non-contiguous stretches of the TCV genomic RNA, has little contiguous sequence similarity with TCV beyond the 3' terminal 7 bases, (Carpenter and Simon, 1996). satC is a chimeric molecule containing nearly full-length satD at its 5' end and two discontinuous segments from TCV genomic RNA at its 3' end (Figure 1.3B; Simon and Howell, 1986). satC is assumed to be generated by recombination events between satD and TCV. diG is a defective deletion version of TCV, consisting of (from 5' to 3') 10 bases from the 5' end of satD, 12 bases of obscure origin, 99 bases from near the 5' end of TCV, and 225 bases that shares 94% sequence similarity with the 3'-terminal sequence of TCV including an imperfect repeat of 36 bases (Li et al., 1989).

While most satRNAs have no effect on, or attenuate the symptoms of their helper virus, satC is virulent, strongly intensifying the symptoms of TCV by changing the mild stunting and chlorotic symptoms of TCV-infected turnip leaves to severely stunted, crinkled, and dark green leaves (Simon and Howell, 1986). In *A. thaliana*, the stunting and delayed bolting attributed to infection by TCV alone turns into a lethal overall necrosis in the presence of satC, within 14- to 21-days postinoculation (dpi) (Figure 1.4; Simon et al., 1992). Symptom intensification by satC occurs despite a reduction in TCV RNA levels in the presence of satC (Li and Simon, 1990). All TCV-tolerant hosts accumulate similar levels of virus and satRNA as symptomatic hosts and remain symptomless in the presence of satC, suggesting that satC is not directly responsible for symptom production but rather creates conditions by which TCV symptom expression is enhanced (Li and Simon, 1990). In addition to satC, diG also intensifies the symptoms of TCV-infected plants, whereas satD is avirulent, without discernible effect on symptoms associated with TCV (Figure 1.4; Simon and Howell, 1986).

Comparison of the symptoms in *Arabidopsis* plants coinoculated with wt TCV and satC or inoculated with CPm3 indicated that the presence of satC and TCV leads to symptoms seemingly identical to those induced by CPm3 (Wang and Simon, 1999). Although satC and diG intensify the symptoms associated with wt TCV, both of them attenuate symptoms of the hybrid virus TCV-CP$_{CCFV}$ (TCV with its CP ORF precisely replaced with that of the related *Cardamine chlorotic fleck virus* [CCFV]) (Table 1.4; Oh et al., 1995). However, satC attenuates symptoms associated with CPm (Figure 1.6B) while diG had no effect on symptoms of CPm (Table 1.4; Kong et al., 1997a; 1997b; Wang and Simon, 1999).

Table 1.4 Symptom modulation of satC and diG in the presence of CP provided by wt or

mutant TCV

	TCV	TCV-CP$_{CCFV}$	CPm
satC	Intensification	Attenuation	Attenuation
diG	Intensification	Attenuation	No effect

Determinants for the differential symptom modulation of satC and diG are localized to their 3'-terminal regions that certain six positional differences when compared with the TCV genomic RNA (Figure 1.7A; Kong et al., 1997a). Further studies indicated that the positions 5 and 6 located within the 3'-terminal hairpin structures (Figure 1.7B) are essential for symptom modulation (Wang and Simon, 2000). Gel mobility shift assays of CP binding to RNA fragments showed that the affinity of CP for the 3'-terminal hairpin of diG is 2-fold greater than for that of the hairpin of satC or a nonviral RNA fragment (Wang and Simon, 2000). It was determined that the ability to attenuate symptoms was correlated with weakened binding of CP to the 3'-terminal hairpin structure (Wang and Simon, 2000).

In this dissertation, I report my findings about mechanisms underlying symptom modulation by satC and CP. In Chapter II, I show that satC and CPm3 symptom intensification correlates with wt levels of CP and decreased levels of virion accumulation. In Chapter III, I report the cloning and analysis of vsRNAs derived from TCV and satC. In Chapter IV, I describe a novel RNA tracking system that reports on TCV location within an infected plant.

Figure 1.7 Sequences and structures of the 3' ends of satC, diG, and the TCV genomic RNA. (A) Alignment of the 3'-end sequences of satC, diG, and TCV. Only differences among the RNAs are shown. The six positional differences are shaded. Short lines indicate absence of the nucleotides in satC and diG when compared with TCV. (B) Computer prediction of the 3'-terminal secondary structures of satC, diG, and TCV (Zuker, 2003). The 3'-terminal structure of satC is supported by solution structure probing results (Zhang et al., 2004). Nucleotides in position 5 and 6 are underlined. V, location of the absent position 5 sequence in satC.

A

257

satC 5'… ACUAGUGCUCUCUGGGUAACCACUAAAAUCCCGAAAGGGUGGGCUUUGGGG
diG   G   C
TCV   U   G   U

Circled: ① ②

356

satC ACCCUCCGAACCAAUAGAUAGCCUCCCUCCU —— CGGACGGGGGGGCCUGCCC-OH
diG   U   A   C   CG—   GG
TCV   U   A   C   CGCG   GG

Circled: ③ ④ ⑤ ⑥

B

TCV

⑤ C
  G   G
  C   C
  U   G
    C G
    C G ⑥
    C G
    C G
    C G
    C G
    U G
    C G
    C G
5'…. AUAG CCUGCCC-OH

satC

⑤ C
    U   G
    C   G
    C   A
    U   C ⑥
     C G
     C G
     C G
     U G
     C G
     C G
5'…. AUAG CCUGCCC-OH

diG

⑤ G
  C   C
  U   G
    C G
    C G
    U G ⑥
    C G
    C G
    C G
    U G
    C G
    C G
5'…. AUA G CCUGCCC-OH
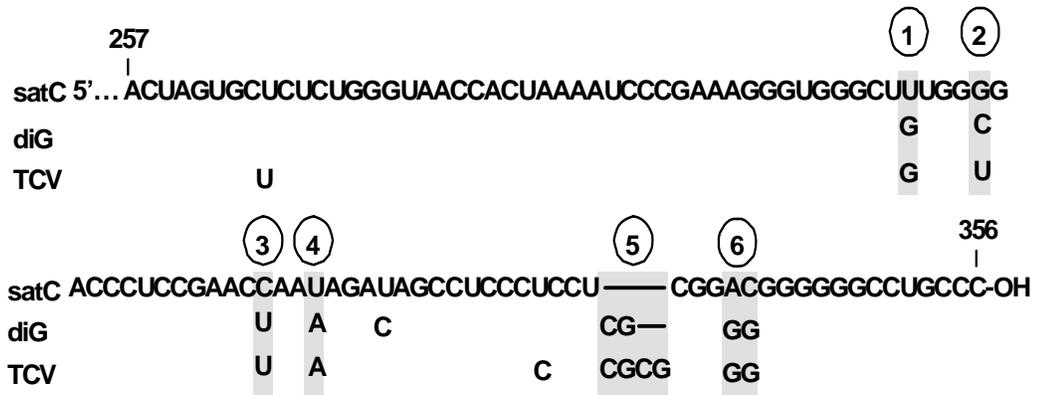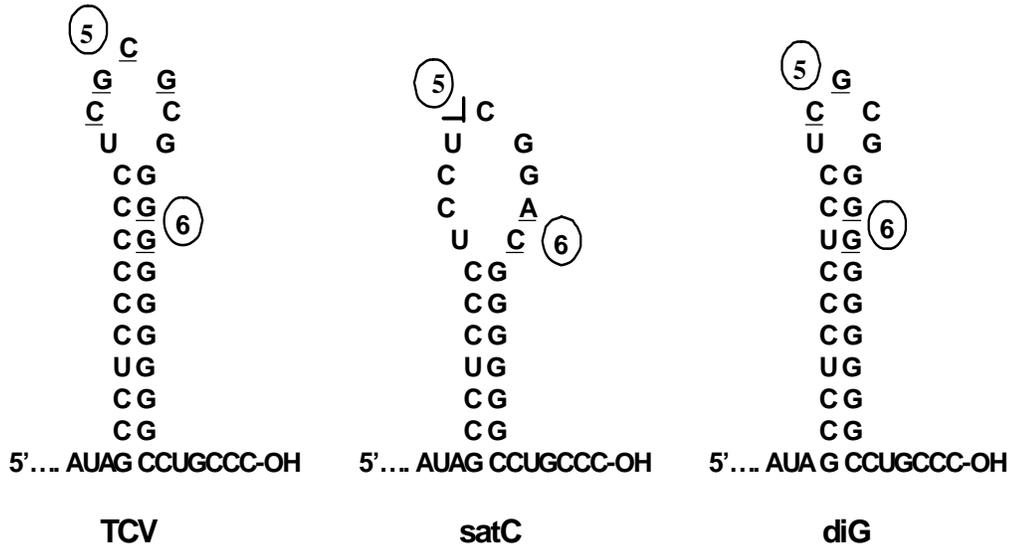
CHAPTER II

ENHANCED PATHOGENESIS ASSOCIATED WITH A VIRULENT TCV MUTANT OR SATELLITE RNA C CORRELATES WITH REDUCED VIRION ACCUMULATION AND ABUNDANCE OF FREE COAT PROTEIN

Introduction

Viral infection often affects a plant's developmental regulation, resulting in diverse symptoms. Disease symptoms can be enhanced by the presence of unrelated viruses (Hull, 2002; Scheets, 1998), which generally involves an increase in the accumulation of one or both viruses. In addition, viral symptoms can be modulated by the presence of unrelated, or partially related satRNAs, which require helper virus-encoded products for replication and systemic spread (Roossinck et al., 1992). While most satRNAs have no effect on, or attenuate the symptoms of their helper virus, symptom enhancement by satRNAs can occur. For example, CMV satRNA D expresses necrotic symptoms in the absence of any helper virus by inducing programmed cell death (Xu and Roossinck, 2000). The satRNA of *Panicum mosaic virus* increases virus titer and enhances systemic spread of the virus allowing the virus to invade previously restricted tissues (Scholthof, 1999).

As described in Chapter I, satC, a non-coding molecule consisting of nearly full-length satD at its 5' end and two TCV segments at its 3' end, intensifies symptoms associated with TCV. Avirulent satD, in contrast, has no discernable effect on symptoms

(Simon and Howell, 1986). In *Arabidopsis thaliana*, satC changes the stunting and delayed bolting symptoms due to infection by TCV alone to lethal overall necrosis (Simon et al., 1992). TCV symptoms can also be modulated by alterations in its 38 kDa CP (Heaton et al., 1991; Wang and Simon, 1999). The CP is involved in a wide variety of functions required for successful host invasion including (i) virion assembly; (ii) systemic movement, but not cell-to-cell movement, in *Arabidopsis thaliana* and *Brassica campestris* and systemic and cell-to-cell movement in other hosts such as *Nicotiana benthamiana* (Hacker et al., 1992); (iii) elicitation of the salicylic acid-dependent defense response in *Arabidopsis* ecotype Dijon (Kachroo et al., 2000); (iv) repression of satC replication (Kong et al., 1997a); (v) suppression of an early step in VIGS (Qu et al., 2003; Thomas et al., 2003); and (vi) modulation of satC-associated symptoms (Wang and Simon, 1999).

As described in Chapter I, when *Arabidopsis* was inoculated with CPm3, which expresses wt levels of a mutant CP with two additional amino acids (glutamic acid and threonine) at the N-terminus (Figure 1.5), symptoms were greatly intensified compared to wt TCV-induced symptoms. The severe symptoms induced by CPm3 appear to be identical to those associated with the presence of satC in wt TCV infections. I now report that enhanced symptoms attributed to either the presence of satC or TCV expressing wt levels of mutant CP with two N-terminal additional amino acids is correlated with a substantial reduction in the level of detectable virions.

Materials and Methods

DNA constructs and plant materials

The plasmids pTCV66, pT7C+, and pT7D+, which contain a T7 RNA polymerase promoter upstream of wt full-length plus-strand sequence of TCV, satC, and satD, respectively, were previously described (Oh et al., 1995; Song and Simon, 1994). CPm, CPm2, and CPm3 are TCV mutants containing base changes in or near the CP gene translation initiation site (Figure 1.5; Wang and Simon, 1999). C56G and Cm5 are satC mutants with mutations in the 3'-terminal hairpin (Wang and Simon, 1999; Stupina and Simon, 1997). All plasmids were linearized with *Sma*I and subjected to in vitro RNA transcription using T7 polymerase to generate RNA transcripts for inoculation of plants or protoplasts. *Arabidopsis* DCL2- and DCL3-defective plants (*dcl2-1* and *dcl3-1,* respective*)* were kindly provided by Dr. James C. Carrington.

Large-scale plasmid DNA isolation

Bacteria (*E. coli*) were grown in 250 ml L-broth (LB) culture at 37°C for 16 hours or overnight with continuous shaking. The cells were collected by centrifugation in a Sorvall GSA rotor at 6000 rpm for 10 minutes and resuspended in 2.5 ml of suspension buffer (25% sucrose and 50 mM Tris-HCl, pH 7.5). To remove the cell wall, 0.4 ml of freshly prepared 10 µg/µl lysozyme was added. The mixture was gently swirled and incubated on ice for 10 min, followed by addition of 0.7 ml of 0.5 M EDTA (pH 8.0). The mixture was incubated again on ice for 10 minutes, followed by addition of 5.3 ml of lysis buffer (0.1% Triton X-100, 62.5 mM EDTA, pH 8.0, and 50 mM Tris-HCl, pH 8.0).

After incubation at 37°C for 10 minutes or 42°C for 5 minutes, the mixture was centrifuged in a Sorvall SS34 rotor at 17,000 rpm for 20 minutes. The supernatant was collected into a 15 ml centrifuge tube and 8.8 g of CsCl and 200 μl of ethidium bromide (10 mg/ml) were added. The mixture was adjusted to a volume of 12 ml with distilled H_2O and then transferred into a quick-seal tube (Beckman, 16 mm X 76 mm). After centrifugation at 20°C in a VTi 65.1 rotor (Beckman) at 65,000 rpm for 4.2 hours or at 45,000 rpm for 12 hours, the lower DNA band was recovered with a 5 ml syringe and extracted 3 times with NaCl-saturated isopropanol. The solution was diluted with 2 volumes of distilled H_2O and then mixed with 6 volumes (original volume) of 100% ethanol. The mixture was incubated at -20°C for at least 2 hours and then centrifuged in a Sorvall SS34 rotor at 10,000 rpm for 10 minutes. The DNA pellet was redissolved in 0.4 ml of distilled H_2O and then transferred to a 1.5 ml eppendorf tube. The dissolved DNA was precipitated with 2.5 volume of 5 M NaOAc/ethanol (1:25), washed with 70% ethanol, dried, and dissolved in an appropriate amount of distilled H_2O. The concentration of DNA was estimated by measuring the absorbance at 260 nm.

In vitro RNA transcription using T7 polymerase

Plasmid DNA was linearized with the appropriate restriction enzyme, extracted with phenol/chloroform, precipitated with 2.5 volume of 5 M NaOAc/ethanol (1:25), washed with 70% ethanol, dried, and dissolved in distilled H_2O. The linearized DNA template (8 μg) was mixed with 6 μl of dithiothreitol (DTT), 12 μl of 5 mM each of ATP, CTP, GTP, UTP, 12 μl of 5X T7 buffer (125 mM NaCl, 40 mM $MgCl_2$, 2mM spermidine, 40 mM Tris-HCl, pH8.0), 60 units of RNAsin (Invitrogen), 80 units of T7

polymerase (Invitrogen), and distilled H_2O to get a final volume of 60 µl. The mixture was incubated at 37°C for 1 hour (genomic RNA) or 2 hours (satRNA).

The synthesized RNA transcripts were directly used for inoculation of plants. For inoculation of protoplasts, the RNA transcripts were extracted with phenol/chloroform, precipitated with 2.5 volume of 5 M NH$_4$OAc (pH5.3)/isopropanol (1:5), washed with 70% ethanol, and dissolved in distilled H_2O. Plus-strand transcripts of TCV, satC, and satD were synthesized using T7 polymerase from *Sma*I-linearized pTCV66, pT7C+, and pT7D+, respectively (Oh et al., 1995; Song and Simon, 1994).

Plant growth and inoculation

Arabidopsis thaliana plants (ecotype Col-0) were grown in a growth chamber at 20°C under a 16-hour light/dark cycle as described by Li and Simon (1990). The oldest leaf pair of seedlings at the 6 to 8 leaf stage was mechanically inoculated with 2 µl (per leaf) of inoculation buffer containing plus-strand TCV RNA transcripts (0.15 µg/µl) with or without satC transcripts (0.015 µg/µl). The inoculation buffer contains 0.05 M glycine, 0.03 M K$_2$HPO$_4$, pH 9.2, 1% Bentonite (clean), and 1% Celite. Plants were photographed at 14 and 21 dpi. Mock plants were treated with inoculation buffer.

RNA extraction from *Arabidopsis* leaves

One gram of uninoculated leaves from infected *Arabidopsis* plants was ground in liquid nitrogen in a 50 ml beaker. Leaf powder was transferred into a 1.5 ml eppendorf tube and extracted with 0.5 ml of phenol and 0.5 ml of extraction buffer containing 0.2 M Tris-HCl, pH 9.0, 0.4 M LiCl, 1% SDS, and 25 mM EDTA. After centrifugation at

13,200 rpm for 5 minutes at 4°C, the aqueous phase was extracted once more with 0.5 ml of phenol/chloroform (1:1) and precipitated with 2.5 volume of 5 M NaOAc/ethanol (1:25). The pellet was resuspended in 300 μl of 2 M LiCl and vortexed well. The solution was then centrifuged at 13,000 rpm for 5 minutes at 4 °C and the pellet was dissolved in 300 μl of distilled H_2O. The RNA was precipitated using 2.5 volume of 5 M NaOAc/ethanol (1:25), rinsed with 70% ethanol, dried, dissolved in 40 μl H_2O, and stored at -80°C.

Preparation and inoculation of protoplasts

Protoplasts were prepared from callus cultures of *Arabidopsis thaliana* ecotype Col-0. The calli were produced from sterilized seeds placed on 1% MS (Murashige-Skoog salts, Gibco BRL) agar media (pH 5.8) supplemented with 2 mg/ml kinetin, 2 mg/ml 2, 4-D (2, 4-dichlorophenoxyacetic acid, Sigma), and 1X vitamins/glycine containing 1 μg/ml nicotinic acid, 10 μg/ml thiamine HCl, 1 μg/ml pyrodoxine, 0.1 mg/ml myoinositol, and 4 μg/ml glycine. The calli were incubated in a growth chamber at 20°C under 35 μmol m^{-2} sec^{-1} lights with a cycle of 16-hour light and 8-hour-dark and passaged every 3 weeks.

To prepare protoplasts, calli in the 4th passage were collected and soaked in 40 ml of 0.6 M mannitol at 25°C for 20 minutes with shaking. The calli were recovered by centrifugation (Beckman GPR-type swinging bucket) at 930 rpm for 5 minutes at 4°C, and then suspended in 50 ml of freshly prepared protoplast isolation medium (PIM, pH 5.8) containing 0.5 g of cellulase (11,900 U/g) and 0.1 g of pectinase (3,140 U/g) (Calbiochem, La Jolla, CA). One liter of PIM contains 1 ml of 1000X vitamin stock (1

mg/ml thiamine-HCl, 0.5 mg/ml pyridoxine-HCl, 0.5 mg/ml nicotinic acid, and 0.1 g/ml myo-inositol), 0.5 ml of 2000X hormone stock (0.4 mg/ml 2, 4-D, 0.4 mg/ml kinetin, and 50 mM KOH), 4.3 g of MS plant salts, 0.1 M sucrose, 3 mM MES, 5 mM $CaCl_2$, and 0.5 M mannitol. The calli/PIM/enzyme mixture was incubated at 26-28°C in the dark for 4 hours with shaking at 75 rpm. The solution was filtered through a 53-μm nylon mesh (Small Parts, Miami Lakes, FL), followed by centrifugation at 930 rpm for 5 minutes at 4°C. The precipitated protoplasts were washed 3 times with 20 ml of 0.6 M mannitol (pre-cooled on ice). The number of cells was calculated using a microscope and hoemocytometer.

Protoplasts (~ 5 X 10^6 cells) in a volume of 100 μl were swirled with 20 μl of TCV genomic RNA transcripts (1 μg/μl), 2 μl of satRNAs (1 μg/μl), 8 μl of 1 M $CaCl_2$, 400 μl of distilled H_2O, and 2.17 ml of 50% PEG (prepared in 50 mM Tris-HCl, pH 7.5). The mixture was incubated at 25°C for 30 seconds, followed by addition of cold 0.6 M mannitol/1 mM $CaCl_2$ and incubated on ice for 20 minutes. The protoplasts were collected by centrifugation at 930 rpm for 5 minutes at 4°C. After washing 3 times with 25 ml of cold 0.6 M mannitol/1 mM $CaCl_2$, protoplasts were resuspended in protoplast culture medium (PCM, pH 5.8) and incubated at 25°C for 40 hours in the dark. One liter of PCM contained 1 ml of 1000X vitamin stock (1 mg/ml thiamine-HCl, 0.5 mg/ml pyridoxine-HCl, 0.1 g/ml myo-inositol, and 0.5 mg/ml nicotinic acid), 0.5 ml of 2000X hormone stock (0.4 mg/ml 2, 4-D, 0.4 mg/ml kinetin, and 50 mM KOH), 4.3 g of MS plant salts, 0.1 M sucrose, 0.4 M mannitol, and 3 mM MES.

Total RNA isolation from protoplasts

Protoplasts in 1 ml of PCM (~1.67 X 10^6 cells) were collected into a 1.5 ml eppendorf tube at 40 hours postinoculation (hpi) and resuspended in 200 μl of extraction buffer (50 mM Tris-HCl, pH 7.5, 5 mM EDTA, 1% SDS, and 100 mM NaCl), followed by addition of 200 μl of phenol/chloroform (1:1) and vigorous vortexing. The mixture was then centrifuged at 13,000 rpm for 5 minutes at 4°C. The supernatant was precipitated with 2.5 volumes of 5 M NaOAc/ethanol (1:25), and washed with 70% ethanol. Pellets were dissolved in 25 μl of distilled water.

RNA gel blot analysis

Four micrograms of total RNA from plants or protoplasts was denatured by heating for 5 minutes at 65°C in 50% formamide and then subjected to electrophoresis through nondenaturing 1.2% agarose gels for detection of viral and subviral RNAs or denaturing 8M urea-5% polyacrylamide gels for detection of vsRNAs and LssRNAs. The gel was treated for 1 hour in 6% formaldehyde with gentle shaking, and then soaked in 10X SSC containing 0.15 M NaCl and 0.015 M sodium citrate for 25 minutes followed by transferring of the RNAs to a NitroPlus membrane (Micron Separations Inc., Westboro, MA). The blot was placed on a UV light box (310 nm, Fotodyne Inc.) for 5 minutes to crosslink the RNA and then dried at 80°C for 10 minutes.

Oligo13 and Oligo16, which are oligonucleotides complementary to either positions 3950-3970 of TCV genomic RNA and positions 250-269 of satC or positions 44-59 of satD (Table 2.1), were labeled with [γ-^{32}P] ATP using T4 polynucleotide kinase and used as probes in the gel blotting analysis of TCV genomic RNA, satC, and satD.

Table 2.1 Oligonucleotides used in Chapter II

Application	Name	Position[a]	Sequence	Polarity[b]
RNA gel blotting	Oligo13	250-269	5'-GTTACCCAAAGAGCACTAGTT	_
	Oligo16	44-59	5'-AGGGCAATGGGCGTCC	_
	OligoC3	206-356	5'-GGGCAGGCCCCCCGTCCGAGGAGGGA GGCTATCTATTGGTTCGGAGGGTCCCCA AAGCCCACCCTTTCGGGATTTTAGTGGT TACCCAGAGAGCACTAGTTTTCCAGGCT AATGCCCGCAGCTAGACGGTGCTGCCGC CGTTTTTGGTCCCATTTACCCTTTGGCTG GAGGGTCTGGGATTCTTTT	_
	OligoCPr	324-356	5'-GGGCAGGCCCCCCGTCCGAGGAGG GAGGCTATC	_
	OligoCPrloop	332-346	5'-CCCGTCCGAGGAGGG	_

[a] Coordinates correspond to those of satC. Oligo13 also corresponds to positions 3950-3970 of TCV genomic RNA. Oligo16 corresponds to positions of satD.

[b] "-"refers to complementarity with satC or satD plus strands.

52

The [α-^{32}P] UTP-labeled full-length TCV plus or minus strands, full-length satC minus strands, or minus-strand satC fragments in different sizes including OliogC3, OligoCPr, and OligoCPrloop (Table 2.1) were prepared using T7 polymerase and used as probes in the blotting analysis of virus-specific small RNAs. Blot prehybridization for 1 hour and hybridization for 2 hours at 42°C were performed in a hybridization buffer containing 5X SSPE, 10X Denhardt's reagent, 0.2% SDS, 0.2 mg/ml freshly denatured salmon sperm DNA, and 50% formamide (every 1% of formamide reduces the Tm by 0.7^{o}C). After hybridization, the blot was washed in a high salt solution containing 6X SSPE and 0.1% SDS for 12 minutes, then washed in low salt solution containing 0.1X SSPE and 0.1% SDS for 20 and 15 minutes, respectively. The blot was covered with a saran wrap and subjected to autoradiography. One liter of 20X SSPE contains 175.3 g NaCl, 27.6 g NaH$_2$PO4, 40 ml of 0.5 M EDTA (pH 8.0) and is adjusted to pH 7.4 using 10 M NaOH. The blots can be stripped in 200 ml of stripping buffer at 65 ^{o}C for 2 hours, and then rehybridized to new probes. Two hundreds of milliliters of the stripping buffer contain 1 ml of 1M Tris-HCl, pH 8.0, 0.5 ml of 0.5 M EDTA, 0.2 ml of 10X Denhardt's reagent, and 198.3 ml of ddH$_2$0.

Protein isolation from protoplasts and gel blot analysis

Protoplasts in 1 ml of PCM (~1.67 X 10^6 cells) were collected in a 1.5 ml eppendorf tube at 40 hpi and resuspended in 30 µl of protein analysis buffer containing 30 mM Tris-HCl, pH 6.8, 2.5% β-mercaptoethanol, 1.5% SDS, and 5% glycerol, followed by vortexing for 5 minutes. The mixture was centrifuged at 13,000 rpm for 5 minutes to collect the supernatant containing proteins.

Total proteins were separated on a 12% SDS-PAGE gel in a running buffer (pH 8.3) containing 50 mM Tris base and 38 mM glycine, and transferred to a NitroPlus membrane (Micron Separations Inc.). Protein blot analysis was performed using the anti-TCV CP polyclonal antibody generated in rabbits injected with purified TCV CP. The anti-CP antibody and the second antibody (anti-rabbit IgG horseradish peroxidase; Gibco BRL) were used in 1:5000 and 1:7500 dilutions, respectively. Dilutions were made in phosphate buffered saline (PBS) containing 6% milk (w/v). Chemiluminescent staining was performed with the Western Lighting Chemiluminescence Reagent kit (Perkin Elmer Life Sciences) using the method as recommended by the manufacture. Membrane incubated with the substrate was covered with plastic saran wrap and exposed to an X-ray film for 60-90 seconds before developing the film.

Virion isolation from protoplasts and gel blot analysis

Protoplasts in 1 ml of PCM (~1.67 X 10^6 cells) were collected in a 1.5 ml eppendorf tube at 40 hpi and resuspended in 200 μl of 0.2 M NaOAc, pH 5.2, followed by addition of 30 µl of sterile glass beads (0.1-0.2 mm in diameter). The mixture was vortexed for three 15-second intervals and placed on ice between each interval. The aqueous phase was recovered by centrifugation at 13,000 rpm for 1 minute. The solid phase was re-extracted twice with 200 μl of 0.2 M NaOAc, pH 5.2. The aqueous phases were combined and incubated on ice for 1 hour, followed by centrifugation at 13,000 rpm for 2 minutes at 4°C. The supernatant was mixed with 1/4 volume of 40% polyethylene glycol (PEG, MW 8000)/1 M NaCl. The mixture was incubated on ice overnight, followed by

centrifugation at 13,000 rpm for 1 hour. The pellet (virions) was dissolved in 30 µl of 10 mM NaOAc, pH 5.5, stored at 4°C.

For virion blotting analysis, 1 µl of virions were separated on a 1% agarose gel prepared in 50 mM Tris base/ 38 mM glycine (pH 8.3). The gel was soaked in 50 mM NaOH for 20 minutes and then in 0.2 M NaOAc pH 5.5 for 20 minutes before blotting to a NitroPlus membrane (Micron Separations Inc., Westborough, MA). Virion blotting analysis was performed using the same antibody and method as those used for the protein gel blotting described above.

Results

Symptom intensification of satC or CPm3 correlates with wt levels of CP and decreased accumulation levels of virion

Since *Arabidopsis* plants infected with CPm3 or wt TCV and satC expressed similar severe symptoms, it seemed possible that the presence of satC might be functionally equivalent to the presence of wt levels of mutant CP that contained an additional glutamic acid and threonine residue at the N-terminus (Figure 1.5). Therefore, I examined if wt levels of mutant CP produced by CPm3 affected the accumulation of virions, and whether virion and CP levels could be correlated with enhanced symptoms. An intermediate construct was included in this study (CPm2), which contained only a single additional amino acid (threonine) at the N-terminus (Figure 1.5). Like CPm3, CPm2 CP was translated from the wt initiation codon and was thus predicted to produce wt levels of a mutant CP.

To compare symptoms induced by mutant and wt TCV in the presence or absence of satRNAs, *Arabidopsis* ecotype Col-0 plants were inoculated with different virus combinations and photographed at 14 and 21 dpi (Figure 2.1). As previously described, wt TCV caused delayed bolting and reduced leaf size. Symptoms were enhanced by coinfection with satC to a spreading necrosis that killed the plants by 21 dpi. The avirulent satD had no discernable effect on symptoms. Plants infected with CPm2 appeared very similar to wt TCV infected-plants at 14 and 21 dpi, and addition of satC, but not satD, intensified symptoms to a lethal necrosis by 21 dpi (Figure 2.1). In contrast, CPm3, in the absence or presence of satC or satD, displayed severe symptoms that were discernable at 14 dpi, and very similar to symptoms produced by wt TCV in the presence of satC at 21 dpi. The symptom modulation by TCV CP and satC is listed in Table 2.2.

To examine virion and CP levels produced by TCV, CPm2 and CPm3 in the presence or absence of satC, protoplasts were prepared from callus cultures of *Arabidopsis* ecotype Col-0 and inoculated with transcripts of TCV genomic RNA alone or together with transcripts of satC or the avirulent satD. Protoplasts inoculated with TCV, CPm2 and CPm3 accumulated similar levels of CP (Figure 2.2, compare CP panel, lanes 1, 4 and 7). CPm3, unlike CPm2, did not generate detectable virions (Figure 2.2, lanes 4 and 7), indicating that the two additional amino acids at the N-terminus of the CP affect virion assembly or stability in host cells. Unexpectedly, the presence of satC in wt TCV infections also had a substantial effect on virion levels. Coinoculation of protoplasts with satC reduced virion levels below detection when the helper virus was wt TCV and by 94% when associated with CPm2 (Figure 2.2, virion panel, lanes 2 and 5). In contrast, virion accumulation was not reduced in the presence of avirulent satD (Figure 2.2, virion

Table 2.2 Summary of symptom modulation by the TCV CP and satC

Constructs	CP sequences[a]	CP levels	Symptom severity	Virion levels[b]	Free CP levels
wt TCV	MENDPR	high	mild	high	intermediate
CPm	M**ET**ENDPR	moderate	mild	low	Moderate (10%)
CPm2	M**T**ENDPR	high	mild	intermediate	moderate
CPm3	M**ET**ENDPR	high	severe	ND	high
wt TCV+C	MENDPR	high	severe	ND	high
CPm+C	M**ET**ENDPR	moderate	30% mild 70% symptomless	low	moderate
CPm2+C	M**T**ENDPR	high	severe	low	high
CPm3+C	M**ET**ENDPR	high	severe	ND	high

[a] Bold amino acid residues denote changes in the N-terminus of the TCV CP.

[b] ND, not detectable.

Figure 2.1 Symptoms of Arabidopsis plants inoculated with either TCV, CPm2 or CPm3 with and without satC or satD. Upper plants were photographed at 14 dpi and lower plants were photographed at 21 dpi. Plants labeled "Mock" were treated with infection buffer alone.

MOCK TCV TCV +C TCV +D CPm2 CPm2 +C CPm2 +D CPm3 CPm3 +C CPm3 +D
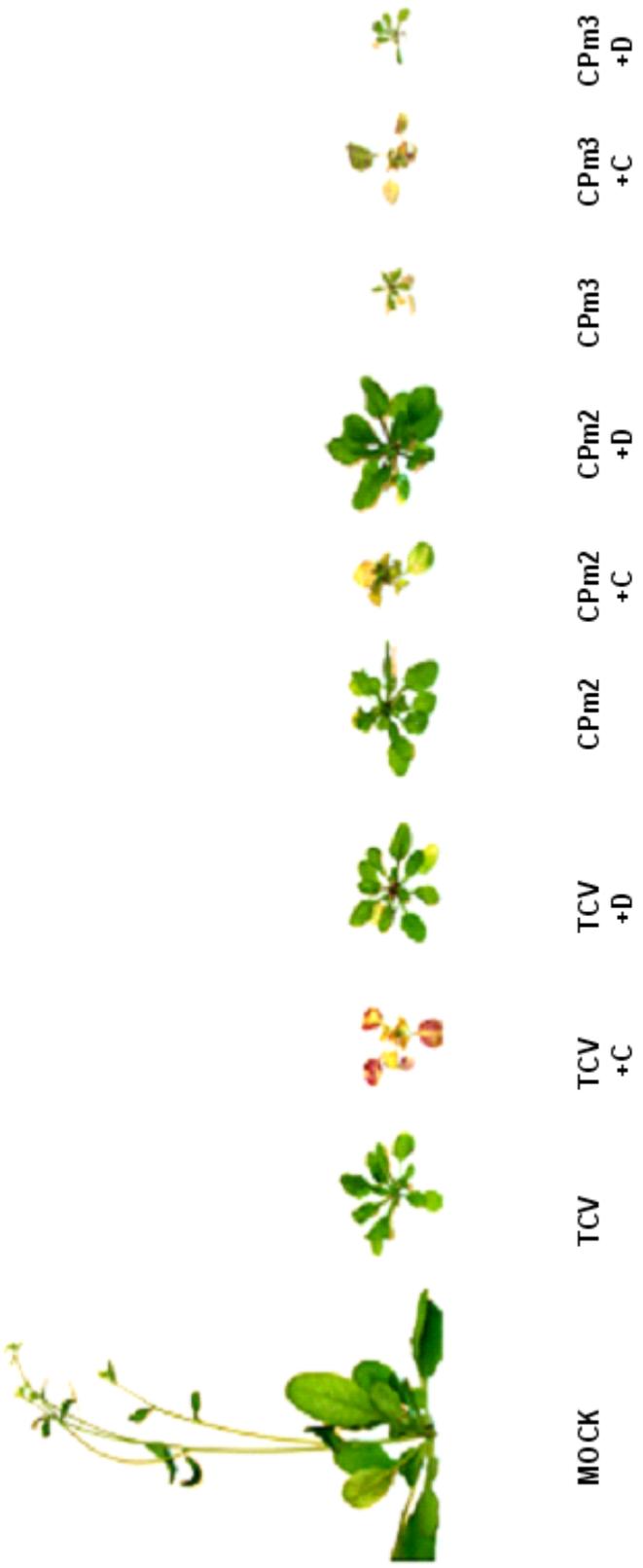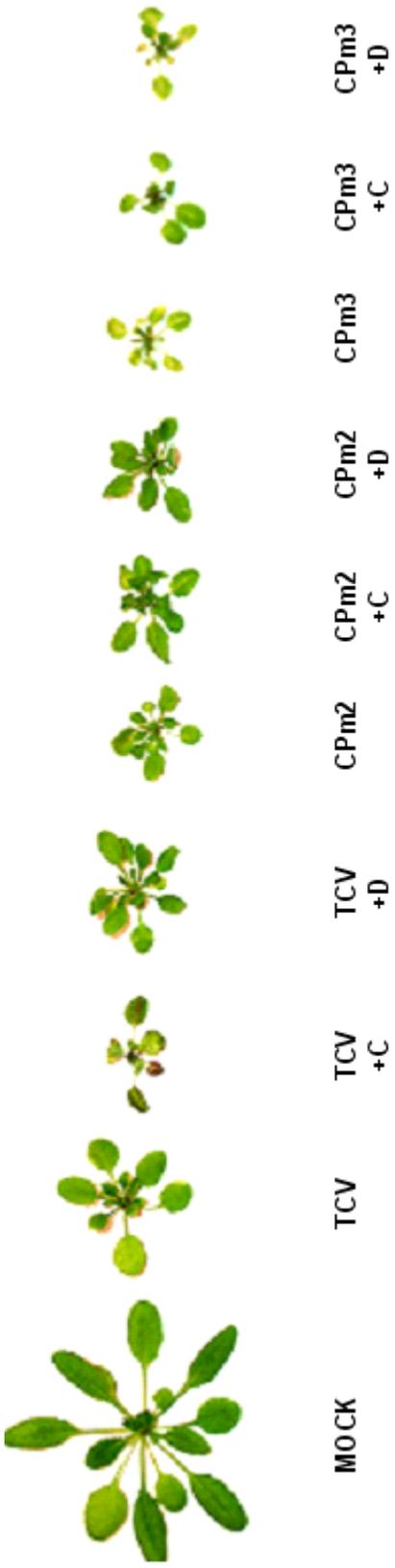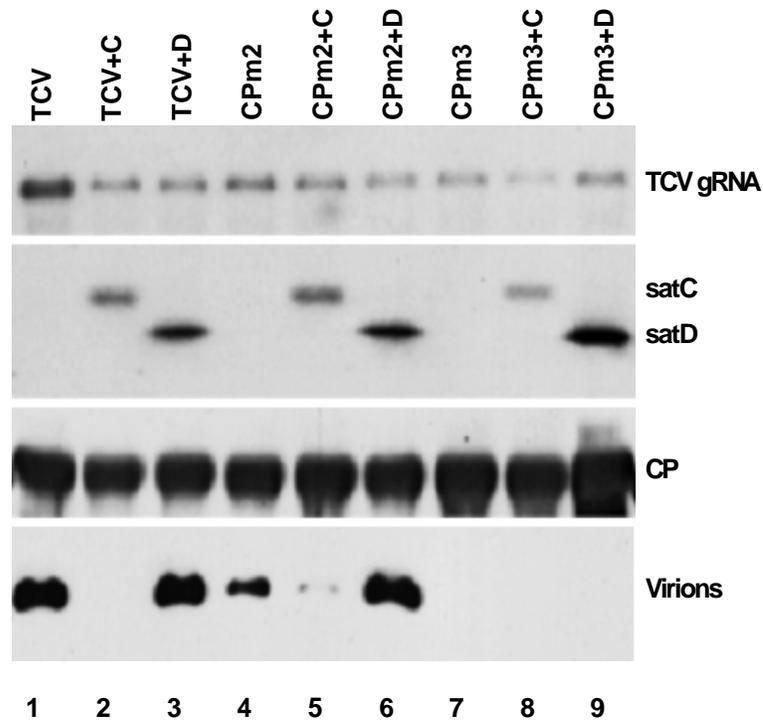
Figure 2.2 Effect of different virus and satRNA combinations on CP and virion accumulation in protoplasts. *Arabidopsis* protoplasts were inoculated with wt TCV or mutant TCV transcripts alone or together with satC or satD transcripts. Total RNA, proteins and virions were extracted at 40 hpi. TCV genomic RNA (TCV gRNA) and satRNAs were detected by RNA gel blot analysis using oligonucleotide probes complementary to both TCV and satC or satD. CP and virions were subjected to electrophoresis on SDS-PAGE gels and detected by chemiluminescence following treatment with anti-TCV CP antibody.

panel, lanes 3 and 6). While the levels of TCV genomic RNA detected in this particular experiment were higher than normally found, the reduced levels of virions associated with the presence of satC or CPm3 is highly reproducible (data not shown). This result demonstrates a novel correlation between severe symptoms in *Arabidopsis* and reduced levels of virions.

Increased levels of free TCV CP correlate with decreased levels of vsRNAs

As described above, CP alteration in CPm3 or the presence of satC interfered with virion accumulation, but did not detectably affect the total levels of CP. This would increase the amount of free CP, enhancing the ability of the virus to suppress RNA silencing since TCV CP is the silencing suppressor (Qu et al., 2003; Thomas et al., 2003). To examine if the additional free CP found with satC or CPm3 inhibits accumulation of vsRNAs, total RNAs were isolated from *Arabidopsis* plants infected with buffer (Mock), TCV, TCV along with satC, or CPm3 at 7 or 9 dpi and levels of the virus-specific RNAs were examined.

As shown in the agarose gel (Figure 2.3A), TCV genomic RNA was not found in Mock plants (lane 1). The wt TCV genomic RNA accumulated to levels that were comparable to those of the 26S ribosomal RNA (lane 2). The presence of satC in wt TCV infections resulted in about a 40% reduction in TCV RNA levels (compare lanes 2 and 3 or lanes 5 and 6). While CPm3 accumulated less efficiently than TCV in protoplasts (Figure 2.2), it accumulated slightly more efficiently than TCV in plants at 7 and 9 dpi (compare lane 2 and 4 or lanes 5 and 7). This difference might be caused by the enhanced ability of the virus to suppress RNA silencing in the presence of the additional free CP

Figure 2.3 Accumulation of virus-specific RNAs in *Arabidopsis* plants infected with buffer (Mock), TCV alone, TCV along with satC, or CPm3. Total RNAs were isolated at 7 or 9 dpi. (A) Agarose gel analysis of the genomic RNA and satC accumulating in infected plants. The total RNAs were separated in a 1.2% agarose gel. Following electrophoresis, the gel was stained with ethidium bromide. Positions of the genomic RNA (gRNA) and satC are indicated. The 26S ribosomal RNA (rRNA) was used as a loading control. (B) RNA gel blot analysis of the small RNAs (21- to 40-nt) derived from the viral and subviral RNAs. The total RNAs were separated through a denaturing 5% polyacrylamide gel-8M urea. The 5S rRNA on the polyacrylamide gel stained with ethidium bromide (prior to gel blotting) was used as a loading control. The blot was hybridized to full-length TCV minus-strand RNA for analysis of small RNAs derived from plus-strand viral and subviral RNAs. satC-specific small RNAs (24- to 40-nt) are indicated with red asterisks. (C) The blot analyzed in B was stripped and then hybridized to full-length TCV plus-strand RNA for detection of the small RNAs derived from minus-strand viral and subviral RNAs.

A

gRNA
26S rRNA

satC

Mock	TCV	TCV+C	CPm3	TCV	TCV+C	CPm3
1	2	3	4	5	6	7

7 dpi   9 dpi

B

Mock   TCV   TCV+C   CPm3   TCV   TCV+C   CPm3

40 nt

24 nt

21 nt

5s rRNA

7 dpi   9 dpi

Probe: full-length TCV minus-strand RNA

C

Mock TCV TCV+C CPm3 TCV TCV+C CPm3

40 nt

24 nt

21 nt

7 dpi   9 dpi

Probe: full-length TCV plus-strand RNA
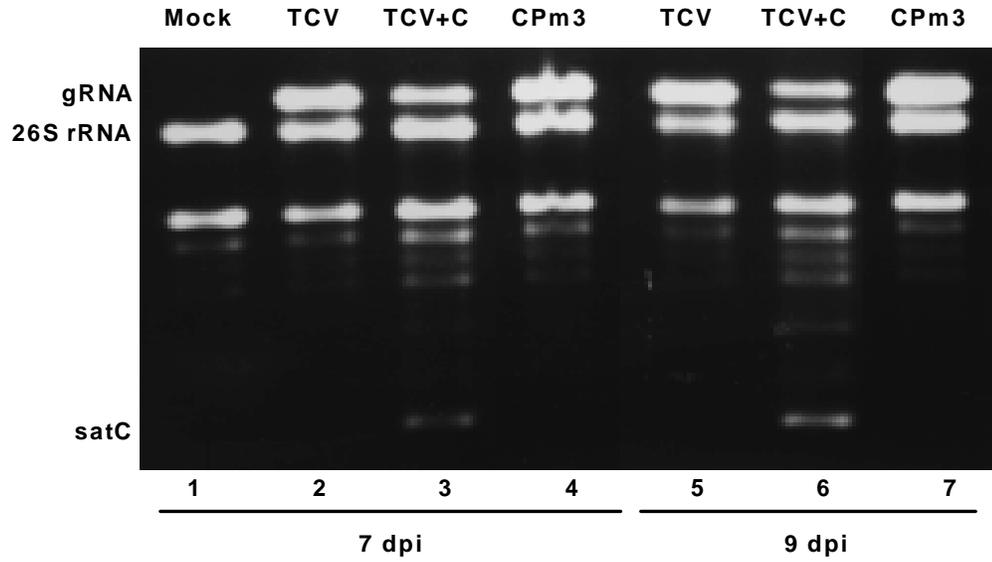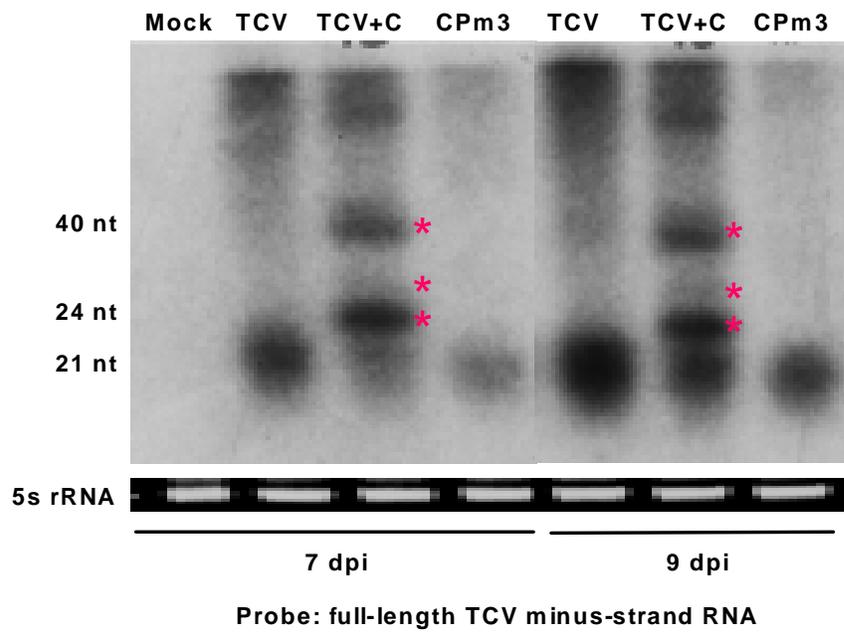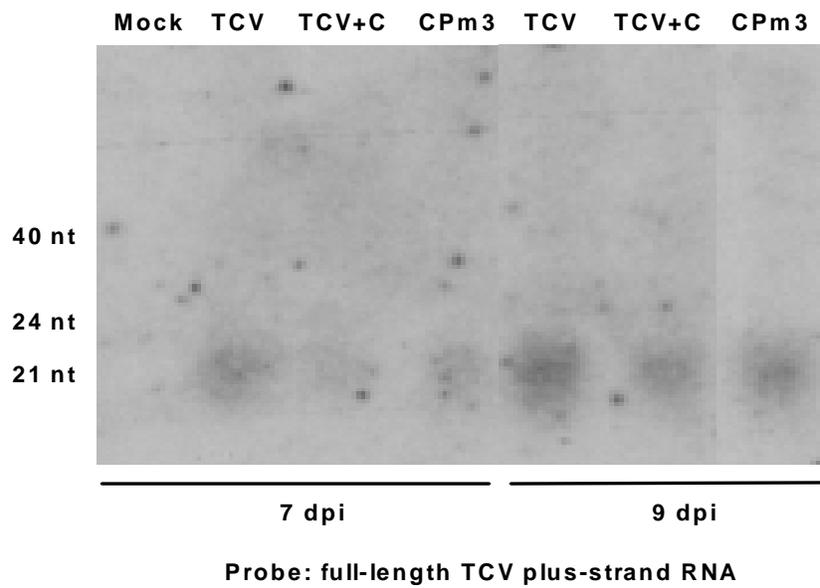
due to reduced virion accumulation in plants infected with CPm3. Enhanced silencing suppression would help the virus to invade new issues in plants, which is not available in protoplasts. The gel in Figure 2.3A also showed that the genomic and satC RNA levels were higher at 9 dpi than at 7 dpi.

The total RNAs were also separated through a denaturing 5% polyacrylamide gel-8M urea and vsRNAs derived from the viral RNAs were detected by RNA gel blot analysis using full-length TCV minus-strand RNA as probe. The RNA gel blot hybridization results indicated that ~21-nt plus-sense vsRNAs were generated in all infected plants except the Mock plants (Figure 2.3B). Levels of the vsRNAs were higher at 9 dpi than 7 dpi, possibly due to continuing accumulation of TCV in plants, which would provide more targets of RNA silencing. In plants infected with TCV along with satC, or CPm3, levels of the 21-nt vsRNAs were about 40% (at either 7 or 9 dpi) of those of the vsRNAs found in the TCV-infected plants. RNA gel blot analysis using full-length TCV plus- strand RNA as probe indicated that minus-sense vsRNAs were also generated with levels higher at 9 dpi than at 7 dpi (Figure 2.3C). The minus-sense vsRNAs found in plants infected with either TCV and satC or CPm3 accumulated to about 40% (at either 7 or 9 dpi) of the vsRNA levels in plants infected with TCV alone. Since CPm3 accumulated slightly more efficiently than TCV in plants as determined at 7 and 9 dpi (Figure 2.3A), the accumulation reduction of vsRNA derived from CPm3 (Figure 2.3B and C) suggested that increased amount of free CP resulted from virion accumulation repression might correlate with decreased vsRNA accumulation.

Small RNAs processed from the 3'-terminal hairpin of satC

Figure 2.3B shows that RNA species of 24- to 40-nt were found in plants infected with TCV along with satC, but not plants infected with TCV alone or CPm3. These small RNAs were different from the 21-nt vsRNAs in at least three aspects. They were (i) larger than the vsRNAs; (ii) satC-specific; and (iii) plus-sense since they were not detectable when TCV plus strand RNA was used as probe (Figure 2.3C). To determine which region of satC gives rise to these new larger single-stranded small RNAs (LssRNAs), total RNAs isolated from plants infected by TCV with or without satC at 7 dpi were analyzed by gel blotting using probes complementary to full-length satC plus-strands or different regions in satC plus strands: the 3'-end 151 nts, the 3'-terminal hairpin, or the loop region of the 3'-terminal hairpin (Figure 2.4A). As shown in Figure 2.4B-E, the LssRNAs were detectable by all of the probes with levels decreasing when shorter probes were used. The results indicate that at least some of these LssRNAs are processed from the loop region of the 3'-terminal hairpin of satC.

Analysis of the putative correlation between LssRNA accumulation and symptom modulation

As described in Chapter I, the ability of satC to attenuate symptoms requires that CP binds only non-specifically to its 3'-terminal hairpin structure since stronger binding to a modified 3'-terminal hairpin eliminated attenuation (Wang and Simon, 2000). To test if accumulation of LssRNAs from the 3'-terminal hairpin is related to symptom modulation, wt satC and a satC mutant, C56G, were examined in plants with TCV-CP$_{CCFV}$ or CPm providing CPs. C56G is satC containing the 3'-terminal hairpin of diG

Figure 2.4 Generation of LssRNA from the 3' end of satC. (A) Probes used in RNA gel blot analysis of LssRNAs. The full-length satC minus-strand RNA, OliogC3, OligoCPr, and OligoCPrloop are represented by lines of different colors. OliogC3, OligoCPr, and OligoCPrloop are complementary to the 3' 151 nts of satC, the 3'-terminal hairpin, and the loop region of the 3'-terminal hairpin, respectively. Sequence is shown in its plus-sense, 5'-to-3' orientation. Numbering is from the 5 end. (B) RNA gel blot analysis of the total RNAs isolated from plants infected with TCV alone (None) or together with satC (C) at 7 dpi. Full-length satC minus-strand RNA was used as probe. The 5S rRNA was used as a loading control. (C-E) The blot analyzed in (B) was stripped and then hybridized to probes as given in the Figure. Red asterisks indicate LssRNA species derived from satC.

A
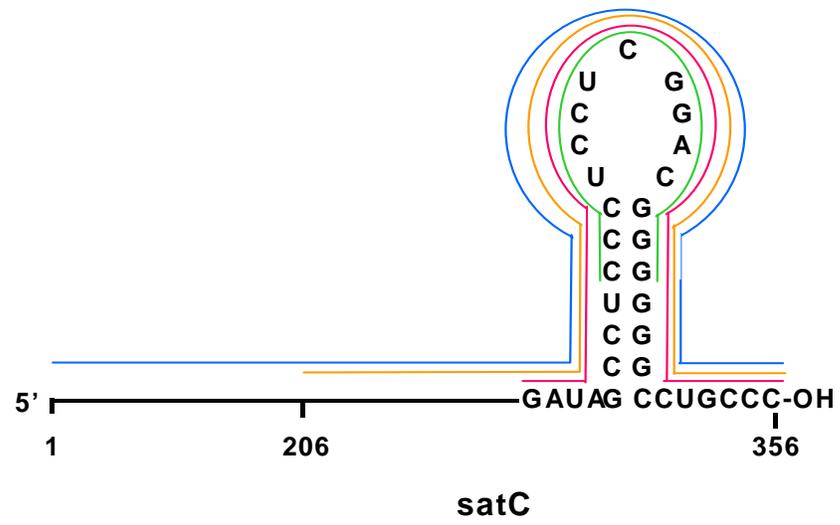
satC

full-length satC minus- strand RNA

OligoC3

OligoCPr

OligoCPrloop

B

None	C

40 nt

Probe: full-length satC
minus- strand RNA

24 nt

21 nt

5s rRNA

C

40 nt

Probe: OligoC3

24 nt

21 nt

D

40 nt

Probe: OligoCPr

24 nt

21 nt

E

40 nt

Probe: OligoCPrloop

24 nt

21 nt
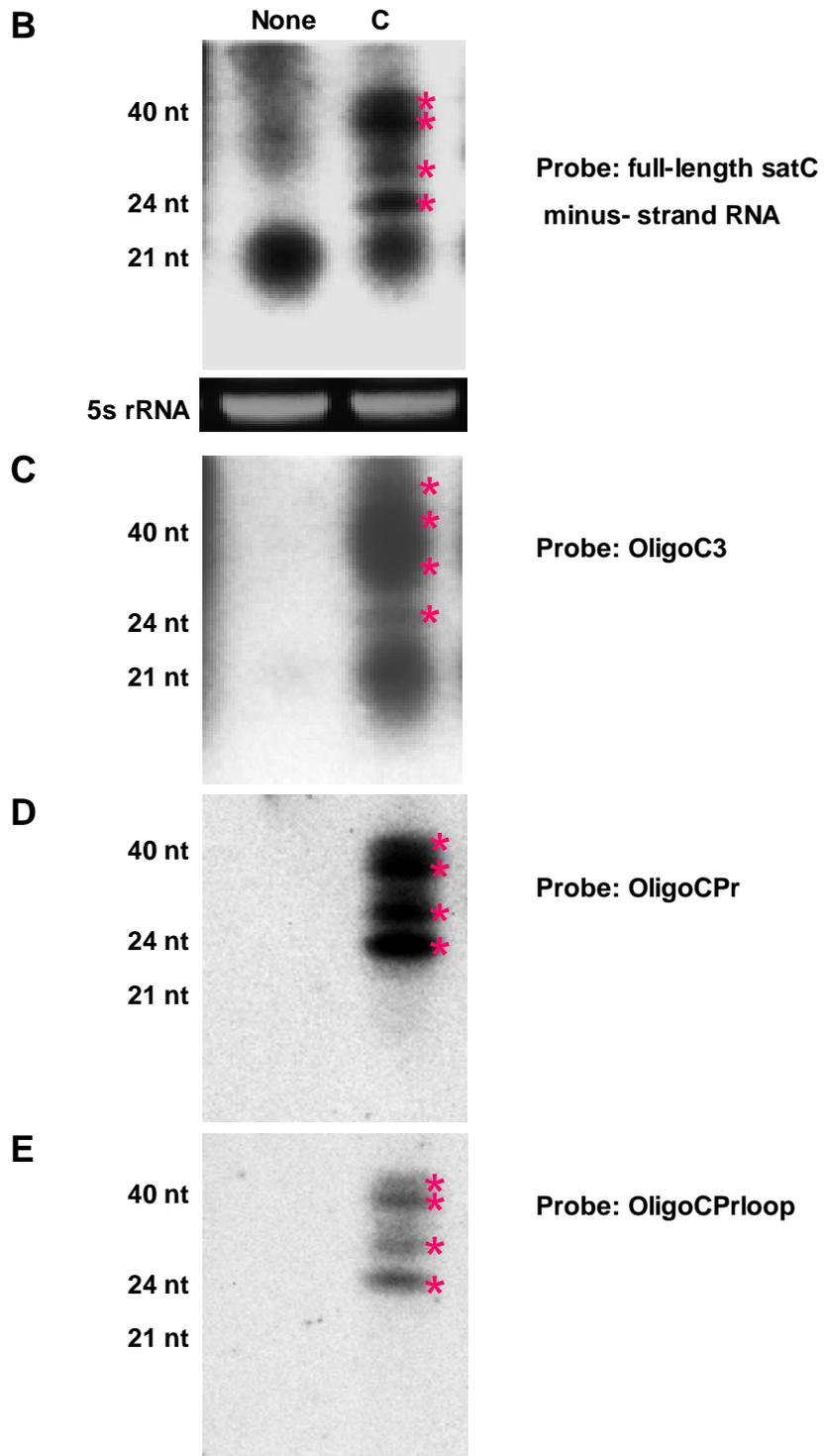
(Figure 1.7). C56G accumulates as efficiently as wt satC in protoplasts, but modulates symptoms of TCV as effectively as diG (Wang and Simon, 2000). As described in Chapter I, TCV-CP$_{CCFV}$ expresses CCFV CP, which shares 65% similarity with that of TCV and accumulates genomic RNAs to levels comparable to those of TCV in inoculated leaves of Col-0 plants (Kong et al., 1997b).

The expectation (Figure 2.5) was that when CP was derived from TCV-CP$_{CCFV}$ or CPm, satC would generate LssRNAs in patterns and levels that would be different from those produced in the presence of wt TCV CP, because satC attenuates symptoms of TCV-CP$_{CCFV}$ and CPm, but intensifies symptoms of TCV (Table 1.4). C56G was expected to generate LssRNAs in different patterns when CPs were derived from TCV, TCV-CP$_{CCFV}$ or CPm, because C56G is phenotypically like diG (Wang and Simon, 2000) and diG intensifies, attenuates, and has no effects on symptoms associated with TCV, TCV-CP$_{CCFV}$, and CPm, respectively (Table 1.4).

As shown by agarose gel electrophoresis (Figure 2.6A), in the presence of CP derived from TCV-CP$_{CCFV}$ and CPm, satC accumulates to about 50% and 40%, respectively, of the levels found with CP translated from wt TCV. A similar reduction in satC accumulation was also observed for C56G. As indicated in the RNA gel blot analysis (Figure 2.6B), satC generates LssRNAs that are in similar patterns (lanes 3, 6, 9; the LssRNA species are indicated with red asterisks), but LssRNA levels are reduced in the presence of CP provided by TCV-CP$_{CCFV}$ or CPm. These decreased LssRNA levels might be caused by the reduced satC accumulation in the presence of CP derived from TCV-CP$_{CCFV}$ and CPm (Figure 2.6A). Similar results were also found for LssRNAs
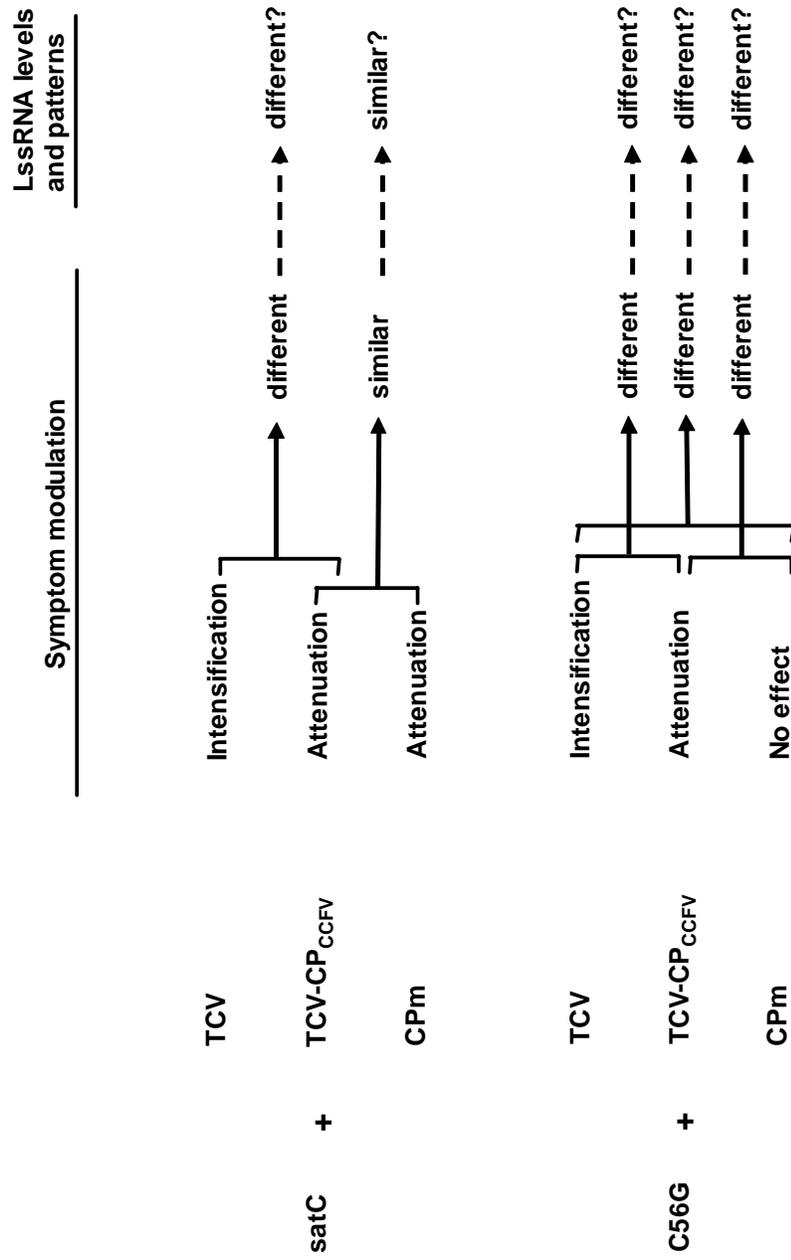
Figure 2.5 Putative correlation between LssRNA accumulation and symptom modulation.

Figure 2.6 RNA gel blot analysis of LssRNAs generated in the presence of CP provided by TCV, TCV-CP$_{CCFV}$, or CPm. Total RNAs were isolated from plants infected with the viral and subviral RNA combinations as given in the Figure at 7 dpi. (A) Agarose gel analysis of the viral and subviral RNAs accumulating in infected plants. The total RNAs were separated in a 1.2% agarose gel. Following electrophoresis, the gel was stained with ethidium bromide. Positions of the genomic RNA (gRNA) and wt satC or C56G are indicated. The 26S rRNA was used as a loading control. (B) RNA gel blot analysis of the LssRNA species derived from satC and C56G. The total RNAs were separated through a denaturing 5% polyacrylamide gel-8M urea. The 5S rRNA was used as a loading control. oligoCPr was used as probe. Single-stranded DNA size markers (M) are shown to the left of the blot. Red and orange asterisks indicate LssRNA species derived from satC and C56G, respectively.
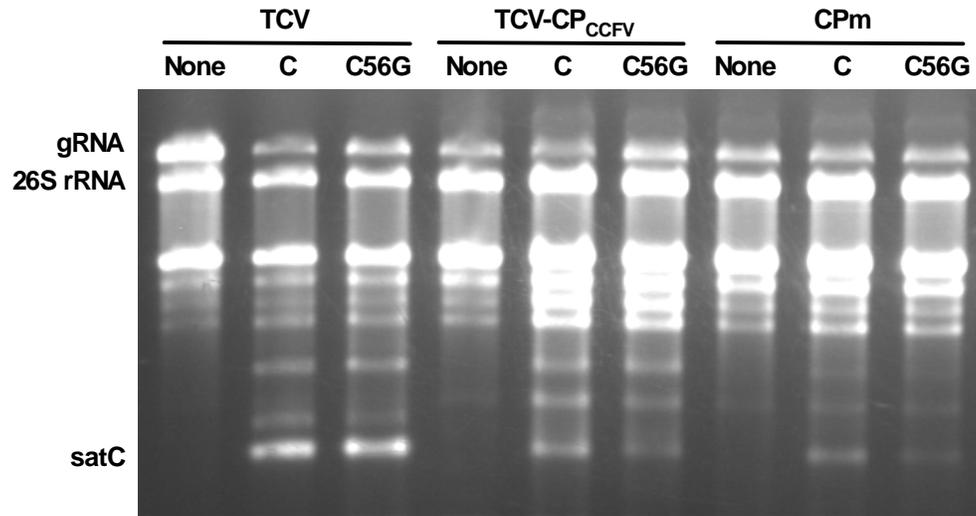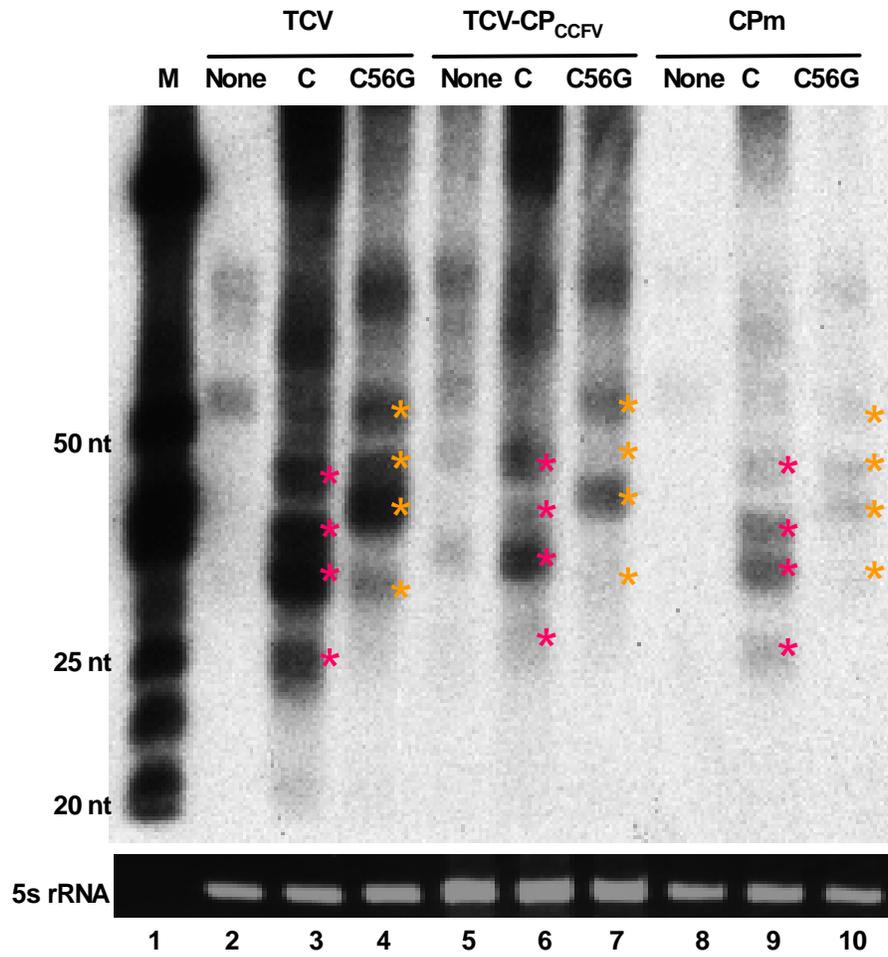
derived from C56G (Figure 2.6B, lanes 4, 7, 10; the LssRNA species are indicated with orange asterisks). Therefore, the current results do not support a significant correlation between accumulation of these LssRNAs and symptom modulation.

LssRNA generation is not related to activity of DCL2 or DCL3

Since LssRNAs have features of vsRNAs (i.e., single-stranded, mainly plus-sense small RNAs), I needed to determine if LssRNAs might be the vsRNA precursors processed by Dicers. To test this hypothesis, LssRNAs produced in DCL2- or DCL3-defective *Arabidopsis* plants (*dcl2-1* and *dcl3-1*, respectively) infected with TCV alone or TCV plus satC or C56G were examined. As shown by agarose gel eletrophoresis, satC or C56G accumulated to similar levels in the tested wt, *dcl2-1*, and *dcl3-1* plants (Figure 2.7A, compare lanes 2, 5, 8 for satC levels; compare lanes 3, 6, 9 for C56G levels). RNA gel blot analysis indicated that satC- or C56G-derived LssRNAs accumulate to similar levels and patterns in the tested wt, *dcl2-1*, and *dcl3-1* plants (Figure 2.7B, compare lanes 3, 6, 9 for satC-derived LssRNAs; and lanes 4, 7, 10 for C56G-derived LssRNAs). Altogether, the results described above suggest that DCL2 and DCL3 are not important for generation of these LssRNAs.

Discussion

When *Arabidopsis* plants were infected with CPm3 or TCV along with satC, disease symptoms were greatly enhanced over those of wt TCV (Wang and Simon, 1999). In this Chapter, I demostrate that the enhanced viral pathogenesis associated with

74

Figure 2.7 RNA gel blot analysis of LssRNAs generated in infected wt or DCL2- and DCL3-defective *Arabidopsis* plants (*dcl2-1* and *dcl3-1,* respectively). The total RNAs were isolated from plants infected with TCV alone (None) or along with satC (C) or C56G at 7 dpi. (A) Agarose gel analysis of the viral and subviral RNAs accumulating in infected plants. The total RNAs were separated in a 1.2% agarose gel. Following electrophoresis, the gel was stained with ethidium bromide. Positions of gRNA and wt satC or C56G are indicated. The 26S rRNA was used as a loading control. (B) RNA gel blot analysis of the LssRNA species derived from satC and C56G. The total RNAs were separated through a denaturing 8M urea-5% polyacrylamide gel. The 5S rRNA was used as a loading control. oligoCPr was used as probe. M, single-stranded DNA size markers. Red and orange asterisks indicate LssRNA species derived from satC and C56G, respectively.

A

	wt			dcl2-1			dcl3-1		
	None	C	C56G	None	C	C56G	None	C	C56G

gRNA
26S rRNA

satC

1   2   3   4   5   6   7   8   9

B

	wt			dcl2-1			dcl3-1		
M	None	C	C56G	None	C	C56G	None	C	C56G

50 nt

25 nt

20 nt

5s rRNA

1   2   3   4   5   6   7   8   9   10
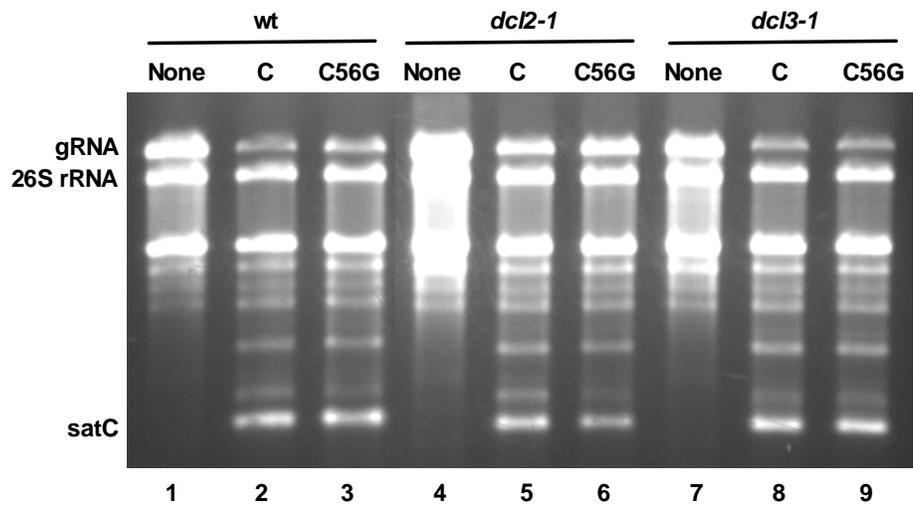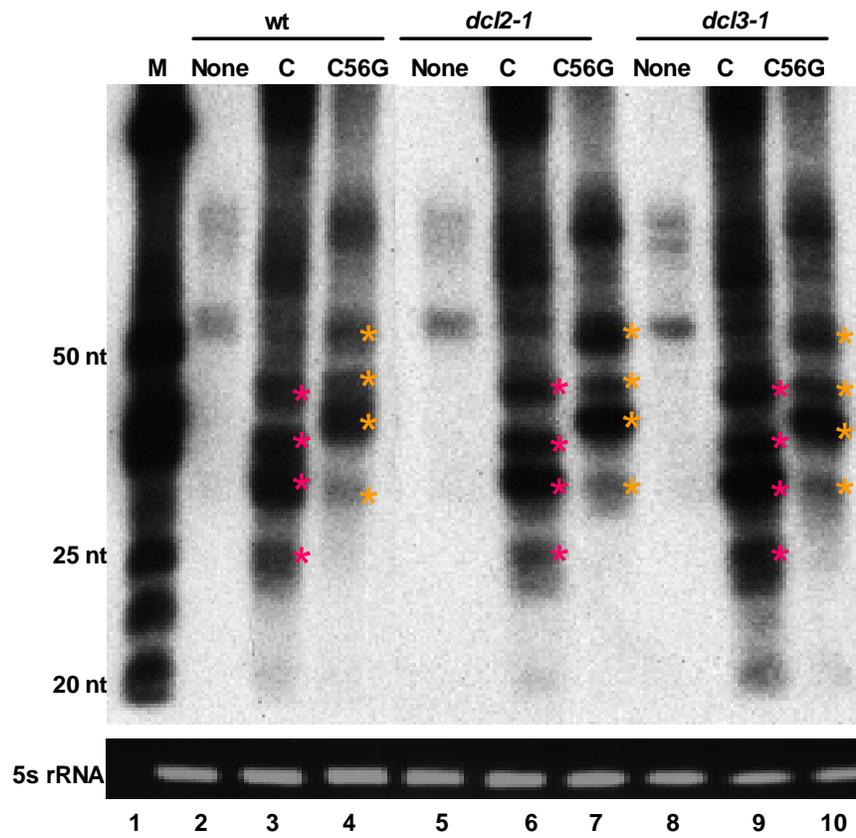
CPm3 or satC correlates with a reduction in virion accumulation and an increase in free CP levels. As described in Chapter I, TCV CP acts as a viral silencing suppressor to interfere with an early step in silencing, prior to the production of small interfering RNAs (Qu et al., 2003; Thomas et al., 2003). When expressed independently of the virus, TCV CP is one of the strongest silencing suppressors discovered to date, with suppressor activity requiring the N-terminal 25 amino acids. However, when CP is expressed from the viral genome, suppression activity associated with TCV is reduced, possibly due to sequestration of the N-terminal RNA-binding domain of the CP within assembling capsid, or a reduction in the amount of CP available at early times of infection when silencing suppression occurs (Qu et al., 2003; Thomas et al., 2003).

Based on these findings and my current results, Figure 2.8 presents a model that explains the virulence associated with satC, the enhanced symptoms associated with CPm3, and the satC-associated symptom attenuation of CPm. I propose that RNA silencing is induced by the presence of both TCV and satC. Infection by wt TCV alone provides only a limited amount of CP to suppress silencing due to the assembly of CP into virions that sequester the CP N-terminus making it unavailable for silencing suppression (Figure 2.8A). In the presence of satC (Figure 2.8B), TCV virion accumulation is substantially reduced providing additional free CP to repress silencing, which results in a more robust infection and enhanced symptom severity. Infection with CPm3 leads to identical effects, with N-terminal CP mutations interfering with assembly of stable virion and resulting in increased levels of free CP (Figure 2.8C). CPm, which contains the same N-terminal CP mutations as CPm3, is also associated with substantially reduced levels of virions (Wang and Simon, 1999). CPm produces only 10% of wt levels

Figure 2.8 Model for symptom intensification by satC and enhanced symptoms of CPm3. Dotted lines in A, D. and E denote weak suppression of VIGS due to reduced availability of CP. The enhanced availability of CP due to satC repression of virion accumulation (B) or reduced virions associated with CPm3 (C) result in increased levels of free CP that strongly suppress silencing leading to enhanced virus colonization of the plant and expressed symptoms. The low levels of CP synthesized by CPm create conditions (CP levels) similar to (A) since CPm CP do not form virions. In (E), symptoms of CPm are substantially reduced since low CP levels are insufficient to repress the additional silencing induced by satC.
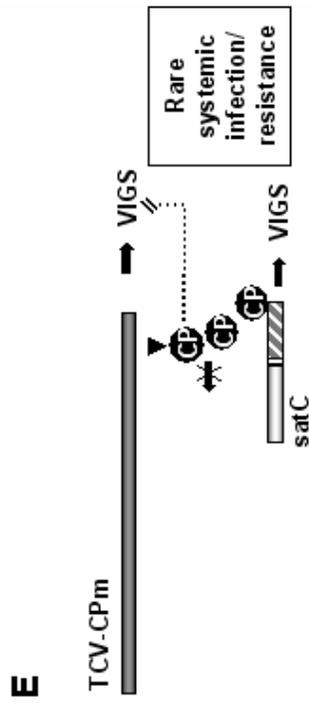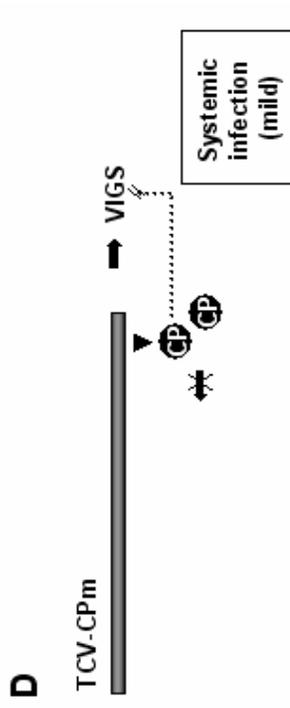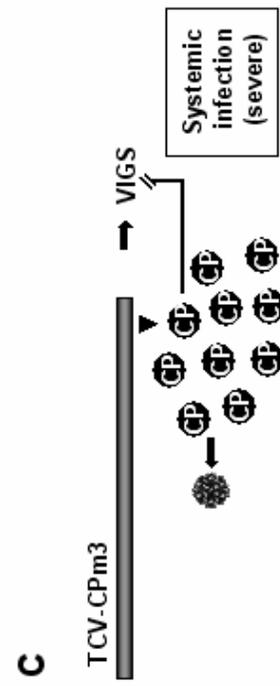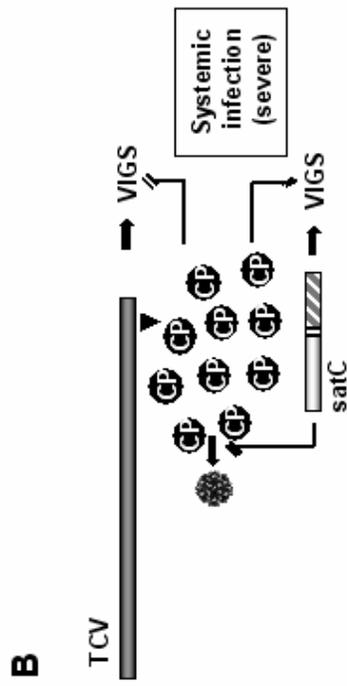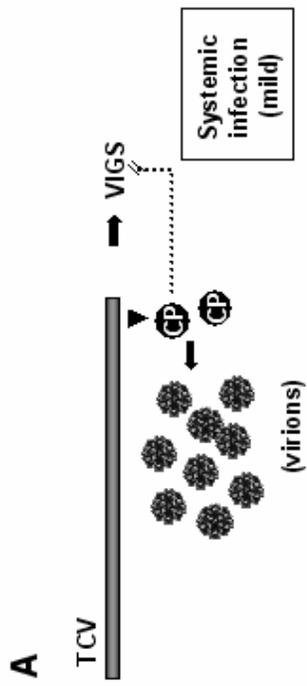
CP, which apparently is sufficient to suppress silencing induced by CPm alone and results in conditions and symptoms similar (but not identical) to infections with wt TCV (compare Figure 2.8A and D). However, I propose that CPm produces insufficient CP to repress the enhanced silencing triggered by the presence of satC in infected cells (Figure 2.8E), leading to symptom attenuation and low or undetectable virus outside the inoculated leaf (Kong et al., 1997a; Kong et al., 1997b).

The interrelationship between satC and TCV suggests that the satRNA is not a simple parasite of the virus. It benefits the helper virus by augmenting the natural ability of the virus to suppress RNA silencing, while also causing a reduction in TCV RNA levels (Li and Simon, 1990). Szittya et al. (2002) have demonstrated that symptom attenuation associated with satC-sized DI RNAs associated with CymRSV is caused by triggering of RNA silencing by the DI RNAs, thus providing precedent for a role of subviral RNAs in silencing. Another example of a satRNA beneficial to its helper virus is the satRNA associated with *Groundnut rosette virus* (GRV). GRV satRNA is required for transcapsidation of GRV by the CP of the assistor virus *Groundnut rosette assistor virus* (GRAV), and thus for transmission between hosts in nature (Robinson et al., 1999).

The region of satC involved in repressing virion accumulation was unexpectedly revealed during a study that used in vivo genetic selection (SELEX: Sytematic Evolution of Ligands by Exponential Enrichment) to study an internal hairpin (M1H) located on minus-strands of satC that serves as a replication enhancer and recombination hot-spot during synthesis of plus-strands (Sun and Simon, 2003; Zhang and Simon, 2003). Fitness of satC containing randomized sequences replacing M1H was correlated with enhanced replication due to the presence of promoter-like elements in the minus-strand and/or

80

enhanced virion inhibition due to formation of a sequence non-specific plus-strand hairpin flanked by CA-rich sequence. The most efficient satRNA at reducing virion accumulation contained either a deletion of the hairpin sequence, or inserts of CA-rich sequence flanking the hairpin, suggesting that the CA-rich sequences flanking M1H in satC are involved in virion suppression.

While ectopic expression of the TCV CP in *Arabidopsis* plants previously indicated that CP dramatically reduces levels of siRNAs generated by silencing (Chapman et al., 2004; Dunoyer et al., 2004), direct evidence that the CP inhibits generation of TCV-derived vsRNAs was lacking, because the CP translated from wt TCV is a weak suppressor (Qu et al., 2003; Thomas et al., 2003). I have found a 60% decrease of vsRNA levels in the presence of increased amounts of free CP in plants infected with CPm3 or TCV along with satC (Figure 2.3). This result strongly supports the model as described above (Figure 2.8), which explains the symptom modulation associated with satC or CPm3.

I also found a new group of small RNAs, the LssRNAs, which are 24- to 40-nt long, satC-specific, single-stranded plus-sense RNAs. RNA gel blot analyses using selected oligonucleotide probes indicated that at least some LssRNAs are processed from the 3'-terminal hairpin of satC, although exact cleavage sites are not currently known. My current data suggests that generation of LssRNAs is not related to either symptom modulation or activities of DCL2 and DCL3. Recent studies indicated that Adenovirus-derived vsRNAs are preferentially generated from the 3' side of the stem of a viral hairpin, like generation of the endogenous miRNAs (Sano et al., 2006). Since LssRNAs are also processed from the viral 3'-terminal hairpin, it is possible that DCL1, the Dicer

required for biogenesis of the miRNAs, is important for generation of LssRNAs. This possibility will be tested in the future. It is also possible that cellular nucleases other than Dicers are involved in this process.

CHAPTER III

TARGETING OF HOST GENE EXPRESSION BY VIRAL-DERIVED

SMALL RNAS

Introduction

Viruses invading plants induce VIGS leading to the processing of viral RNAs by Dicers into ~21 nt vsRNAs that load into RISC to direct cleavage of complementary viral RNAs. These vsRNAs may also base pair with complementary host mRNAs to guide degradation of host mRNAs, which may alter the plant's developmental regulation, generating discernible symptoms. As described in Chapter I, vsRNAs derived from non-coding viroids and CMV satY appear able to promote pathogenesis (Wang et al., 2004) while a role in modulation of host gene expression has been proposed for small RNAs derived from animal DNA virus (the Herpesviruses and Adenoviruses) transcripts (Pfeffer et al., 2005; Sano et al., 2006; Sullivan and Ganem, 2005). vsRNAs derived from CymRSV are about 20- to 21-nt long and primarily derived from discrete "hotspot" regions on plus strands of the viral RNA (Molnar et al., 2005). Specific plant mRNAs targeted by vsRNAs, however, have not been identified.

As described in Chapter I, virus-encoded silencing suppressor proteins may interfere with endogenous silencing pathways, altering developmental regulation and thus contributing to symptom development. TCV CP is a viral suppressor of RNA silencing (Qu et al., 2003; Thomas, et al., 2003) and ectopic CP expression substantially reduced

levels of 21- and 24-nt siRNAs while enhancing at least one miRNA (Chapman et al., 2004; Dunoyer et al., 2004). While ectopic expression of some viral silencing suppressors in infected cells can produce developmental abnormalities similar to those associated with viral infection (Kasschau et al., 2003) or silencing pathway mutants (Voinnet, 2005), expression of TCV CP had little (Chapman et al., 2004) or no effect (Dunoyer et al., 2004) on host morphology.

To determine whether symptoms associated with TCV infection result from vsRNA targeting of host mRNAs, I cloned TCV- and satC-specific vsRNAs. Both sets of vsRNAs were purine-rich, and nearly all were derived from plus-strands. BLAST searching revealed 12 putative host mRNA targets for one of the TCV hotspot vsRNA, TvsRNA5, and six of seven genes selected for this study had transcript levels reduced 2.4- to 4-fold by TCV infection. Plants infected with TCV containing a deletion in the TvsRNA5 region exhibited reduced symptoms despite wt levels of virus accumulation and retained near wt levels of the three TvsRNA5-targeted mRNAs tested. These results indicate that vsRNAs derived from invading RNA viruses can specifically target host gene expression, which affects virus symptom expression and may produce a more favorable environment for virus infection.

Materials and Methods

Growth and inoculation of *Arabidopsis* plants

Arabidopsis plants (ecotype Col-0) were grown in a growth chamber at 20°C with a 16-h light/dark cycle as described in Chapter II. TCV or satC RNAs synthesized using T7 polymerase from *Sma*I-linearized DNA plasmids were inoculated into the oldest pair leaves of *Arabidopsis* seedlings at the 6 to 8 leaf-stage as described in Chapter II. Control (mock) plants were inoculated with inoculation buffer only. Systemically infected leaves were collected at 7 dpi, pooled, and then frozen at $-80^{o}C$ prior to RNA extraction.

RNA extraction

About 500 mg of leaves of *Arabidopsis* plants systemically infected with TCV with or without satC were ground in liquid nitrogen and resuspended in 10 ml of TRIzol® Reagent (Invitrogen). The suspension was then mixed with 3 ml of cholorform followed by vortexing and centrifugation in a Sorvall SS34 rotor at 13,000 rpm for 10 minutes at 4°C. The aqueous phase (~6 ml) was re-extracted with 6 ml of chloroform and precipitated with an equal volume of isopropanol. The RNA pellets were washed with 70% ethanol, dried, and dissolved in 200 μl of RNase-free H_2O. The RNA was then used for real-time PCR, 5' RACE or subjected to further purification for cloning of small RNAs.

Cloning of small RNAs

To clone small RNAs, the RNAs extracted from *Arabidopsis* plants using the method described above were further purified using the RNA/DNA Midi kit (Qiagen) and the protocol supplied by the manufacturer to obtain low molecular mass RNAs. Twenty micrograms of low molecular mass RNAs was subjected to electrophoresis through an 8% denaturing polyacrylamide gel followed by ethidium bromide staining. Using a denatured 10-nt DNA ladder for size standards, the 15- to 40-nt RNA region was excised from the gel, sliced, transferred into a 1.5 ml eppendorf tube, and incubated in 3 volumes of 0.3 M NaCl at 4°C overnight with vigorous shaking. After incubation, the solution was collected and mixed with an equal volume of phenol/chloroform (1:1), followed by vigorous vortexing and centrifugation at 13,000 rpm for 5 minutes at 4°C. The supernatant was precipitated with 2.5 volumes of 5 M NaOAc/ethanol (1:25). After washing with 70% ethanol, the RNA pellets were dried and dissolved in 25 µl of distilled water.

The small RNAs were cloned using previously described methods (Lau, et al., 2001; Llave et al., 2002) with a few modifications (see Figure 3.1 for procedure flow chart). Briefly, gel-purified RNAs isolated using the method described above were ligated to a 5' adaptor that contains hydroxyl groups (OH) at both ends to prevent adaptor self-ligation (Dharmacon; sequences of all oligonucleotides used in this Chapter are listed in Table 3.1) using T4 RNA ligase (Amersham). The ligation products were separated on an 8% denaturing polyacrylamide gel. RNAs of ~ 35-60 nt were gel-purified, precipitated with ethanol, and then ligated to a 3' adaptor (Dharmacon) using T4 RNA ligase. The 3' adaptor contains a 5'-monophosphate group and a 3' inverted deoxy-thymidine (3'-idT)

Figure 3.1 Flow chart for cloning of vsRNAs from plants infected with TCV in the presence or absence of satC. Gel-purified RNAs were ligated to 5' and 3' adapters using T4 RNA ligase. The adapters were terminally modified to prevent self-ligation. Final ligation products were reverse transcribed and amplified by PCR. OH, hydroxyl group; P, monophosphate group; idT, inverted deoxythymidine group; RT, Superscript II reverse transcriptase; Taq, Taq DNA polymerase. See text for details.
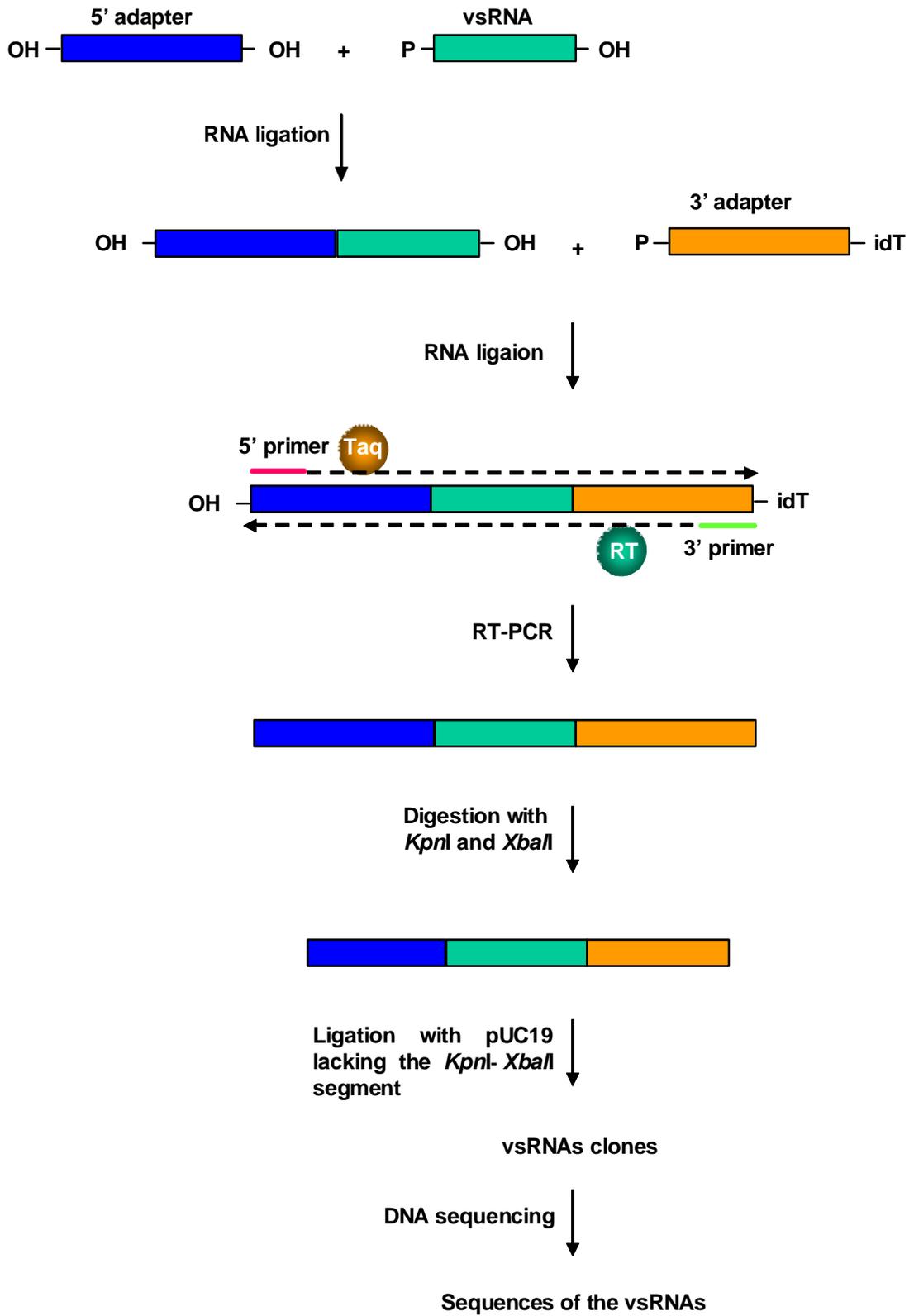
Table 3.1 Oligonucleotides used in Chapter III

Application	Name	Sequence[a]	Polarity[b]
vsRNA cloning	5' adaptor	5'-TACAATACGACTCACT*AAA*	
	3' adaptor	5'-P-*UUU*AACCGCATCCTTCTC-idT	
	Oligo5F	5'-CGGCGG**GGTACC**CCGTACTAATACGACTCACTAAA	+
	Oligo3R	5'-GCGC**TCTAGA**GCGAGAAGGATGCGGTTAAA	−
Real-time RT-PCR	oligo(dT)$_{20}$	5'-TTTTTTTTTTTTTTTTTTTT	−
	At2g22090F	5'-TCCATTATTTTTCCTTTTGTTGG	+
	At2g22090R	5'-CAATATTCGTCCCCACCATC	−
	At2g24762F	5'-AAGAAACAACGAGTCAGTGAGC	+
	At2g24762R	5'-ATTTCCCGTGAAAACACGAA	−
	At2g32960F	5'-TGAGTTACCTGAGGAATCATCAAA	+
	At2g32960R	5'-GATTACAAATGAATCAAAAGAAAAGA	−
	At3g07810F	5'-TCATTGTTCCTCCTAGGCTTTT	+
	At3g07810R	5'-CTCGCCGGAGACTGATACA	−
	At4g11010F	5'-TCCCTCTTCCTCTTGTCTTTTG	+
	At4g11010R	5'-CCCGGAATGTGTTTGTATCC	−
	At4g19110F	5'-GTCTTTGCCTCGTCAATGGT	+
	At4g19110R	5'-GACCCAAGTCGATCTTTATTGC	−
	At5g42860F	5'-ACCCCAAAGCAGAAGAATCA	+
	At5g42860R	5'-GAATTTGATACTTTGCGTGAAAAA	−
	TCP4F	5'-GGTCCCCTTCAGTCCAGTTACAGTC	+
	TCP4R	5'-AGGAAGGTGATGGTGGTGGTT	−
5' RACE	AAP	5'-GGCCACGCGTCGACTAGTAC<u>GGGIIGGGIIGGGIIG</u>	+
	GSP1	5'-AATAAAAGATAAAAATAGTTTTTTCT	−
	GSP2	5'-GTACATCAACAGAAACGAGTT	−

[a] Bold residues denote a *Kpn*I site in Oligo5F and an *Xba*II site in Oligo3R. Bases in italics indicate the RNA residues in the 5' and 3' adapters. The 3' portion of AAP is underlined, which is complementary to the homopolymeric tail of dCTP-tailed cDNA. I, deoxyinosine residue; P, monophosphate group; idT, inverted deoxythymidine group.

[b] "+" and "-" polarities refer to homology and complementarity with *Arabidopsis* mRNAs, respectively.

to prevent 3' end ligation. Final ligation products were subjected to reverse transcription using reverse transcriptase Superscript II (Invitrogen) and Oligo3R as primer. Reverse transcription products were amplified by PCR using primers Oligo5F and Oligo3R, which contain *Kpn*I and *Xbal*I sites, respectively. PCR products were digested with *Kpn*I and *Xbal*I, and separated on a 3% agarose gel. DNA fragments of 55-80 nt were eluted from the gel and ligated to pUC19 lacking its *Kpn*I-*Xbal*I fragment. The resulting clones were pre-screened for virus-specific sequences by hybridization to full-length TCV or satC plus- and minus-strand probes using the RNA gel blotting method described in Chapter II and then sequenced.

Real-time RT-PCR

Real time RT-PCR was performed using Invitrogen's SuperScript™ III Platinum® Two-Step qRT-PCR Kit with SYBR® Green according to the manufacturer's protocol (see Figure 3.2 for procedure flow chart). Briefly, the oligo(dT)$_{20}$-directed reverse transcription was carried out at 42°C for 50 minutes in a 20-µl reaction containing 10 µl of 2X RT Reaction Mix, 2 µl of RT Enzyme Mix, 1 µl of total RNA (1 µg/µl) extracted from plants infected with TCV alone or along with satC. The 2X RT Reaction Mix contains 2.5 µM oligo(dT)$_{20}$, random hexamers (2.5 ng/µl), 10 mM MgCl$_2$, and dNTPs (dATP, dCTP, dGTP, dTTP). The RT Enzyme Mix contains SuperScript™ III RT and RNaseOUT™. The reaction was terminated by heating at 85°C for 5 minutes, and then chilled on ice. The resulted cDNAs were treated with 1 µl of *E. coli* RNase H (2 U/ µl) at 37°C for 20 minutes, and then diluted 10-fold. Each 8 µl of the diluted cDNA sample
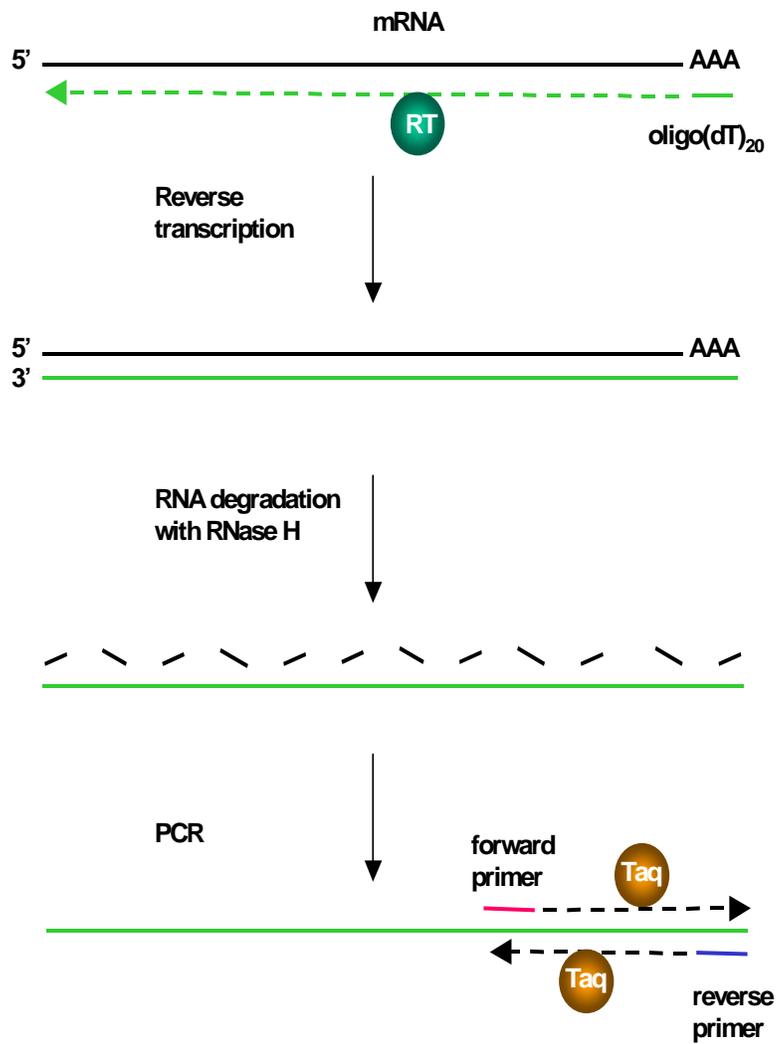
Figure 3.2 Flow chart for real-time PCR of *Arabidopsis* mRNAs. RT, Superscript II reverse transcriptase; Taq, Taq DNA polymerase. See text for details.

(~40 ng of input RNA) was added to a 25-µl PCR reaction containing 12.5 µl of SuperMix-UDG, 0.5 µl of 10 µM forward primer, 0.5 µl of 10 µM reverse primer. The forward primers used for PCR assay of mRNAs of *Arabidopsis* genes At2g22090, At2g24762, At2g32960, At3g07810, At4g11010, At4g19110, At5g42860 and TCP4 are At2g22090F, At2g24762F, At2g32960F, At3g07810F, At4g11010F, At4g19110F, At5g42860F, and TCP4F, respectively. The corresponding reverse primers are At2g22090R, At2g24762R, At2g32960R, At3g07810R, At4g11010R, At4g19110R, At5g42860R and TCP4R, respectively. Primers were designed using OligoPerfect™, a primer design software program provided by Invitrogen. Amplification was carried out with a 3-Step Cycling program (50°C for 2 minutes; 95°C for 2 minutes; and 45 cycles of: 95°C for15 seconds, 55°C for 30 seconds, and 72°C for 30 seconds) in a Prism 7700 Sequence Detection System (Applied Biosystems) in real time. The melting curves were analyzed as described in the instrument documentation provided by Invitrogen. Real time PCR data were analyzed using the delta-delta Ct method (Pfaffl, 2001). Ct represents the cycle threshold, e.g., the cycles necessary to detect a signal. Experiments were carried out in triplicate using three different preparations of RNA combined from 2 to 3 plants. Relative expression ratios of different samples and mock were normalized to actin-2, the constitutive marker gene (Sigma). The efficiencies of all primer pairs were between 99-103% and standard curves were generated for all pairs. PCR products were also monitored following electrophoresis through 2% agarose gels stained with ethidium bromide for production of a single species.

5'-RACE

     5'-RACE (rapid amplification of cDNA ends) PCR was carried out according to Invitrogen's 5'-RACE PCR protocol (Catalog # 18374-058) with modifications (see Figure 3.3 for procedure flow chart). Briefly, 5 µl of total RNA (1 µg/µl) isolated from plants was mixed with 2.5 µl of 1 µM GSP1 (gene-specific primer 1) in a 0.5 ml eppendorf tube. The mixture was incubated at 70°C for 10 minutes and chilled on ice for 1 minute to denature the RNA, which was followed by addition of 2.5 µl of 10X PCR buffer (200 mM Tris-HCl, pH 8.4, 500 mM KCl), 2.5 µl of 25 mM MgCl$_2$, 1 µl of 10 mM each of dATP, dCTP, dGTP, dTTP, and 2.5 µl of 0.1 M DTT. The mixture was adjusted to a volume of 24 µl with distilled H$_2$O and then incubated for 1 minute at 42°C. The mixture was collected by brief centrifugation and gently mixed with 1 µl of SuperScript™ II RT (200U/µl), followed by incubation at 42°C for 50 minutes to synthesize enough cDNA. The reverse transcription reaction was terminated by incubation at 70°C for 15 minutes and then cooled down to 37°C. The reaction mixture was treated with RNase A at a final concentration of 0.1 µg/µl and RNase H (1U/ µl) at 37°C for 30 minutes. The first-strand cDNA was purified using a S.N.A.P. column (Invitrogen) and the method recommended by the manufacturer to eliminate unused primer and dNTPs. The purified cDNA was mixed with 5 µl of 5X tailing buffer (50 mM Tris-HCl, pH 8.4, 125 mM KCl, 7.5 mM MgCl$_2$) and 2.5 µl of 2 mM dCTP. The mixture was adjusted to a volume of 24 µl with distilled H$_2$O, heated at 94°C for 3 minutes, chilled on ice for 1 minute, and collected by brief centrifugation. After addition of 1 µl of terminal deoxynucleotidyl transferase (15 U/µl), the mixture was incubated at 37°C for

Figure 3.3 Flow chart for 5' RACE of *Arabidopsis* mRNAs. RT, Superscript II reverse transcriptase; TDT, terminal deoxynucleotidyl transferase; Taq, Taq DNA polymerase; GSP1, gene-specific primer 1; AAP, abridged anchor primer; GSP2, gene-specific primer 2. See text for details.
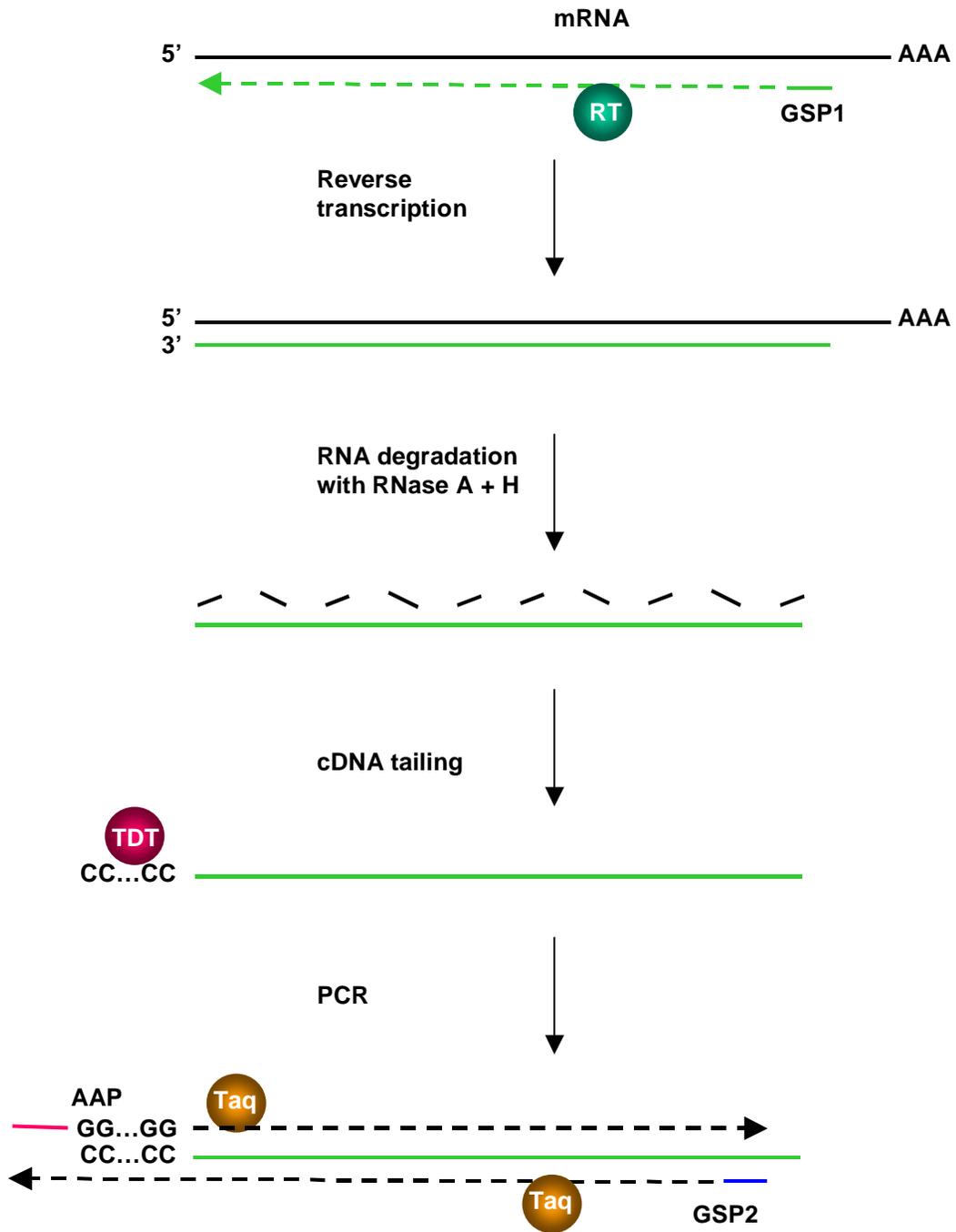
10 minutes to tail the cDNA. The reaction was terminated by incubation at 65°C for 10 minutes. To amplify the dCTP-tailed cDNA by PCR, 5 μl of the tailed cDNA was mixed with 5 μl of 10X PCR buffer (200 mM Tris-HCl, pH 8.4, 500 mM KCl), 3 μl of 25 mM MgCl$_2$, 1 μl of 10 mM each of dATP, dCTP, dGTP, dTTP, 2 μl of 10 μM nested GSP2 (gene-specific primer 2), 2 μl of 10 μM AAP (abridged anchor primer), and 0.5 μl of *Taq* DNA polymerase (5 units/μl). The 3' poly(G) portion of AAP (Table 3.1), which is complementary to the homopolymeric tail of dCTP-tailed cDNA, contains deoxyinosine residues (I) to create a melting temperature (Tm) for the 16-base anchor region (66.6°C) that is comparable to that of a typical 20-base primer with 50% GC content. Deoxyinosine basepairs with all four bases with different affinities. The mixture was adjusted to a volume of 50 μl with distilled H$_2$O and PCR was carried out in a thermal cycler using the cycling protocol recommended by the manufacturer. Ten microliters of the 5' RACE products were analyzed by 1.2% agarose gel electrophoresis using appropriate size standards.

Results

TCV and satC vsRNAs are mainly derived from plus-strand hotspot regions

To identify vsRNAs derived from TCV gRNA and satC, 10 *Arabidopsis* Col-0 seedlings at the six to eight leaf stage were inoculated with either TCV or TCV and satC. At 7 dpi, the onset of visible symptoms, leaves from infected plants were pooled, and small RNAs (under 50 nt) were isolated and cloned. To avoid sequencing non-viral siRNAs and miRNAs, clones were initially pre-screened for virus-specific sequences by

hybridization to full-length TCV or satC plus- and minus-strand probes. Approximately 40% of the small RNA population that was amenable to cloning was virus-specific. Most of the TCV vsRNA clones contained sequence from plus-strands (57/62) and 45 of the 57 plus-strand vsRNAs were derived from five hotspot regions containing at least six members each (labeled TvsRNAs1-5) (Table 3.2). Endpoints within each hotspot region were slightly staggered, denoting that the excision events were imprecise. TvsRNA sequences ranged in size from 19 to 24 nt, with the majority (52 of 62) being 20 to 22 nt. Nearly all sequences were purine-rich, with an average purine content of 68 ± 8.9% (hotspot sequences were only considered once), compared with a TCV genomic RNA purine content of 54%. In addition, there were 22 GGG(G) or AAA(A) elements compared with only five CCC(C) or UUU(U) elements. All TvsRNAs appear to have been excised from hairpin or interior paired regions of TCV, as determined by mFold computer modeling (Zuker, 2003; Figure 3.4).

Of the 37 satC vsRNA (CvsRNA) sequences cloned, all but three were from two regions of satC: positions 128-154 in plus-strands (CvsRNA1) and positions 21-40 in minus-strands (CvsRNA2) (Table 3.3). As with TCV vsRNAs, CvsRNAs were purine-rich with an average purine content of 62 ± 5.6% compared with satC G/A content of 54%. The lengths of CvsRNAs were also similar to those of TCV gRNA, with 35 of 37 being 20 to 22 nt in length (Figure 3.5 B and C). Members of CvsRNA1 and CvsRNA2 had slightly staggered ends, indicating similar imprecise excision as was found for TCV TvsRNAs. mFold RNA structure predictions (Zuker, 2003) combined with solution structure probing of the 5' portion of satC (G. Zhang and A. E. Simon, unpublished) revealed that both hotspots lie within one strand in extensively paired regions (Figure

Table 3.2 The vsRNAs derived from plus- and minus-strands of TCV.

Strand	Position[a]	Sequence	Copy #	Length (nt)	Group
Plus	310-331	AGCGGGGCGGAUAUAGAAAUAG	2	22	TvsRNA1 (10/60)
	311-332	GCGGGGCGGAUAUAGAAAUAGA	7	22	
	312-333	CGGGGCAGAUAUAGAAAUAGACU	1	23	
	375-395	CGGGGCGGAUAUAGAAAUAGAC	2	22	TvsRNA2 (16/60)
	376-396	UUUGGUGGAGGCGGUAGGUAG	10	21	
	377-398	UGGUGGAGGCGGUAGGUAGUAC	1	22	
	377-395	UCUGGUGGAGGCGGUAGGUAG	3	21	
	1003-1022	GAAAGAGUCUUUUACGCUUGA	3	21	TvsRNA3 (6/60)
	1005-1025	AAAGAGUCUUUUACGUUGAAGC	2	22	
	1005-1028	AAGAGUCUUUUACGUUGAAGAUGC	1	24	
	2792-2812	UGGGCGAUAAAGUGGCAGAAG	3	21	TvsRNA4 (6/60)
	2796-2815	CGATAAAGTGGCAGAAGAAG	2	20	
	2796-2817	CGATAAAGTGGCAGAAGAAGGG	1	22	
	3850-3870	UAAGAAAAGAAAACAAAAAC	4	21	TvsRNA5 (6/60)
	3851-3870	AAGAAAAGAAAACAAAAACC	2	20	
	616-636	CGCGGAAGACATTCAGGTCGT	1	21	
	696-715	AAGUGCGGAAGUGGUGGGUC	1	20	
	831-851	UGGUCGGGAGGGAGACUCAAA	1	21	
	950-970	GACUUUGGAGUCCACAACAA	1	21	
	1449-1467	UGAGUAACACCUGGGAUAA	1	19	
	1801-1821	UGAUGAAGUCGACAGGGUGC	1	21	
	2809-2830	AGAAGGGCUGGUCAACCCUAAC	1	22	
	3093-3113	CAGCUCAUUAAGGAGGCGGCC	1	21	
	3545-3564	CAAGGGGACAGCUGGGUGGG	1	20	
	3603-3624	TTGACATTGTTCTACGAGAAGG	1	22	
	3755-3773	UGAGGAGCAGCCAAAGGGU	1	19	
Minus	42-63	AUCGUGAAUAGAGAGAAGGUUG	1	22	
	766-786	UCAGGCAGUCGGCAUAAUCG	1	21	
	2630-2650	AAGTAGGAGGACCAGTGAGAG	1	21	
	3379-3360	ATGAGCTTGCCGAAATCGAC	1	20	
	2975-2995	CUUCUGGUUAUGCCGUCCCUG	1	21	

[a] Coordinates correspond to those of TCV.

Figure 3.4 Position of the TCV vsRNAs on local structures determined by mFold (Zuker, 2003). Arrowheads bracket the furthest endpoints of the encompassed TvsRNA sequences.
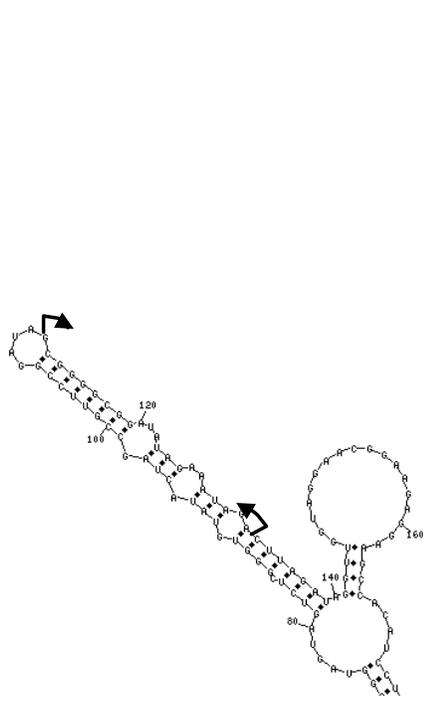
TvsRNA1
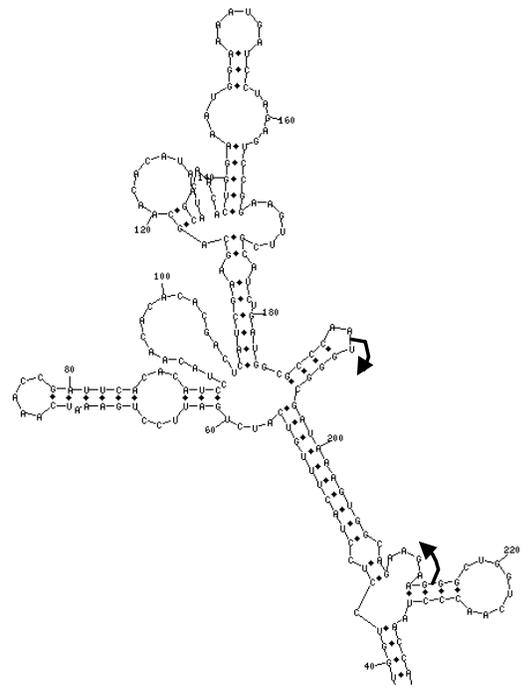
TvsRNA4
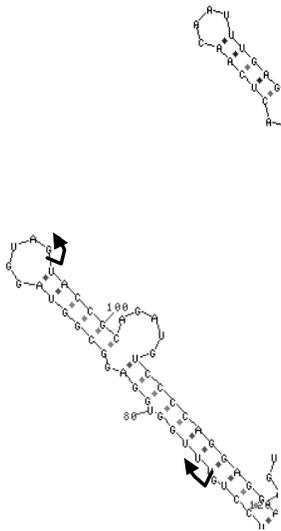
TvsRNA2
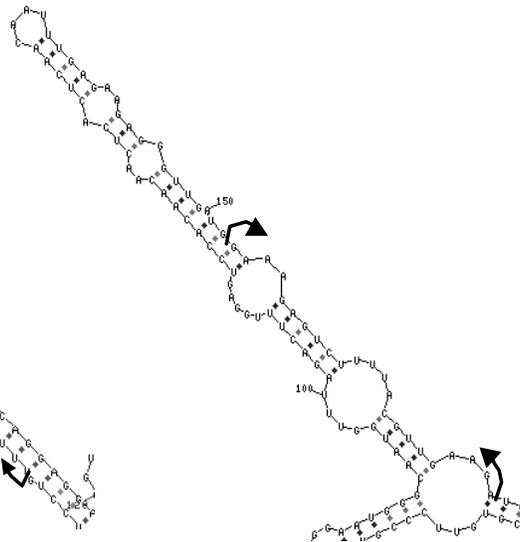
TvsRNA3
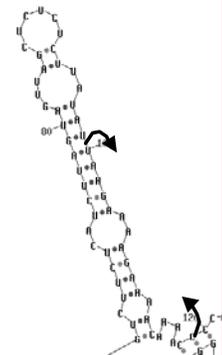
TvsRNA5

Table 3.3 The vsRNAs derived from plus- and minus-strands of satC.

Strand	Position [a]	Sequence	Copy #	Length (nt)	Group
Plus strand	128-147	CCAUCAAGUACGGGAGCGUG	1	20	CvsRNA1 (26/40)
	129-148	CAUCAAGUACGGGAGCGUGA	1	20	
	130-151	AUCAAGUACGGGAGCGUGAAAA	1	22	
	131-150	UCAAGUACGGGAGCGUGAAA	8	20	
	131-152	UCAAGUACGGGAGCGUGAAAAC	2	22	
	131-153	UCAAGUACGGGAGCGUGAAAACC	1	23	
	132-153	CAAGUACGGGAGCGUGAAAACC	1	22	
	133-153	AAGUACGGGAGCGUGAAAACC	6	21	
	133-154	AAGUACGGGAGCGUGAAAACCU	2	22	
	134-154	AGUACGGGAGCGUGAAAACCU	3	21	
	140-160	GGAGCGUGAAAACCUGGCUGU	1	21	
	189-210	CAGCCAAAGGGUAAAUGGGACC	1	22	
Minus strand	21-40	CAUUAGUUGCGUAGUAUUGU	3	20	CvsRN2 (10/40)
	22-40	CAUUAGUUGCGUAGUAUUGGU	5	21	
	22-40	CAUUAGUUGCGUAGUAUUGGU	1	21	
	25-40	UAGUUGCGUAGUAUUGGU	1	18	
	12-33	UGCGUAGUAUUGUAUGAAACCC	1	22	
	171-187	AGGGUCUGGGAUUCUUUUGAG	1	21	

[a] Coordinates correspond to those of satC.

102

3.5A and B). In addition, one CvsRNA (positions 189-210) was excised from the M1H hairpin region, which is a required hairpin in plus-strands (Sun and Simon, 2003). It is noted that no LssRNA-sized small RNAs (24- to 40-nt) were found among the satC-derived small RNAs (Table 3.3), although 18- to 40-nt RNA species were eluted from the gel during the small RNA cloning (see Materials and Methods).

TvsRNA5 downregulates complementary *Arabidopsis* mRNAs

TvsRNA5 (5'UAAGAAAAGAAAACAAAAACC), the most purine-rich of the TvsRNAs, is located between positions 3850 to 3969 in the 3' untranslated region (UTR) of TCV. This sequence comprises the 3' side of the well-studied M3H hairpin, which also contains a sequence repeat that acts as an enhancer and recombination hotspot in its minus-sense orientation (Carpenter et al., 1995). I chose to examine if this particular vsRNA targets host transcripts for the following reasons: small deletions in this region are not detrimental to TCV accumulation (Carpenter et al., 1995); the 3' UTR location allows for sequence alterations without affecting viral ORFs; and the sequence had extensive complementary to the largest number of host genes.

BLAST searching the *Arabidopsis* genome against the reverse complement of TvsRNA5 revealed complementarity (at least 16/16 or 19/20) to 12 genes, some of which encode RNA-binding proteins, protein kinases, senescence-associated proteins, protein phosphatases and specific transcription factors (Figure 3.6A). To determine if TCV infection affects the expression of some of these genes, seven were selected for analysis. For all seven, the complementary pyrimidine-rich sequence is located within the 3' UTR. mRNAs from two genes (At4G19110.1 and At2G24762; all genes are identified by their

Figure 3.5 Position of the satC vsRNAs on structures determined by mFold (Zuker, 2003). For the satC plus (+) strand, only the 5' domain derived from satD, is presented. The putative structure for satC full length minus (-)-strand is shown. Arrowheads bracket the furthest endpoints of the encompassed CvsRNA sequences.

SatC (+) 5' domain

B

CvsRNA2

Full-length SatC (-)
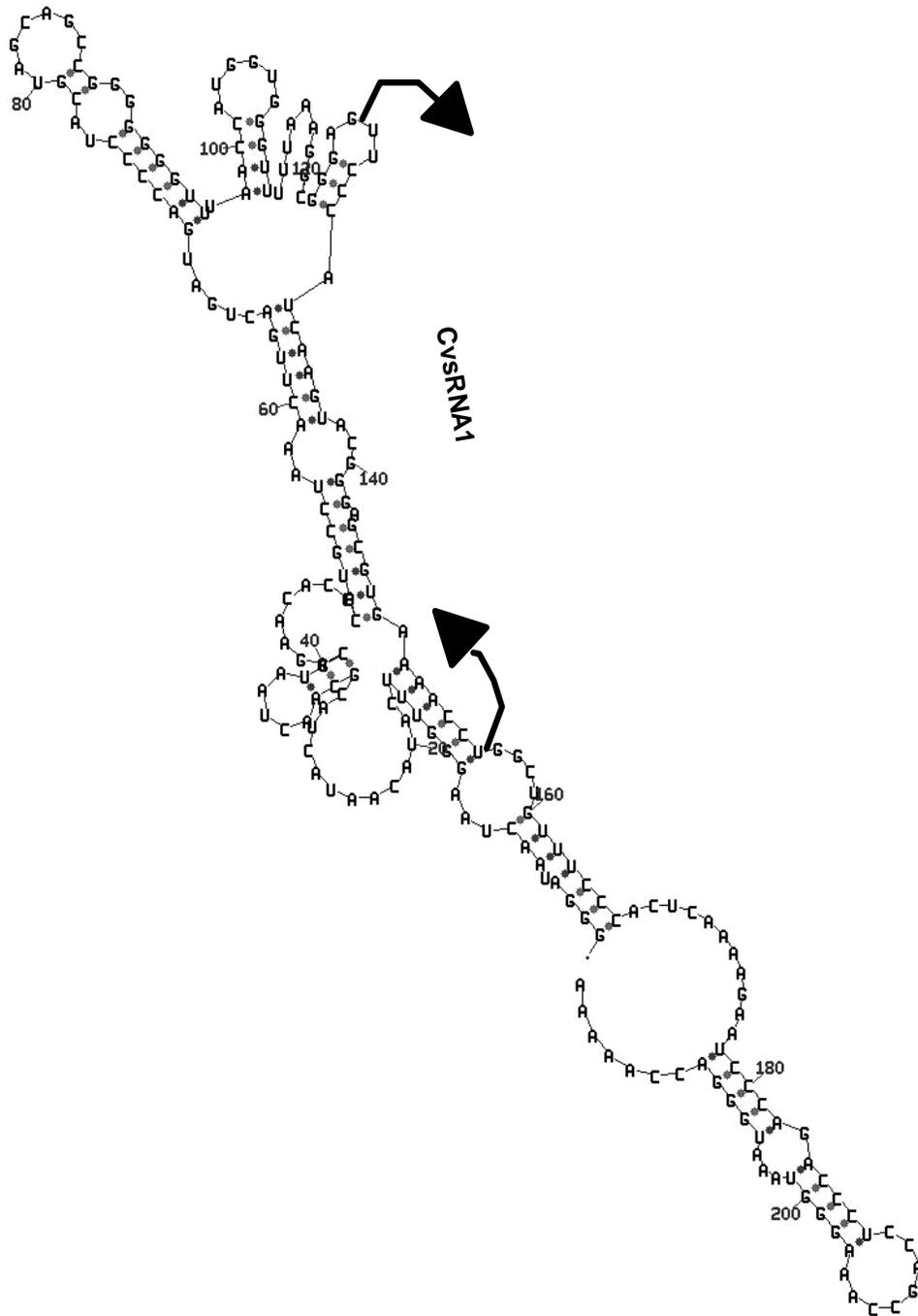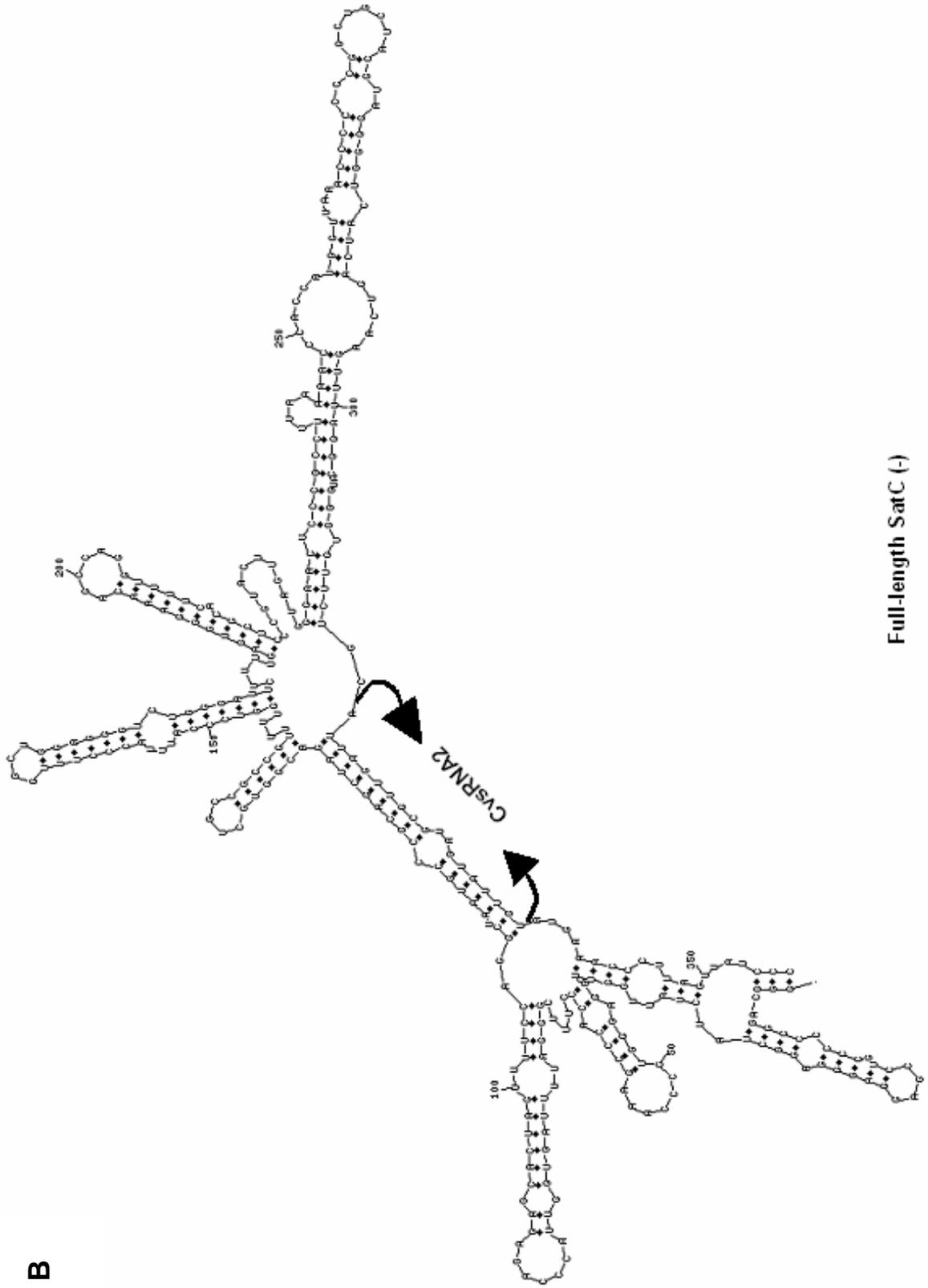
Figure 3.6 Expression of genes with sequences complementary to TvsRNA5 in virus-infected plants. (A) Complementarity between TvsRNA5 and transcripts of seven Arabidopsis genes identified by BLAST. The accession numbers and encoded protein functions (if known) are given. All sequences are located in the 3' UTR of the mRNAs. mRNA sequences are shown in 5' to 3' orientation. (B) mRNA accumulation levels as determined by real-time PCR. Plants were either mock inoculated (Mock) or inoculated with TCV alone or TCV and satC. RNA was extracted at 7 dpi from leaf tissue pooled from five plants, and subjected to real-time PCR using gene-specific primers. PCR was repeated three times. Error bars denote standard deviation.

A

2446 UGCUUUUGUUUUCUUUUCUUA   At4G19110   **Serine/threonine**
    | |||||||||||||||||||| **protein kinase**
TCV CCAAAAACAAAAGAAAAGAAU 3850

568   CUUUUUUGUUUUCUUUUCUUC   At2G24762   **Unknown**
    ||||||||||||||||||||
TCV CCAAAAACAAAAGAAAAGAAU 3850

2058 UAUUUUUGUUUUCUUUUCUUC   At3G07810   **Putative hnRNP**
    ||||||||||||||||||||
TCV CCAAAAACAAAAGAAAAGAAU 3850   **RNA-binding protein**

1218 ACAUUUUGUUUUCUUUUUUUU   At5G42860   **Unknown chloroplast**
    |||||||||||||||| :|| **protein**
TCV CCAAAAACAAAAGAAAAGAAU 3850

819 GGUUUUUCUUUUCUUUUCUUA   At4G11010   **Nucleoside diphosphate**
   ||||||| |||||||||||| **kinase 3, mitochondrial**
TCV CCAAAAACAAAAGAAAAGAAU 3850

1480 AUGUUUUGUUUUCUUUUCUUU   At2G22090   **UBP1 interacting**
    ||||||||||||||||||| **protein 1a**
TCV CCAAAAACAAAAGAAAAGAAU 3850

1107 GGUUUUUGUUUUCUUUUUCUG   At2G32960   **Tyrosine specific**
   |||||||||||||||||| : | :   **protein phosphatase**
TCV CCAAAAACAAAAGAAAAGAAU 3850

B

accession numbers) can pair 18/18 residues, while four (At3G07810.1, At2G22090, At5G42860 and At2G32960) can pair 17/17 residues (Figure 3.6A). mRNA from one gene (At4G11010) is complementary to 20 of 21 residues.

To determine if genes complementary to TvsRNA5 have altered expression in the presence of the virus, *Arabidopsis* seedlings were inoculated with TCV, TCV and satC, or inoculation buffer (Mock). At 7 dpi, RNA was extracted and pooled from 2 to 3 plants each and mRNA transcripts quantified by real-time PCR. Accumulation of transcripts corresponding to six of the seven genes was 2.4- to 4-fold lower in virus-infected plants compared with levels of transcripts in control, mock-inoculated plants (Figure 3.6B). The expression of one gene, At2G32960 was unchanged by TCV infection (see Discussion for possible explanation). The additional presence of satC did not substantially affect the level of expression of any of the genes. Since gene selection for analysis was based solely on sequence complementarity to TvsRNA5, these results suggest a possible connection between reduced gene expression and the presence of TCV vsRNA5 in the cellular small RNA population.

TCV with a deletion in the TvsRNA5 region is unable to downregulate expression of three targeted genes

To confirm that reduced transcript levels were due to the presence of TvsRNA5, plants were inoculated with TCV containing a deletion of positions 3854-3860 in the TvsRNA5 region (the construct TCVΔvs5, which was generated by Dr. Clifford D. Carpenter) (Figure 3.7A). It had been previously show that TCV with this deletion accumulates to wt levels in turnip, while TCV with a deletion of four additional bases

Figure 3.7 Effect of deleting TvsRNA5 sequence in the TCV genome on expression of putative targeted genes. (A) Location of the deletion in TvsRNA5 sequence in TCVΔvs5. The deleted sequence is boxed. (B) Levels of TCV and TCVΔvsRNA5 gRNA accumulating in infected *Arabidopsis* leaves at 7 dpi. RNA was pooled from 2 to 3 plants. Following electrophoresis, the gel was stained with ethidium bromide. The position of genomic RNA (gRNA) is indicated. The two non-viral RNAs are cytoplasmic ribosomal RNAs, which can be used as loading controls. (C) Expression of genes with sequences complementary to TvsRNA5 in virus-infected plants. mRNA accumulation levels were determined by real-time PCR. Plants were either mock inoculated (Mock) or inoculated with wt TCV (TCV) or TCVΔvs5. RNA was extracted at 7 dpi from leaf tissue pooled from 2 to 3 plants, and subjected to real-time PCR using gene-specific primers. PCR was repeated twice with different sets of plants. (D) Phenotype of rosette leaves of mock-, wt TCV-, and TCVΔvs5-infected plants at 14 dpi. Two plants for each treatment are shown. Note that young rosette leaves in the center of the plant expand more fully in plant infected with TCVΔvs5 compared with plants infected with wt TCV.

A

TvsRNA5:

UAAG$\boxed{\text{AAAAGAA}}$AACAAAAACC

C

B

D

Mock　　　　wt TCV　　　TCVΔvs5
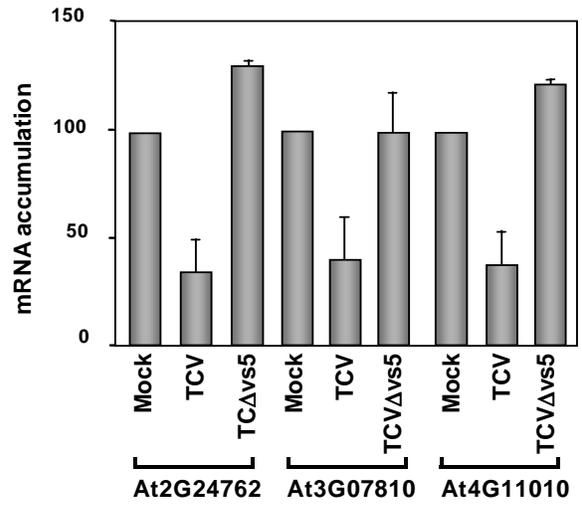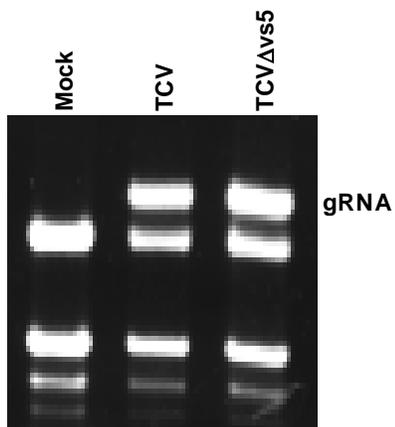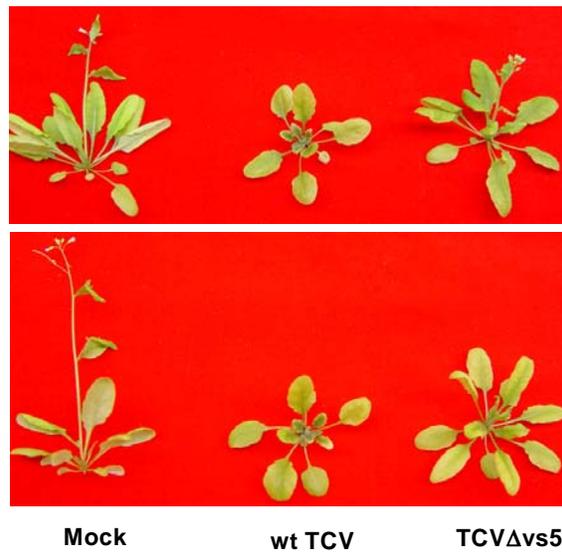
(3854-3864) accumulated to less than 20% of wt levels (Carpenter et al., 1995). Arabidopsis plants were inoculated with TCV, TCVΔvs5, or inoculation buffer, and RNA extracted and pooled from 2-3 plants each at 7 dpi. TCV and TCVΔvs5 accumulated to very similar levels in infected leaf tissue as determined by electrophoresis of total RNA followed by ethidium bromide staining (Figure 3.7B). Real-time PCR analysis was conducted for transcripts of three genes that were downregulated by the presence of wt TCV (At2G24762, At3G07810 and At4G11010). As found previously, transcript levels of the three genes were reduced in plants infected with wt TCV compared with mock-inoculated plants (2.4- to 2.9-fold; Figure 3.7C). However, in plants infected with TCVΔvs5, transcript levels for all genes were at or above levels found in mock-inoculated plants. These results strongly suggest that TvsRNA5 is able to reduce levels of transcripts with complementary sequences.

To ascertain if reduced accumulation of TvsRNA5-targeted genes affects symptom expression, plants infected with wt TCV or TCVΔvs5 were examined for symptoms at 10 and 14 dpi. At both time points, plants infected with TCVΔvs5 exhibited attenuated symptoms compared with those infected with wt TCV (Figure 3.7D). In TCV-infected *Arabidopsis*, young leaves failed to fully expand after 7 dpi and bolting was delayed or plants failed to bolt. In contrast, TCVΔvs5-infected plants had leaves only slightly reduced in size at 10 and 14 dpi compared with mock-inoculated plants. In addition, all plants bolted, although the bolt was stunted compared with mock-inoculated plants. These results strongly suggest that TvsRNA5 reduces the expression of transcripts with complementary sequences, which either directly or indirectly are responsible for a subset of symptoms expressed by TCV.

5' RACE assay of fragments produced by putative TvsRNA5-guided RISC cleavage of plant mRNA

Since TvsRNA5 is able to reduce levels of transcripts with complementary sequences (Figure 3.6 and 3.7) and its putative target sequence is in the 3' UTR of all these mRNAs, it is possible that reductions in mRNA are caused by RISC-mediated cleavage or decreasing the stability of the mRNA. It was recently reported that an animal miRNA affects the AU-rich stability determinant in the 3' UTR of an mRNA (Jing et al., 2005). TvsRNA5-guided cleavage events should be in predicted locations of host mRNAs (Figure 3.6A) and produce fragments of shortened sizes. Therefore, 5' RACE (see Materials and Methods) was performed to amplify the 3' fragment generated by putative cleavage of At3G07810. The expectation was that the presence of full-length At3G07810 mRNA in plants would result in an approximately 2800-bp cDNA fragment, and that in wt TCV-infected plants, level of this cDNA would be much lower due to the RNA cleavage. Amplification of the 3' fragment generated by putative cleavage of At3G07810 would generate a 450-bp cDNA fragment.

PCR products were separated on a 1.2% ethidium bromide-staining agarose gel along with 1kb and 100 bp ladders (M1 and M2, respectively, Figure 3.8). As shown in Figure 3.8, one 700-bp DNA fragment was amplified by the 5' RACE PCR of the 700-nt control RNA (CK), which was provided by the manufacturer. However, no detectable products were found in other samples that do not contain the control RNA. Therefore, the current results cannot determine whether or not At3G07810 mRNA is cleaved or not.
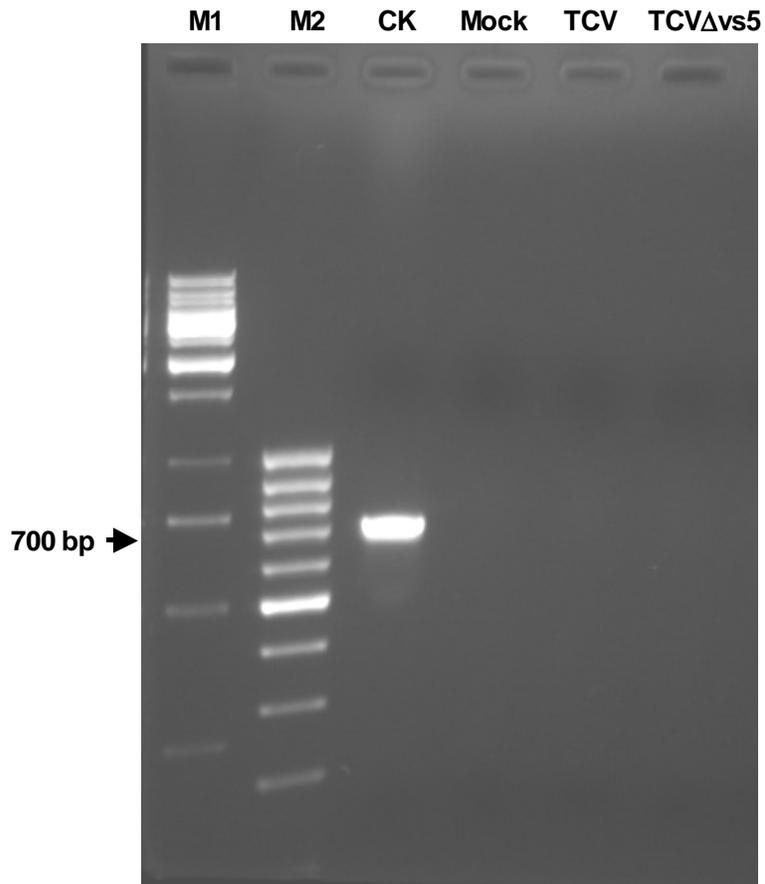
Figure 3.8 5' RACE assay of putative fragments produced by TvsRNA5-guided cleavage of *Arabidopsis* At3G07810 mRNA. Plants were either mock inoculated (Mock) or inoculated with wt TCV or TCVΔvs5. RNA was extracted at 7 dpi from leaf tissue pooled from five plants, and subjected to 5' RACE. PCR products were separated on a 1.2% ethidium bromide-staining agarose gel. M1, 1 kb DNA ladder; M2, 100 bp DNA ladder; CK, control.

The presence of satC reduces levels of TCP4 mRNA in infected *Arabidopsis* plants

As described in Chapter I, coinoculation of satC and TCV into plants leads to severe leaf crinkling, which is not visible in plants inoculated with TCV alone. Very similar leaf crinkling can be observed in *Arabidopsis* plants with mutations in its JAW locus that encodes an miRNA (miR-Jaw) (Palatnik et al., 2003). These mutations resulted in a substantial increase in levels of miR-JAW and a concomitant decrease in levels of miR-JAW-targeted gene transcripts, which are members of the TCP family of transcription factors (Palatnik et al., 2003). BLAST searches of the *Arabidopsis* genome against the reverse complement of CvsRNA1 revealed complementarity to TCP4, a member of the TCP family. The TCP4 mRNA is complementary to 19 of 22 CvsRNA1 residues with several mismatches (Figure 3.9A).

To test whether the presence of satC affects levels of TCP4 mRNA, *Arabidopsis* plants were inoculated with TCV, TCV and satC, or inoculation buffer (Mock). At 7 dpi, RNA was extracted and pooled from 2 to 3 plants each and levels of TCP4 mRNA transcripts were assayed by real-time PCR. As shown in Figure 3.9B, TCP4 transcripts in the mock plants and the TCV-infected plants accumulated to similar levels, suggesting that TCV does not affect levels of TCP4 mRNA. However, in plants coinfected with TCV and satC, TCP4 transcripts accumulated to only about 25% of those in the mock plants, suggesting that satC affects TCP4 expression, possibly by CvsRNA1-directed cleavage of TCP4 transcripts.

A

```
CvsRNA 1      CCAAAAGU—GCGAGGG—CAUGAAC
              | | | | | | | |   | | | | | | |   | | | |
TCP4 1201     GGUUUCUGUUCGCUCCUCCUACUC
```

B
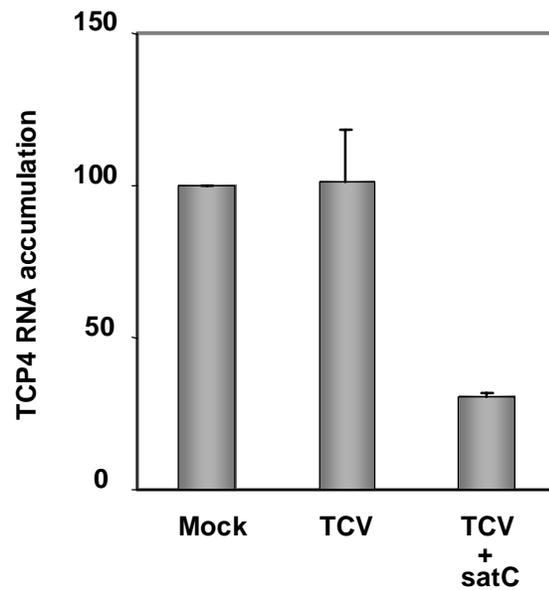
Figure 3.9 The presence of satC affects accumulation levels of TCP4 mRNAs in infected plants. (A) Complementarity between CvsRNA1 and TCP4 mRNA revealed by BLAST. (B) Levels of TCP4 mRNA at 7 dpi as determined by real-time PCR.

Discussion

In this Chapter, I cloned and sequenced vsRNAs derived from TCV or satC that are in comparable sizes and distribution to those previously reported for CymRSV (Molnár et al., 2005). TCV and satC vsRNAs ranged in size from 18-24 nt, similar to the size range of host miRNAs (18-25 nt) (Bartel, 2004; Kidner and Martienssen, 2005). The vast majority (92%) of TvsRNAs were derived from plus-strands, compared with 80% positive polarity for CymRSV vsRNAs (Molnár et al., 2005). Seventy-three percent of TCV vsRNAs were excised from one of five hotspot regions, with members containing slightly staggered ends. Many CymRSV vsRNAs were also clustered with slightly staggered ends, and duplexes accumulating in infected tissue contained mismatches indicating the two strands in excised RNA duplexes were not perfectly paired (Molnár et al., 2005). Results with TCV therefore support the hypothesis that vsRNAs are derived from structured regions of RNA viral genomes but not from fully dsRNA species. The enzyme responsible for biogenesis of vsRNAs in the cytoplasm where RNA viruses replicate is not known, although a transient reduction in TCV vsRNA levels was reported in TCV-infected *dcl2-1* plants (Xie et al., 2004). Interestingly, vsRNAs have only been found associated with nuclear replicating DNA viruses in animal cells (Pfeffer et al., 2005; Sullivan and Ganem, 2005). This could reflect differences in dicers and RNA silencing pathways in plants and animals (Chen, 2005; Du and Zamore, 2005).

Of the seven host genes with complementarity to TvsRNA5 selected for analysis, six showed reduction in mRNA levels from 2.6- to 4-fold in the presence of wt TCV. Microarray analysis of expression differences in Arabidopsis plants infected with TMV

118

revealed only 35 genes reduced between 1.9- and 4.6-fold among the 8,000 to 10,000 mRNAs analyzed (Golem and Culver, 2003). Similar studies using CMV (Dinesh Kumar, personal communication) or TuMV (Steven Whitham, personal communication) revealed expression reductions for only 400 of 25,000 mRNAs or 220 of 24,000 mRNAs, respectively.

The one gene that was not detectably altered in virus-infected plants (At2G32960) had 17 consecutive bases complementary to TvsRNA5, similar to the level of complementarity for other TvsRNA5-targeted mRNAs and for host miRNA targeting (Roades et al., 2002; Schwab et al., 2005). Analysis of known miRNA-mRNA pairs indicate that exact matches are uncommon at the very 5' and 3' ends, (Haley and Zamore, 2004; Mallory et al., 2004). The poor complementarity between positions 1-4 at the 5' end of TvsRNA5 and At2G32960 transcripts, with four mismatches or G:U pairs, may therefore account for lack of altered gene expression. Alternatively, the structural context of the target sequence in At2G32960 mRNA may make the region inaccessible for pairing with TvsRNA5.

The sequences complementary to TvsRNA5 in all six targeted mRNAs are located in the 3' UTR. In plants, target sequences for miRNAs are normally within the coding region (Roades et al., 2002), however, several sequence targets of *Arabidopsis* miR156 are within the 3' UTR (Bartel, 2004). As shown in Figure 3.8, 5' RACE was performed to test if TvsRNA5-specific reductions in mRNA levels are due to cleavage of the RNAs or involvement with 3' UTR mRNA stability determinants. In this experiment, the failure of cDNA amplification might be caused by some suboptional PCR conditions such as primer designs, which need to be modified or corrected in the future. RNA decay

mediated by numerous intracellular mechanisms would shorten the fate of RNA in cells, which may prevent recovery of the fragments. To enhance the recovery of these potential fragments, *Arabidopsis* Xrn4 mutants, which are compromised in the miRNA-mediated decay pathway and thus contain elevated levels of 3' ends following RISC-mediated cleavage events (Souret et al., 2004), may be used.

The 5' RACE can also be preformed to test if the TCP4 mRNA reduction in the presence of satC results from RNA cleavage guided by CvsRNA1 or other satC-derived vsRNAs. Although 18- to 40-nt RNA species were eluted from the gel during the small RNA cloning, satC-specific LssRNAs were not recovered. Explanations for this result are possible: (i) the single-stranded LssRNAs may be much more unstable than the vsRNAs generated by Dicer processing in cells; (ii) LssRNAs may not be completely denatured in 8% denaturing polyacrylamide gel, which may inhibit the ligation to adapters by keeping some secondary structures folded; and (iii) LssRNAs may be terminally methylated by cellular enzymes, which may inhibit ligation to adapters.

CHAPTER IV

A NOVEL PROCEDURE FOR THE LOCALIZATION OF VIRAL RNAS IN PROTOPLASTS AND WHOLE PLANTS

Introduction

The ability to track the movement of viruses non-evasively using co-expressed reporter proteins has provided a wealth of information on cell-to-cell and long distance movement of some viruses in host plants (Baulcombe et al., 1995; Cheng et al., 2000; Roberts et al., 1997). Methods for co-expression of reporter proteins such as the *Aequorea victoria* green fluorescent protein (GFP) have relied on the engineering of new viral mRNA transcripts expressed from natural or ectopic subgenomic RNA promoters (Baulcombe et al., 1995), the fusion of reporter proteins to amenable viral proteins such as the CP or movement proteins (Heinlein et al., 1995; Santa Cruz et al., 1996), or the addition to, and subsequent cleavage from, viral expressed polyproteins (Dolja et al., 1992; Verver et al., 1998). In addition, some viruses encode proteins not required for systemic movement within the host (as opposed to transfer between hosts) and such proteins can be replaced with reporter proteins (Gardiner et al., 1988; Scholthof et al., 1993). Such methods require substantial modification of the viral genome and can lead to alterations in viral accumulation or pathogenesis (Cohen et al., 2000). Furthermore, such methods have only been successfully applied to a small percentage of RNA viruses, since many viruses, especially those packaged in size restrictive icosahedral capsids (Qu and

Morris, 1997), cannot tolerate insertion of large non-viral segments or loss of any open reading frames (ORFs). Thus, alternative procedures are necessary for the non-evasive detection of most viruses.

TCV is an example of an RNA virus that cannot tolerate added genomic sequences and requires all five of its ORFs for replication and systemic movement (Figure 4.1A). Unlike rod shaped viruses such as TMV or PVX that are relatively unaffected by the insertion of additionnal sequences, TCV has a strict genome size preference and cannot tolerate insertions of more than a few hundred bases (Qu and Morris, 1997). Furthermore, all TCV ORFs overlap, and encoded proteins are non-functional when fused to GFP (Cohen et al., 2000).

Recently, a novel technique was established for the direct real time visualization of mRNAs in living yeast cells. The technique made use of a well studied interaction between the CP of MS2 bacteriophage (CP_{MS2}) and a 19 base MS2 hairpin (hp), which naturally results in repression of translation of the phage replicase (Fouts, et al., 1997; Valegard et al., 1997). By fusing CP_{MS2} to GFP and a nuclear localization signal (NLS), the fusion protein was transported into the nucleus upon expression in transfected yeast. However, addition of six CP_{MS2} hp binding sequences to the 3' UTR of specific yeast mRNAs resulted in binding of the fusion protein to the mRNA thus relocating the fusion protein to the cytoplasmic environ containing the mRNA where GFP fluorescence was readily detectable (Bertrand et al., 1998).

This technique has now been adapted for localization of viral RNAs within whole plants. Transgenic plants expressing the GFP-NLS-CP_{MS2} fusion protein were generated and GFP only became cytoplasmically localized when transgenic plants were infected

Figure 4.1 Basic components of the RNA tracking system. (A) Location of the inserted hp in the TCV genome. The 19 base hp (in blue) targeted by CPMS2 was inserted just 3' of the TCV CP ORF. (B) Sequence of the 19 base hp (in blue) and flanking sequences in TCV-hp. TCV sequences are in black except for the stop codon of the CP ORF, which is in red. Bases in green are linker sequences designed to allow multiple head-to-tail inserts of the hp, had it been required. (C) Schematic of the rationale behind the RNA tracking procedure. Large circles represent individual cells. Expression of the GFP-NLS-CPMS2 fusion protein alone leads to nuclear (N) sequestration of the fusion protein.   In the presence of TCV-hp, CPMS2 (red hexagon) binds to the 19 base hp in the TCV-hp 3' UTR thus GFP (green hexagon) is retained in the cytoplasm.

A

TCV (4054 b)

B

CP_{MS2}-targeted hairpin

3792

AAUU UAG UAC UUGGCGCGC GACGCGUCG GUAAUAGUGUA

TCV CP ORF

C
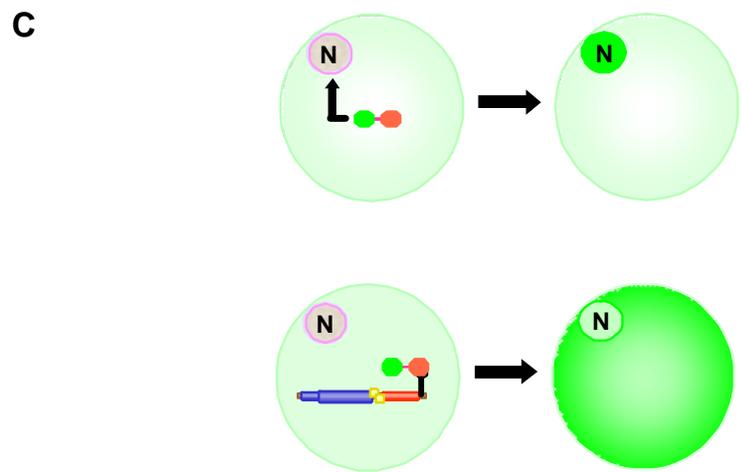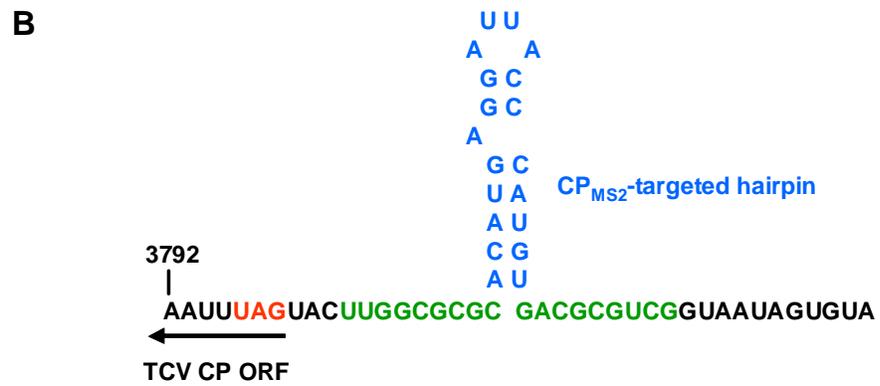
with TCV containing a single CP_{MS2} binding hp (Figure 4.1 A and B). Neither the presence of the 19 base hp in the viral 3' UTR, nor the interaction of the virus with the fusion protein, detectably impaired any viral function. Thus this technique should be amenable to the study of viruses with transformable plant (or animal) hosts and should also prove useful for the detection of host RNAs engineered to contain the 19 base hp.

Materials and Methods

Constructs

To insert the 19-base hp target (Figure 4.1B) of CP_{MS2} into the 3' UTR of TCV, a linker (Table 4.1) with *Bss*HII and *Mlu*I recognition sites was introduced into the TCV *Sna*BI site previously constructed at position 3802 by deletion of one base in pTCV66 (Carpenter et al., 1995). The linker was used to ensure head-to-tail insertion of multiple hairpins, if more than one hp was necessary to sequester GFP in the cytoplasm. Insertion of the linker into *Sna*BI-digested pTCV66 was performed using T4 DNA ligase (Invitrogen) (see Figure 4.2 for procedure flow chart). The resulting ligation products were digested with *Bss*HII and *Mlu*I, and gel purified to produce a linear plasmid molecule lacking the *Bss*HII-*Mlu*I fragment. A DNA fragment containing the 19 base hp sequence flanked by *Bss*HII and *Mlu*I sites was synthesized by Invitrogen, treated with *Bss*HII and *Mlu*I, gel-purified, and then ligated to the plasmid lacking the *Bss*HII-*Mlu*I fragment to generate pT7TCV-hp. pT7CPm3-hp was generated by using the same method to insert a hp into pT7CPm3, which contains a T7 RNA polymerase promoter upstream of full-length plus-strand sequence of CPm3 (Wang and Simon, 1999).

Table 4.1 Oligonucleotides used in Chapter IV

Application	Name	Sequence[a]
Plasmid construction	Linker	5'-TTG**GCGCGC**CAACG**ACGCGT**CG
	OliogMS2F	5'-GA**AGATCT**<u>ATGGCTCCAAAGAAGAAGAGAA AGGT</u>**C**GCTTCTAACTTTACTCAG
	OligoMS2R	5'-GA**AGATCT**CTAGTAGATGCCGGAGTTTGC

[a] The SV40 NLS sequence in OliogMS2F is underlined. Bold residues denote *Bss*HII and *Mlu*I sites in Linker and a *Bgl*II site in both OliogMS2F and OligoMS2R.
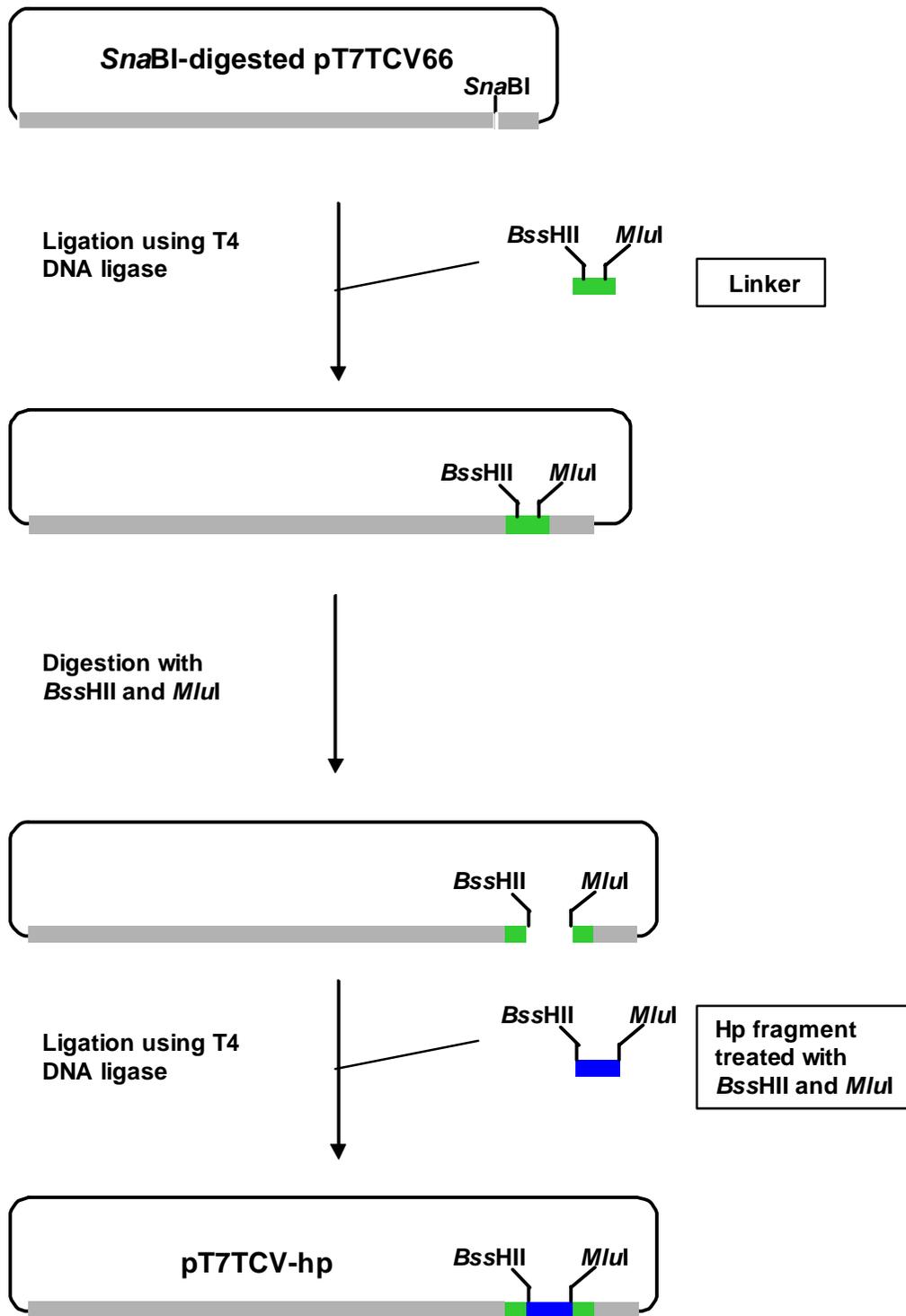
Figure 4.2 Flow chart for construction of pT7TCV-hp. See text for details.

An expression vector for GFP-NLS-CP$_{MS2}$ was constructed using pAVA321 containing a dual *Cauliflower mosaic virus* (CaMV) 35S promoter, the TEV translational enhancer, GFP coding sequence and the CaMV 35S transcriptional terminator (Figure 4.3, upper panel; von Arnim et al., 1998), which was kindly provided by A.G. von Arnim. The CP$_{MS2}$ ORF was obtained from pG14-MS2-GFP/LEU (Bertrand et al., 1998), which was kindly provided by R.H. Singer. A fragment containing the CP$_{MS2}$ ORF was amplified by PCR from pG14-MS2-GFP/LEU using OliogMS2F and OliogMS2F as primers (Table 4.1). The NLS of SV40, which is functional in *Arabidopsis* (Chiu et al., 1996; Van der krol and Chua, 1995), is included in the sequence of OliogMS2F (Table 4.1). The PCR products were digested with *Bgl*II, gel-purified, and then inserted into the *Bgl*II site at the 3' end of the GFP ORF in pAVA321, generating pGNC (Figure 4.3, lower panel). The pGNC was transformed into *E. coli* competent cells (Invitrogen) using the method recommended by the manufacturer and selected for Kanamycin resistance. pGNC DNA was prepared using the large-scale plasmid DNA isolation method described in Chapter II.

For use in plant transformation, the GFP-NLS-CP$_{MS2}$ expression cassette was removed from pGNC with *Pst*I, gel-purified, and then inserted into the *Pst*I site of the T-DNA vector pCGN 1547 (Calgene, Davis, CA), generating pTGNC. pTGNC was then transformed into the *Agrobacterium tumefaciens* strain ASE competent cell (Monsanto) using an electroporation method as recommended by the manufacturer. The plasmids were selected for chloramphenicol and Kanamycin resistance.

Figure 4.3 The plasmids pAVA321 ans pGNC. Some of the restriction enzyme sites contained in the plasmids are shown. Arrows indicate the direction of transcription. P35S, a dual CaMV 35S promoter; TE, TEV translational enhancer; GFP, GFP coding sequence; T35S, CaMV 35S transcriptional terminator.
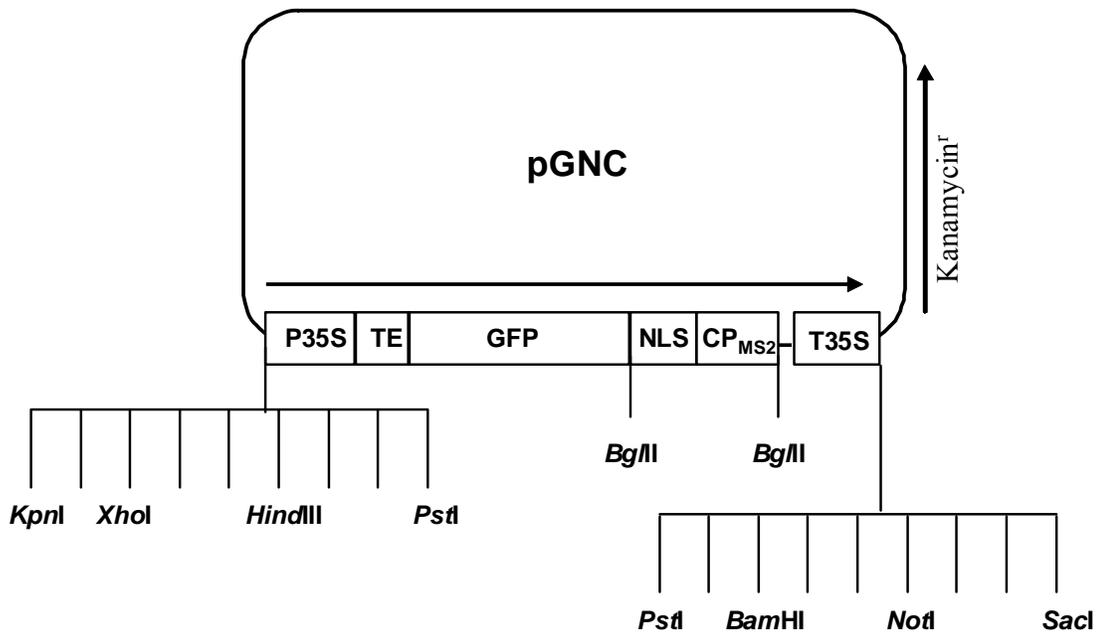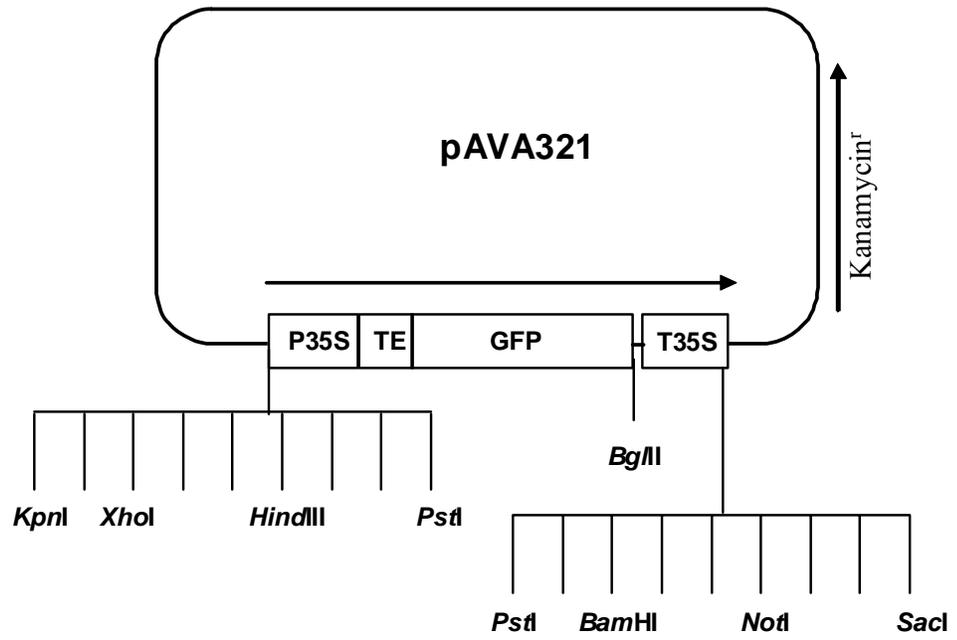
Protoplast transfection

Arabidopsis protoplasts were freshly prepared using the method described in Chapter II. Protoplast transfections with a combination of plasmid DNA and viral RNA transcripts were performed as described previously for tobacco mesophyll protoplasts (Chiu et al., 1996; Liu et al., 1994). Briefly, 20 µg of pGNC or pAVA321 DNA with or without 20 µg of viral RNA transcripts, which were prepared using T7 RNA polymerase from *Sma*I-linearized pT7TCV-hp or pT7CPm3-hp, were mixed with protoplasts (0.5 X 10^6 cells) in transfection buffer A containing 0.4 M mannitol, 20 mM $CaCl_2$, and 5 mM MES, pH 5.7 to get a final volume of 250 µl. The mixture were then added to 250 µl of transfection buffer B (pH 10.0), which contains 40% polyethylene glycol (PEG) 4000, 0.4 M mannitol, and 100 µM $Ca(NO_3)_2$. After incubation at 25°C for 10 minutes, the mixture was added to 3 ml of PCM, followed by incubation at 25°C for 18 to 24 hours in the dark.

Plant transformation

Agrobacterium-mediated plant transformation with pTGNC was performed using the vacuum infiltration method as previously described (Clough and Bent, 1998) with modifications. Briefly, *Arabidopsis* ecotype Col-0 seeds were grown in a growth chamber at 20°C with a 16-hour light/8-hour-dark cycle as described in Chapter II. Primary bolts of plants starting to flower were removed to induce more secondary bolts. Plants containing the maximum number of immature flower clusters (about six-week old) were used for transformation. *Agrobacterium* containing pTGNC were grown in 250 ml LB containing chloramphenicol (30 µg /ml) and kanamycin (50 µg/ml) at 28°C for 24 hours

with continuous shaking (150 rpm). The bacterial cells were collected by centrifugation in a Sorvall GSA rotor at 3000 g for 15 minutes and resuspended in 5% sucrose solution with OD_{600} adjusted to 0.8. The resulting bacterium solution was then mixed thoroughly with Silwet L-77 with the concentration of Silwet L-77 adjusted to 0.02-0.05%. Infiltration was performed by placing the above-ground parts of plant in the prepared bacterium solution followed by application of a 20-second vacuum in a vacuum chamber. The infiltrated plants were covered with a plastic dome, placed at the dark overnight, and then moved to normal growth condition to set seeds. Putative transformed seeds were selected for kanamycin resistance on 0.5X MS agar media (pH 5.8) containing 0.5% MS, 0.8% agar, and 100 mg/L kanamycin. Transgenic progeny were screened for GFP-fluorescent nuclei using confocal microscopy.

GFP visualization by confocal microscopy

Protoplasts transfected with plasmid DNA with or without viral RNA were observed in a Lab-Tek Chamber (SlideSystem-2 Well Chambered Cover-glass, Nunc, Nalgene, NY Catalog #, 155382). Transgenic *Arabidopsis* plants were inoculated with viral RNA transcripts using the methods described in Chapter II. At 14 dpi, leaves were excised from infected plants, mounted in water on a slide (Micro Slide, Corning Glass Works, Catalog # 2948), and covered with a coverslip (#1 micro cover glass, VWR Scientific, PA, Catalog # 48366067). This coverslip was used in order to focus a short working distance lens. The slide was sealed around the coverslip with nail polish to prevent evaporation of water and stabilize the coverslip. A Zeiss LSM510 laser scanning confocal microscopy equipped with an argon ion laser was used to visualize GFP

localization in living cells. GFP was excited with blue laser light at 488 nm and transmitted through a 505/550 nm band pass emission filter. Laser power between 5% and 30% was used.

Results and Discussion

Insertion of the CP_{MS2} binding sequence into the 3' UTR of the TCV genome does not affect viral accumulation or pathogenicity

My rationale for adapting the Bertrand et al. (1998) procedure to detect RNA virus movement in whole plants was based on the fact that most plant cells having compact nuclei that would allow nuclear localized GFP to be easily distinguished from cytoplasmic GFP. By constitutively expressing a fusion protein containing GFP, a NLS, and the CP_{MS2} (GFP-NLS-CP_{MS2}), the protein should be sequestered in the nuclei of all cells capable of expressing the 35S promoter (Figure 4.1C, upper panel). However, a cytoplasmic RNA containing the 19 base hp target of CP_{MS2} should cause the GFP fusion protein to bind to the RNA and thus be localized mainly in the cytoplasmic venue of the bound RNA (Figure 4.1C, lower panel).

As detailed in Materials and Methods, the GFP-NLS-CP_{MS2} fusion protein expression plasmid pGNC contains dual CaMV 35S promoters, the TEV translational enhancer, an inframe fusion of the GFP ORF (von Arnim et al., 1998), an NLS functional in *Arabidopsis* (Chiu et al., 1996; Van der krol and Chua, 1991) and the CP_{MS2} ORF (Bertrand et al., 1998). Protoplasts transfected with this construct displayed bright green fluorescence in nuclei when examined by confocal microscopy under blue light at 18 to

24 hour post-transfection with only traces of fluorescence visible in the cytoplasm (Figure 4.4, D-F). This was in contrast to the overall fluorescence found in cells transfected with a construct containing the identical 35S promoter but expressing only GFP (Figure 4.4, B and C).

To achieve cytoplasmic localization of GFP-NLS-CP$_{MS2}$, the 19 base MS2 hp needed to be inserted into the TCV genome without interfering with replication or movement of the virus. Although six hp were added to yeast mRNAs to achieve cytoplasmic relocalization of the fusion protein (Bertrand et al., 1998), the much higher levels of TCV RNA accumulation in infected cells (detectable by ethidium bromide staining following agarose gel electrophoresis of total cellular RNA) suggested that a single hp might suffice for relocalizing the fusion protein to the cytoplasm where TCV and other RNA viruses replicate. To avoid interfering with translation, the 19 base hp flanked by a linker sequence was inserted in the TCV 3' UTR five bases downstream of the CP ORF termination codon at a *Sna*BI site in the corresponding cDNA, generating TCV-hp (Figure 4.1B). This enzyme recognition site was previously engineered into wtTCV genomic RNA by deletion of a single base at position 3802, and minor alterations at this location in the TCV genome did not disrupt TCV accumulation in plants and protoplasts (Carpenter et al., 1995).

To determine if insertion of the 19 base hp into this location in the TCV genome affected viral accumulation in *Arabidopsis* ecotype Col-0 protoplasts, in vitro synthesized transcripts of wt TCV and TCV-hp were inoculated into protoplasts and viral accumulation assayed at 40 hpi. As shown in Figure 4.5A, TCV-hp genomic RNA (lanes 2 and 4) accumulated to a similar level as wt TCV genomic RNA (lanes 1 and 3). The

Figure 4.4 GFP fluorescence in *Arabidopsis* protoplasts. Protoplasts were transfected with buffer (A), pAVA321 expressing GFP alone (B and C), pGNC alone (D-F), pGNC and wtTCV transcripts (G-I), or pGNC and TCV-hp (J-L). The fluorescent signal was detected using a laser scanning confocal microscope under blue light at 18 to 24 hpi. Bar = 5 μm.
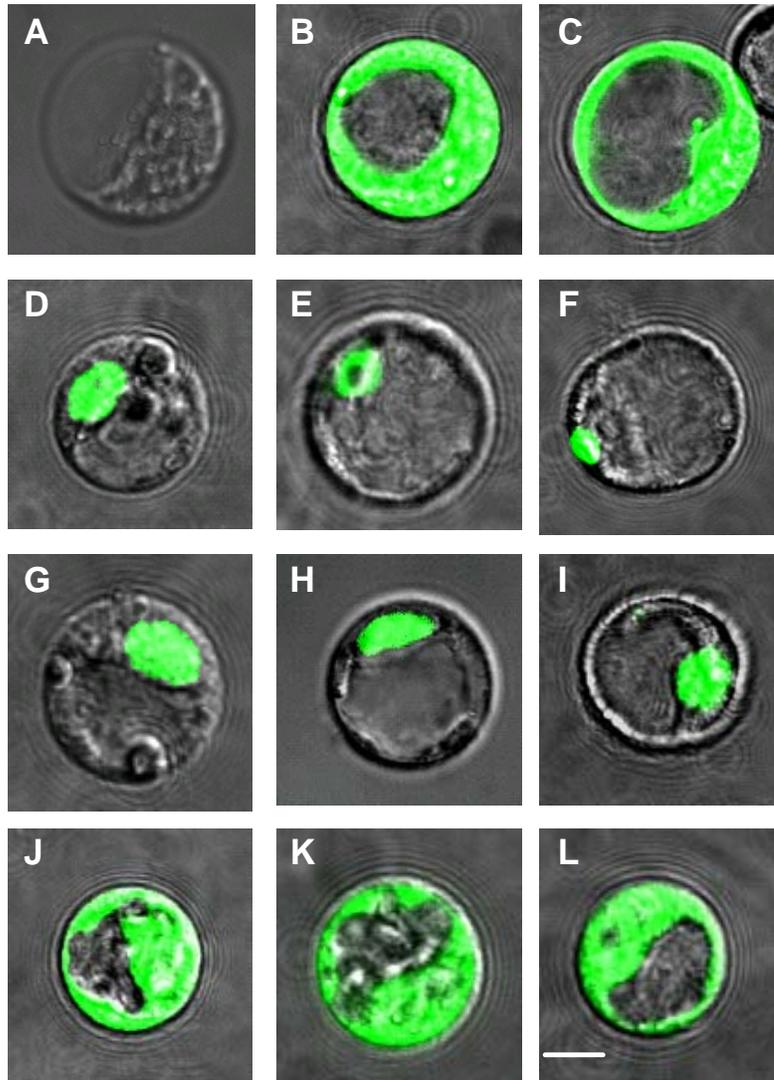
Figure 4.5 Accumulation of TCV-hp in protoplasts and virulence in plants. (A) Accumulation of wt TCV and TCV-hp in *Arabidopsis* protoplasts. Protoplasts were inoculated with wtTCV or TCV-hp transcripts and total RNA extracted at 40 hpi. RNA was subjected to electrophoresis and stained with ethidium bromide. Two repetitions of the experiment are shown. (B) Symptoms associated with infection of wt TCV or TCV-hp in *Arabidopsis* plants at 14 dpi. Seedlings of *Arabidopsis* ecotype Col-0 were inoculated at the six to eight leaf stage with buffer alone (Mock), wt TCV or TCV-hp transcripts, as indicated.

A

wt TCV TCV-hp wt TCV TCV-hp

← TCV

1   2   3   4

B

Mock   wt TCV   TCV-hp
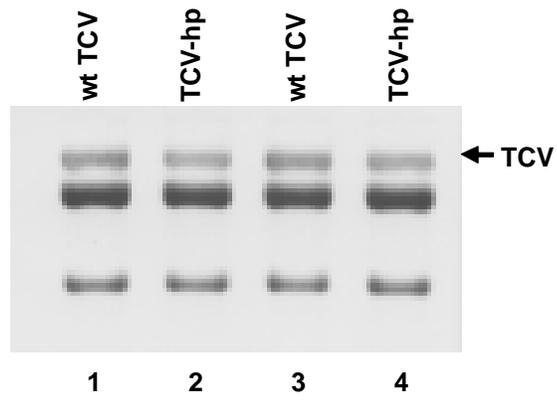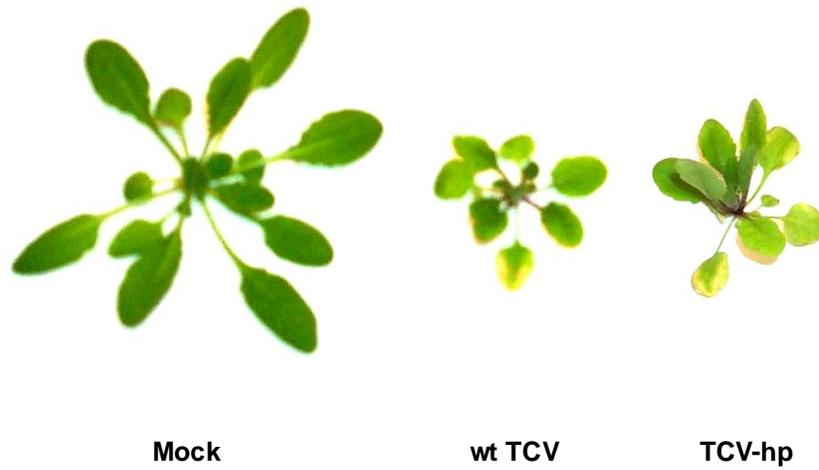
inserted hp was also tested for affect on virus pathogenesis by inoculating wt TCV and TCV-hp RNA transcripts onto *Arabidopsis* Col-0 seedlings. At 14 dpi, there was no detectable difference in symptoms caused by wt TCV or TCV-hp (Figure 4.5B), indicating that the insertion did not substantially affect TCV interaction with the host plant.

Replication of TCV-hp in protoplasts can relocate GFP-NLS-CP$_{MS2}$ from the nucleus to the cytoplasm

To test if the single hp insert in TCV-hp was able to localize the GFP-NLS-CP$_{MS2}$ fusion protein in the cytoplasm, protoplasts were transfected with pGNC and wt TCV or TCV-hp transcripts. As shown in Figure 4.4G-I, GFP fluorescence remained localized in the nuclei of protoplasts co-transfected with pGNC and wt TCV but became cytoplasmic when cells were co-transfected with TCV-hp RNA (Figure 4.4, J-L). This result indicated that the presence of wt TCV had no effect on GFP-NLS-CP$_{MS2}$ localization and did not promote any detectable non-specific nuclear leakage or non-specific binding of the fusion protein to wt TCV RNA. In addition, binding of the fusion protein to the 3' UTR of TCV-hp still permitted TCV-hp accumulation in the cytoplasm, indicating that the viral RNA-dependent RNA polymerase responsible for TCV replication was able to perform its function in the presence of the fusion protein. If TCV-hp had been unable to accumulate in cells in the presence of GFP-NLS-CP$_{MS2}$, I could have modified the 19 base hp to reduce the binding efficiency of CP$_{MS2}$ since mutations in the hp that either increase or decrease binding have been well characterized (Lim et al., 1994; Romaniuk et al., 1987).

139

Generation of transgenic *Arabidopsis* constitutively expressing GFP-NLS-CP$_{MS2}$

To determine if this method could be used to detect virus in whole plants, the GFP-NLS-CP$_{MS2}$ expression cassette was transformed into *Arabidopsis* ecotype Col-0 by *Agrobacterium*-mediated vacuum infiltration. Transformants were selected for kanamycin resistance and then examined by confocal microscopy for nuclear localized GFP, which was especially evident in transparent roots. As shown in Figure 4.6, GFP was also visible in nuclei of leaf epidermal cells, trichomes, and petioles of positive plants. This coincides with the constitutive CaMV 35S promoter-regulated gene expression in tissues as reported previously (Chytilova et al., 1999). GFP fluorescence was more readily detected in younger leaves than in older leaves, consistent with previous reports that younger tissue has higher levels of protein expression from the 35S promoter (Chytilova et al., 1999; Williamson et al., 1989). Positive plants were allowed to self-fertilize and progeny were subjected to a similar selection strategy. Selected positive progeny were self-fertilized, and their progeny were screened for GFP-fluorescent nuclei. Homozygous progeny of a homozygous parent were selected for further analysis. These transgenic plants have been named "AtGNC ".

Visualization of TCV movement in AtGNC plants

The oldest leaf pair (1st and 2nd real leaves) of AtGNC seedlings (six to eight leaf stage) was inoculated with TCV-hp RNA transcripts and leaves examined at 2 to 16 dpi. No differences in symptoms were expressed by the AtGNC-infected plants compared with wt Col-0-infected plants throughout the experiment (data not shown). In inoculated leaves, cytoplasmic GFP fluorescence was readily detectable in small clusters of

Figure 4.6 GFP fluorescence in nuclei of transgenic AtGNC plants (two-week old) expressing the GFP-NLS-CPMS2 fusion protein. Green fluorescent nuclei were detected in leaf epidermal cells (A, bar = 20 μm); leaf epidermal cells under lower magnification (B, bar = 50 μm). The false red background is shown for easy detection of the signal; leaf trichome cell (C); petiole (D); and root (E). Bars (C-E) = 50 μm. All images were generated using composite fluorescent and transmitted light.
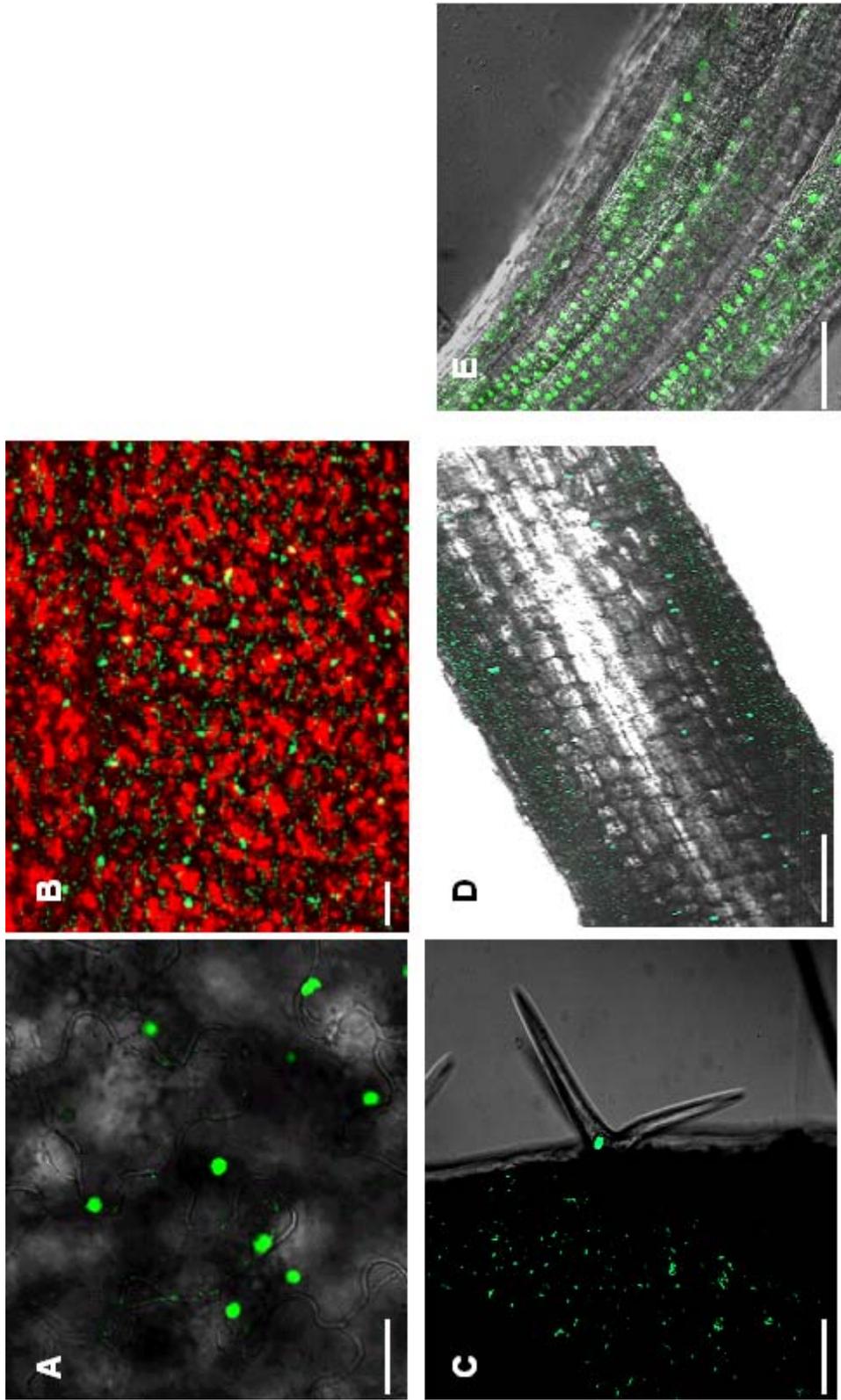
epidermal cells by 2 dpi (Figure 4.7, A-C), indicating that TCV was replicating and able to traffic cell-to-cell despite the cellular presence of a foreign binding protein. No cytoplasmic GFP fluorescence was detected in non-inoculated transfected leaves using identical imaging conditions (data not shown). Irregularly shaped fluorescent clusters of at least 20 cells were detected at 3 dpi (Figure 4.7, F-H). The irregular shapes of the infection sites may have resulted from directional cell-to-cell movement influenced by veins close to inoculated cells or the direction of the assimilate flow. Bright foci of GFP fluorescence were also detected at 2 dpi in some trichomes and trichome support cells (a collection of large, regularly shaped epidermal cells that surround the base of the unicellular trichome) (Figure 4.7, D and E). No cytoplasmic GFP fluorescence was detected in any cells adjacent to the trichome support cells. It is likely that trichome infection in the inoculated leaves resulted from the manual inoculation procedure (rubbing the leaf with viral transcripts and an abrasive) with the virus descending into the base support cells as opposed to movement into these cells from surrounding epidermal cells (see below).

Individual leaves excised from one TCV-hp infected AtGNC plant and one mock-inoculated AtGNC plant were observed for cytoplasmic GFP fluorescence at 16 dpi. As shown in Figure 4.8, top row, little, if any fluorescence was detected (cytoplasmic or nuclear) in uninfected leaves under the same imaging conditions used to detect the very strong cytoplasmic GFP fluorescent signals found in most infected leaves. The levels and pervasiveness of cytoplasmic fluorescence in TCV-hp-infected leaves varied substantially depending on the age of the leaf, with weak fluorescence visible in the 3rd and 5th leaves and very strong fluorescence detected throughout the 9th leaf (Figure 4.8, middle and

Figure 4.7 GFP distribution in inoculated leaves of TCV-hp-infected AtGNC plants. Cytoplasmic fluorescence at 2 dpi in epidermal cells (A and C, bars = 50 μm; B, bar = 26 μm) and trichomes support cells (D and E, bars = 80 μm). Red arrows denote the trichome branches and the regularly shaped support cells. Infection sites comprising at least 20 visible cells at 3 dpi. (F-H), bars = 100 μm. Images A, B, C, F, G, and H were generated using the fluorescent channel only. Images D and E were generated using composite fluorescent and transmitted light.
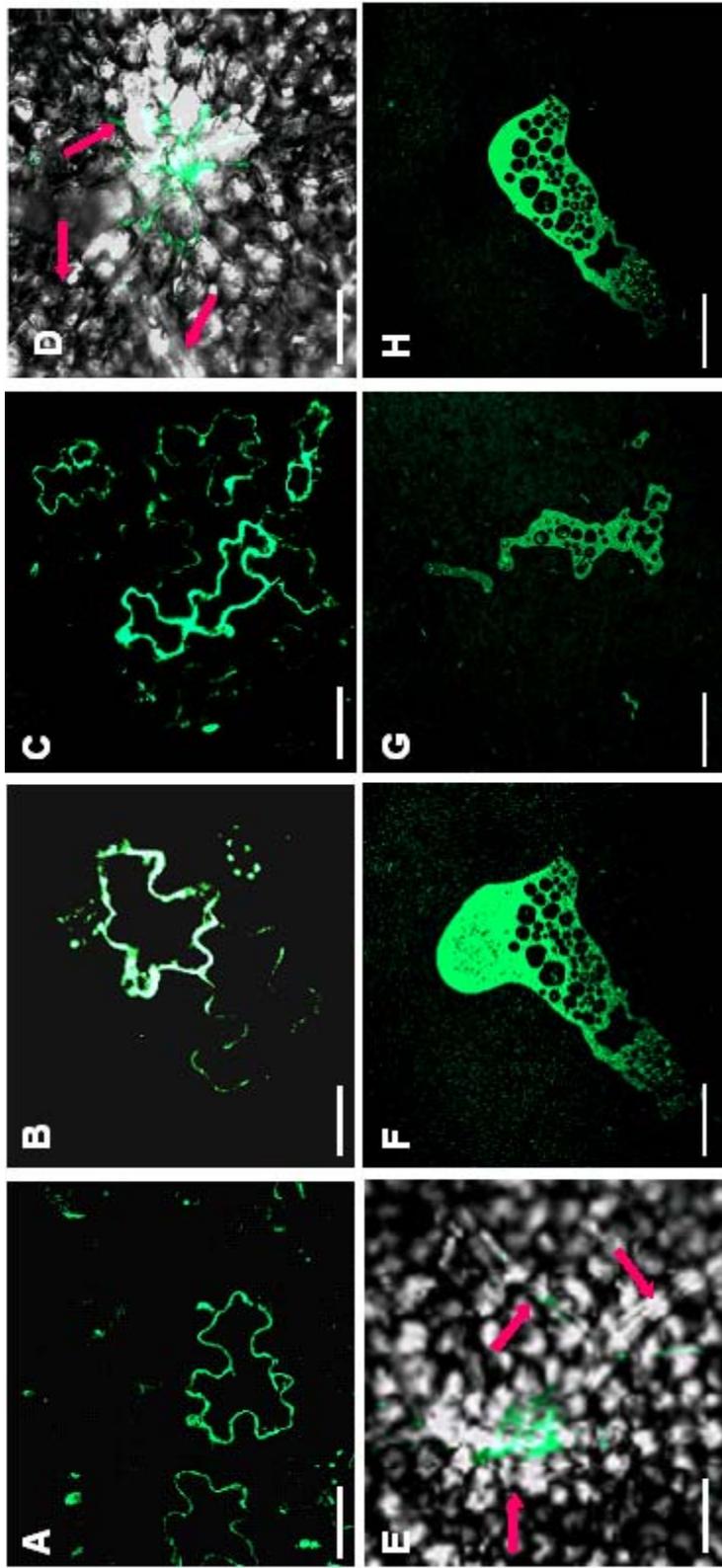
Figure 4.8 GFP distribution in systemically infected leaves of AtGNC plants. Individual leaves were removed from a single plant at 16 dpi and subjected to confocal microscopy. All images are produced by fluorescence and transmitted light. Bars = 400 μm. Top row are four leaves from one AtGNC plant at 16 days after mock inoculation with infection buffer. Numbers (3rd, 5th, 7th, 11th) refer to the age of the leaves, with the 3rd leaf being the oldest systemically infected leaf and the 11th being the youngest. Middle and bottom rows are the 3rd through the 11th leaf of a TCV-hp infected AtGNC plant. The 10th and 11th leaves are composite images generated from three separate images to visualize most of the leaf. 10th (mag) is a magnified region in the vicinity of the midvein from the 10th leaf shown to the left (bar = 100 μm). Arrow in the 7th leaf points to trichome support cells clearly adjacent to a secondary vein. Bright, isolated fluorescent foci in the 10th leaf are also emanating from trichome support cells.
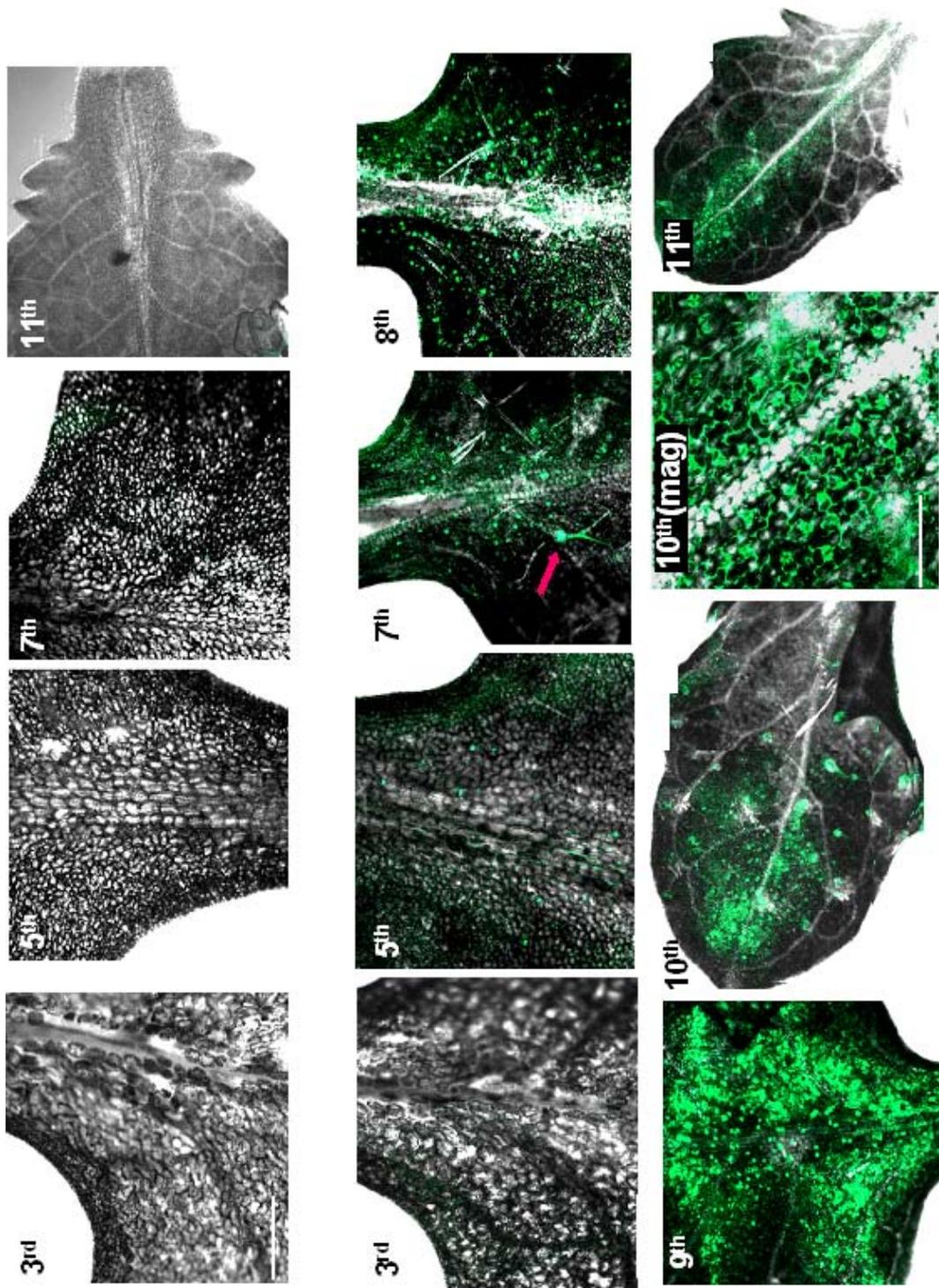
bottom rows). The reduced levels of GFP cytoplasmic fluorescence in older leaves can be explained by a decline in TCV accumulation known to occur in older tissues (Simon, unpublished). However, reduced expression of the GFP-NLS-CP$_{MS2}$ fusion protein in older leaves might also contribute to reduced GFP fluorescence, a possibility that is currently under investigation.

Examination of the 10th and 11th (youngest) leaves showed a striking pattern of GFP fluorescence, with the majority in the vicinity of the midvein (see Figure 4.8, bottom row, 10th and 11th leaf). This result suggests that TCV is exiting the phloem through the primary vein and then spreading cell-to-cell. In addition, trichomes and their support cells that were visibly adjacent to secondary and tertiary veins showed extremely bright fluorescence (Figure 4.8, middle and bottom rows, 7th land 10th leaf). This result suggests that TCV, when present in *Arabidopsis* minor veins, is unable to unload except into trichome support cells. From these cells, there was no detectable movement into surrounding epidermal cells, suggesting that trichome support cells may be symplastically isolated. While virus movement in multicellular trichomes is known to occur (Angell et al., 1995; Derrick et al., 1992), little is known about the cells at the base of trichomes. Restriction of virus movement from trichome support cells (also seen in inoculated leaves, Figure 4.8, D and E) may provide the plant with a means of containing viral infection following vector attack of protruding trichomes.

TCV accumulation surrounding the midvein of newly infected systemic leaves was also found using a complementation strategy to track TCV movement in *Arabidopsis* (Cohen et al., 2000). GFP-tagged TCV was generated by fusing GFP to the TCV CP and then inoculating virus into *Arabidopsis* expressing TCV CP from the 35S promoter.

Although systemic movement of the virus was achieved, no symptoms were detected, suggesting that either low levels of TCV were accumulating or that the method affected virus-host interaction. This is in contrast to the current method, where no differences were discernable in the timing or expression of TCV-associated symptoms in AtGNC plants.

Visualization of TCV movement in a virion-free form in AtGNC plants

As described in Chapter I, virion formation is not required for TCV movement and TCV may move as a ribonucleocomplex (Wang and Simon, 1999). Protoplast assays of CPm3 in Chapter II indicated that CPm3 does not generate detectable virions due to the two additional amino acids at the N-terminus of the CP that may affect virion assembly in host cells. Now AtGNC plants were used to study movement of virus in a virion-free form by comparing movement of TCV-hp and CPm3-hp, which is TCV-hp containing the CPm3 mutation. As shown in Figure 4.9A, cytoplasmic GFP fluorescence in inoculated leaves was readily detectable in more epidermal cells of CPm3-hp-infected plants than those infected with TCV-hp at 2 dpi. This result indicates that the cell-to-cell viral movement is enhanced when TCV infects hosts in a virion-free form. Systemically infected leaves excised from infected AtGNC plants were also observed for cytoplasmic GFP fluorescence at 17 dpi. The 10th (youngest) leaf of TCV-hp-infected plant showed a narrow pattern of GFP fluorescence, while GFP fluorescence in the 10th leaf of the plant infected with CPm3-hp had spread into the whole leave (Figure 4.9B), suggesting that long-distance movement of TCV were also enhanced in the absence of detectable virions.

Figure 4.9 GFP distribution in leaves of AtGNC plants infected with TCV-hp or CPm3-hp. Individual leaves were removed from plants and subjected to confocal microscopy. All images are produced by fluorescence and transmitted light. (A) Inoculated leaf at 2 dpi. Bars = 100 μm. (B) Systemically infected (youngest expanded) leaf at 17 dpi. Bars = 500 μm. The composite images were generated from three separate images to visualize most of the leaf.

A
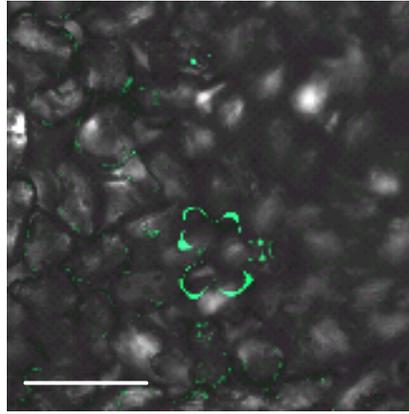
2 dpi: TCV-hp   2 dpi: CPm3-hp

B

10th   10th
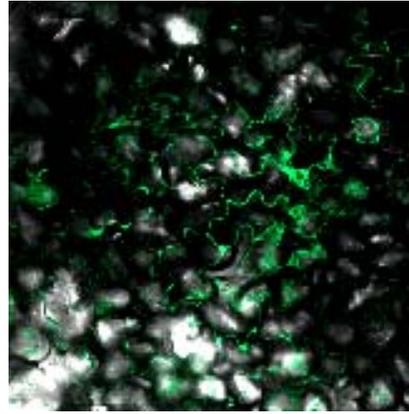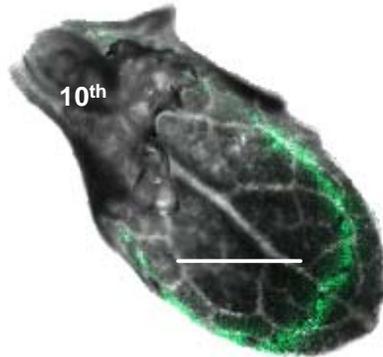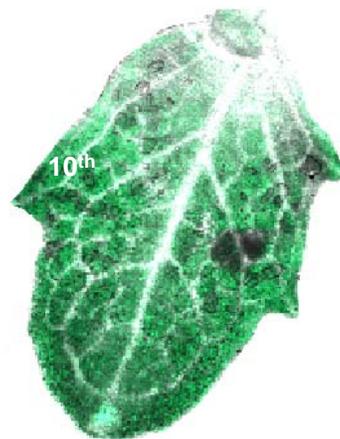
17 dpi: TCV-hp   17 dpi: CPm3-hp

The enhanced cell-to-cell and long-distance movement of CPm3 observed using AtGNC plants might be caused by multiple facts. As described in Chapter I, TCV may move as a ribonucleocomplex. Since CP is required for viral long-distance movement, increased levels of free CP due to reduced virion formation may help the virus to move in plants by facilitating formation of a ribonucleocomplex, which might consist of viral RNA, movement proteins and CP. Enhanced viral movement would benefit the virus by permitting it to rapidly colonize young host tissues. The TCV CP was previously found to be required for virus systemic movement, but not cell-to-cell movement, in *Arabidopsis thaliana* (Hacker et al., 1992). The observed cell-to-cell movement enhancement in AtGNC plants could also be caused by enhanced silencing suppression attributed to the higher level of free CP, since the CP is the RNA silencing suppressor (Qu and Morris, 2003; Thomas et al., 2003).

The potential usage of this technique

My results demonstrate that AtGNC plants can be used to examine cell-to-cell and long-distance movement of viruses that are pathogens of *Arabidopsis*. Generation of other GNC transgenic plants should allow for examination of local and systemic movement of a large number of viruses recalcitrant to previous procedures. The viral genome requires minimal disruption, only the addition of a 19 base hp and a limited linker sequence to allow insertion of properly oriented multiple hps, if necessary. One possible limitation of the technique, however, is that detection of GFP fluorescence requires that cells express the GFP-NLS-CP$_{MS2}$ fusion protein and such expression from the 35S promoter is not completely constitutive (Benfey and Chua, 1990). My initial use

of the system to examine TCV movement confirms previous findings that the virus only appears to move cell-to-cell after exiting from the primary vein in *Arabidopsis* and also provides novel information on trichome support cells. AtGNC plants have similar appearance, development and fertility as the parental ecotype and exhibit identical symptoms as wt plants when inoculated with TCV-hp. These plants, and other species of plants expressing GFP-NLS-CP$_{MS2}$, should also prove useful for detection of host RNA movement intra- and intercellularly, tissue specific expression of mRNAs without modification of their ORFs, and possibly as a quick selection for transformed plants.

CONCLUSIONS

In this dissertation, I report my studies on the mechanisms involved in symptom modulation by TCV and satC. satC is not a simple parasite of the virus. It does compete with the viral genomic RNA for use of virus-encoded proteins for its amplification in plants. The presence of satC always results in a reduction in viral RNA levels in protoplasts and whole plants. Nevertheless, satC benefits infection of TCV and intensifies symptoms of TCV in all symptomic hosts. My finding that satC interferes with virion accumulation helps in understanding how satC benefits TCV, since increased levels of free CP that result from reduced levels of virions could augment the silencing suppressor activity of the CP and thus enhance viral colonization of plants.

As described in Chapter IV, increased levels of free CP due to a reduction in virion accumulation may help the virus to move in plants by facilitating formation of a ribonucleocomplex, possibly consisting of viral RNA, movement proteins, and CP. Enhanced viral movement would benefit the virus by permitting it to rapidly colonize young host tissues. Enhanced TCV cell-to-cell and long-distance movement has been observed in AtGNC plants using the virus-tracking method that I established. CPm3, which has reduced virion levels and severe symptoms, shows more rapid and extensive spread than wt TCV in inoculated and uninoculated leaves.

In addition to the indirect contribution to symptoms by affecting virion accumulation, satC may directly lead to symptoms, since co-infection of satC and TCV leads to severe leaf crinkling, which is not displayed in plants infected with TCV alone. The satC-associated leaf crinkling is very similar to that observed in *Arabidopsis* plants

with mutations in the JAW locus. This locus encodes a microRNA, miR-Jaw, which regulates expression of the TCP gene family (Palatnik et al., 2003). I found that mRNA of TCP4, a member of the TCP family, is complementary to 19 of 22 CvsRNA1 residues with several mismatches and that the presence of satC is associated with a reduction in mRNA levels of TCP4 in plants. These results suggest that satC may induce disease by producing vsRNAs, such as CvsRNA1, that may basepair with, and guide cleavage of, TCP4 transcripts. The putative phenotypic changes in plants caused by satC might provide a more amenable environment for successful infection of TCV.

The mutualistic relationship between satC and TCV suggests that both participants gain fitness from the interaction. An other interaction that benefits both virus and satellite RNA is observed for GRV and its satellite RNA. GRV does not encode a CP (Murant et al., 1995; Taliansky and Robinson, 2003) and is dependent on the CP of GRAV for virion assembly (Mayo et al., 1999). The 900-nt satRNA of GRV is dependent on GRV-encoded protein for amplification, but required for GRV virion assembly and thus aphid transmission of virions (Mayo et al., 1999). It is not known whether decreased levels of TCV virions due to the presence of satC impede beetle-mediated transfer of virus between hosts in the field. Alternatively, more rapid and extensive colonization of the plant might help beetles transfer a limited, but sufficient amount of virions between hosts. The presence of PMV satRNA also enhances systemic spread of the virus by allowing the virus to invade previously restricted tissues, although the mechanisms involved are not clear (Scholthof, 1999).

As described in Chapter I, the TCV CP is a pathogenicity determinant involved in multiple processes such as facilitating viral movement, eliciting hypersensitive response

in *Arabidopsis thaliana* ecotype Dijon, suppressing RNA silencing in host plants, facilitating TCV accumulation and repressing satC replication (Kong et al., 1997a). Symptom modulation by changes in the levels of CP in the presence or absence of satC is shown in Table 2.2. When ectopically expressed in plants, CP is one of the strongest silencing suppressors discovered to date (Chapman et al., 2004; Dunoyer et al., 2004; Qu et al., 2003; Thomas et al., 2003), with suppressor activity requiring the N-terminal 25 amino acids (Thomas et al., 2003). However, when CP is translated from the wt TCV genomic RNA, the suppression activity is dramatically reduced, possibly due to sequestration of the N-terminal 25 amino acids of the CP within assembling capsids at early times of infection when CP is necessary for silencing suppression (Qu et al., 2003; Thomas et al., 2003). This hypothesis is supported by my finding that reduced virion accumulation with satC or CPm3 is correlated with symptom enhancement. Symptom enhancement could result from enhanced silencing suppression and therefore increased viral colonization of the plant in the presence of high levels of free CPs when virion levels are reduced.

In addition to symptom modulation by CP, TCV appears to cause symptoms by generating vsRNAs. I found that expression of six of seven *Arabidopsis* genes tested was reduced 2.4- to 4-fold in TCV-infected plants at 7 dpi. Transcript levels of three of these genes were restored to normal in plants infected with TCV containing a deletion affecting generation of one TCV vsRNA, TvsRNA5. This deletion does not significantly affect viral accumulation, but leads to symptom attenuation. These results suggest that at least some vsRNAs excised from plant RNA viral genomes are specifically altering the expression of host genes leading to phenotypic changes in the plant. To my knowledge,

these are the first host gene transcripts whose levels are decreased in the presence of a complementary vsRNA.

Analysis of virus spread using co-expressed reporter proteins has provided important details on cell-to-cell and long distance movement of viruses in plants. However, most viruses cannot tolerate insertion of large non-viral segments or loss of any ORFs, procedures required to detect viruses non-evasively. As described in Chapter IV, I have modified a technique used to localize mRNAs in yeast (Bertrand et al., 1998) for detection of viral RNAs in AtGNC plants. This technique should be amenable for detection of any virus with a transformable plant (or animal) host and may also prove useful for localizing properly engineered host RNAs.

As summarized above, studies of symptom modulation by TCV and satC, as well as establishment of the novel virus-tracking method in plants help us to understand mechanisms underlying the interaction between plant viruses and their hosts. However, many questions remain to be answered. For example, (i) how many *Arabisopsis* genes are down-regulated by the presence of TCV and satC? (ii) Are some host genes up-regulated by TCV and satC? (iii) What is the function of LssRNA? To answer these questions, 5' RACE assays need to be performed in the future to investigate the putative RISC cleavage of host mRNA guided by TCV- and satC-specific vsRNAs.

REFERENCES

Adenot, X., Elmayan, T., Lauressergues, D., Boutet, S., Bouche, N., Gasciolli, V., Vaucheret, H., 2006. DRB4-dependent TAS3 trans-acting siRNAs control leaf morphology through AGO7. Curr Biol. 16, 927-932.

Ahlquist, P., 2002. RNA-dependent RNA polymerases, viruses, and RNA silencing. Science 296, 1270-1273.

Ahlquist, P., 2006. Parallels among positive-strand RNA viruses, reverse-transcribing viruses and double-stranded RNA viruses. Nat Rev Microbiol. 4, 371-382.

Allen, E., Xie, Z., Gustafson, A.M., Carrington, J.C. 2005. microRNA-directed phasing during *trans*-acting siRNA biogenesis in plants. Cell 121, 207-221.

Altschul, S.F., Madden, T.L., Schaffer, A.A., Zhang, J., Zhang, Z., Miller, W., Lipman, D.J., 1997. Gapped BLAST and PSI-BLAST: a new generation of protein database search programs. Nucleic Acids Res. 25, 3389-3402.

Ambros, V., 2001. microRNAs: tiny regulators with great potential. Cell 107, 823-826.

Anandalakshmi, R., Pruss, G.J., Ge, X., Marathe, R., Mallory, A.C., Smith, T.H., Vance, V.B., 1998. A viral suppressor of gene silencing in plants. Proc. Natl Acad. Sci. USA 95, 13079-13084.

Andersson, M.G., Haasnoot, P.C., Xu, N., Berenjian, S., Berkhout, B., Akusjärvi, G., 2005. Suppression of RNA interference by adenovirus virus-associated RNA. J Virol. 79, 9556-65.

Angell, S.M., Baulcombe, D.C., 1995. Cell-to-cell movement of potato virus X revealed by microinjection of a viral vector tagged with the β-glucuronidase gene. Plant J. 7, 135-140.

Aravin, A., Tushl, T., 2005. Identification and characterization of small RNAs involved in RNA silencing. FEBS Lett. 579, 5830-5840.

Bartel, D.P., 2004. MicroRNAs: genomics, biogenesis, mechanism, and function. Cell 116, 281-297.

Baulcombe, D., 2004. RNA silencing in plants. Nature 431, 356-363.

Baulcombe, D.C., Chapman, S., Santa Cruz S., 1995. Jellyfish green fluorescent protein as a reporter for virus infections. Plant J. 7, 1045-1053.

Baumberger, N., Baulcombe, D. C., 2005. Arabidopsis ARGONAUTE1 is an RNA slicer that selectively recruits microRNAs and short interfering RNAs. Proc. Natl. Acad. Sci. USA 102, 11928-11933.

Benfey, P.N., Chua, N.H., 1990. The cauliflower mosaic virus 35S promoter: Combinatorial regulation of transcription in plants. Science 250, 959-966.

Bernstein, E., Caudy, A.A., Hammond, S.M., Hannon, G.J., 2001. Role for a bidentate ribonuclease in the initiation step of RNA interference. Nature 409, 363-366.

Bertrand, E., Chartrand, P., Schaefer, M., Shenoy, S.M., Singer, R.H., Long, R.M., 1998. Localization of *ASH1* mRNA Particles in Living Yeast. Mol. Cell. 2, 437-445.

Bohmert, K., Camus, I., Bellini, C., Bouchez, D., Caboche, M., Benning, C., 1998. AGO1 defines a novel locus of *Arabidopsis* controlling leaf development. EMBO J. 17, 170-180.

Borsani, O., Zhu, J., Verslues, P.E., Sunkar, R., Zhu, J.K., 2005. Endogenous siRNAs derived from a pair of natural *cis*-antisense transcripts regulate salt tolerance in *Arabidopsis*. Cell 123, 1279-1291.

Boutet, S., Vazquez, F., Liu, J., Béclin, C., Fagard, M., Gratias, A., Morel, J.B., Crété, P., Chen, X., Vaucheret, H., 2003. *Arabidopsis HEN1*: A genetic link between endogenous

miRNA controlling development and siRNA controlling transgene silencing and virus resistance. Curr. Biol. 13, 843-848.

Brigneti, G., Voinnet, O., Li, W.-X., Ji, L.-H., Ding, S.-W., Baulcombe, D.C., 1998. Viral pathogenicity determinants are suppressors of transgene silencing in Nicotiana benthamiana. EMBO J. 17, 6739-6746.

Bucher, E., Sijen, T., De Haan, P., Goldbach, R., Prins, M., 2003. Negative-strand tospoviruses and tenuiviruses carry a gene for a suppressor of gene silencing at analogous genomic positions. J. Virol. 77, 1329-1336.

Buck, K.W., 1996. Comparison of the replication of positive-stranded RNA viruses of plants and animals. Adv. Virus Res. 47, 159-251.

Cai, X., Lu, S., Zhang, Z., Gonzalez, C.M., Damania, B., Cullen, B.R., 2005. Kaposi's sarcoma-associated herpesvirus expresses an array of viral microRNAs in latently infected cells. Proc Natl Acad Sci USA 102, 5570-5575.

Cai, X., Schafer, A., Lu, S., Bilello, J.P., Desrosiers, R.C., Edwards, R., Raab-Traub, N., Cullen, B.R., 2006. Epstein–Barr Virus MicroRNAs Are Evolutionarily Conserved and Differentially Expressed. PLoS Pathog. 2, e23.

Carpenter, C.D., Oh, J.W., Zhang, C., Simon, A.E. 1995. Involvement of a stem-loop structure in the location of junction sites in viral RNA recombination. J. Mol. Biol. 245, 608-622.

Carpenter, C.D., Simon, A.E., 1996. In vivo restoration of biologically active 3' ends of virus-associated RNAs by nonhomologous RNA recombination and replacement of a terminal motif. J. Virol. 70, 478-486.

Carrington, J.C., Ambros, V., 2003. Role of microRNAs in plant and animal development. Science 301, 336-338.

Carrington, J.C., Kasschau, K.D., Mahajan, S.K., Schaad, M.C., 1996. Cell-to-cell and long-distance transport of viruses in plants. Plant Cell 8, 1669-1681.

Chapman, E.J., Prokhnevsky, A.I., Gopinath, K., Dolja, V.V., Carrington, J.C., 2004. Viral RNA silencing suppressors inhibit the microRNA pathway at an intermediate step. Genes Dev. 18, 1179-1186.

Chen, J., Li, W.X., Xie, D., Peng, J.R., Ding, S.W., 2004. Viral virulence protein suppresses RNA silencing-mediated defense but upregulates the role of microRNA in host gene expression. Plant Cell 16, 1302-1313.

Chen, X., 2005. MicroRNA biogenesis and function in plants. *FEBS Lett.* 597, 5923-5931.

Chen,J., Noueiry, A., Ahlquist, P., 2001. Brome mosaic virus Protein 1a recruits viral RNA2 to RNA replication through a 5' proximal RNA2 signal. J Virol. 75, 3207-3219.

ChendrimadA, T.P., Gregory, R.I., Kumaraswamy, E., Norman, J., Cooch, N., Nishikura, K., Shiekhattar, R., 2005. TRBP recruits the Dicer complex to Ago2 for microRNA processing and gene silencing. Nature 436, 740-744.

Cheng, N.H., Su, C.L., Carter, S.A., Nelson, R.S., 2000. Vascular invasion routes and systemic accumulation patterns of tobacco mosaic virus in *Nicotiana benthamiana*. Plant J. 23, 349-362.

Chiu, W.L., Niwa, Y., Zeng, W., Hirano, T., Kobayashi, H., Sheen J., 1996. Engineered GFP as a vital reporter in plants. Curr. Biol. 6, 325-330.

Chytilova, E., Macas, J., Galbraith D.W., 1999 Green fluorescent protein targeted to the nucleus, a transgenic phenotype useful for studies in plant biology. Ann. Bot. 83, 645-654.

Citovsky, V., Knorr, D., Schuster, G., Zambryski, P., 1990. The P30 movement protein of tobacco mosaic virus is a single-strand nucleic acid binding protein. Cell 60, 637-648.

Clough, S.J., Bent, A.F., 1998. Floral dip: a simplified method for Agrobacterium-mediated transformation of Arabidopsis thaliana. Plant J. 16, 735-743.

Cohen, Y., Gisel, A., Zambryski P.C., 2000. Cell-to-cell and systemic movement of recombinant green fluorescent protein-tagged turnip crinkle viruses. Virology 273, 258-266.

Cronin, S., Verchot, J., Haldeman-Cahill, R., Schaad, M.C., Carrington, J.C., 1995. Long-distance movement factor: a transport function of the potyvirus helper component proteinase. Plant Cell 7, 549-559.

Dalmay, T., Hamilton, A.J., Rudd, S., Angell, S., Baulcombe, D.C., 2000. An RNA-dependent RNA polymerase gene in *Arabidopsis* is required for posttranscriptional gene silencing mediated by a transgene but not by a virus. Cell 101, 543-553.

Dalmay, T., Rubino, L., Burgyan, J., Russo, M., 1992. Replication and movement of a coat protein mutant of cymbidium ringspot tombusvirus. Mol. Plant-Microbe Interact. 5, 379-383.

Dalmay, T.D., Horsefield, R., Braunstein, T.H., Baulcombe, D.C., 2001. *SDE3* encodes an RNA helicase required for post-transcriptional gene silencing in *Arabidopsis*. EMBO J. 20, 2069-2078.

Dangl, J. L., Jones, J. D., 2001. Plant pathogens and integrated defence responses to infection. Nature 411, 826-833.

de Carvalho-Niebel, F., Frendo, P., Van Montagu, M., Cornelissen, M., 1995a. Post-transcriptional cosuppression of beta-1,3-glucanase genes does not affect accumulation of transgene nuclear mRNA. Plant Cell. 7, 347-58.

de Carvalho-Niebel, F., Frendo, P., Inze, D., Cornelissen, M., Van Montagu, M., 1995b. Co-suppression of beta-1,3-glucanase genes in Nicotiana tabacum. Curr Top Microbiol Immunol. 197,91-103.

Denli, A.M., Tops, B.B., Plasterk, R.H., Ketting, R.F., and Hannon, G.J., 2004. Processing of primary microRNAs by the Microprocessor complex. Nature 432, 231-235.

Denti, M.A., Boutla, A., Tsagris, M., Tabler, M., 2004. Short interfering RNAs specific for potato spindle tuber viroid are found in the cytoplasm but not in the nucleus. Plant J. 37, 762-769.

Deom, C.M., Oliver, M.J., Beachy, R.N., 1987. The 30-kilodalton gene product of tobacco mosaic virus potentiates virus movement. Science 237, 389-394.

Derrick, P.M., Barker, H., Oparka, K.J., 1992. Increase in plasmodesmatal permeability during cell-to-cell spread of tobacco rattle tobravirus from individually inoculated cells. Plant Cell 4, 1405-1412.

Ding, S.W., Li, W.X., Symons, R.H., 1995 A novel naturally occurring hybrid gene encoded by a plant RNA virus facilitates long distance virus movement. EMBO J. 14, 5762-5772.

Dolja, V.V., Haldeman, R., Robertson, N.L., Dougherty, W.G., Carrington, J.C., 1994. Distinct function of capsid protein in assembly and movement of tobacco etch potyvirus. EMBO J. 13, 1482-1491.

Dolja, V.V., Olja, V.V., McBride, H.J., Carrington, J.C. 1992. Tagging of plant potyvirus replication and movement by insertion of beta-glucuronidase into the viral polyproteins. Proc. Natl. Acad. Sc. USA 89, 10208-10212.

Dorlhac de Borne, F., Vincentz, M., Chupean, Y., Vaucheret, H., 1994. Co-suppression of nitrate reductase host genes and transgenes in transgenic tobacco plants. Mol Gen Genet. 243, 613-621.

Du, T., Zamore, P.D., 2005. microPrimer: the biogenesis and function of microRNA. Development 132, 4645-4652.

Dunoyer, P., Himber, C., Voinnet, O., 2005. DICER-LIKE 4 is required for RNA interference and produces the 21-nucleotide small interfering RNA component of the plant cell-tocell silencing signal. Nat. Genet. 37, 1356-1360.

Dunoyer, P., Lecellier, C. H., Parizotto, E. A., Himber, C., Voinnet, O., 2004. Probing the microRNA and small interfering RNA pathways with virus-encoded suppressors of RNA silencing. Plant Cell 16, 1235-1250.

Dunoyer, P., Pfeiffer, S., Fritsch, C., Hemmer, O., Voinnet, O., Richards, K.E., 2002. Identification, subcellular localization and some properties of a cysteine-rich suppressor of gene silencing encoded by peanut clump virus. Plant J. 29, 555-567.

Dunoyer, P., Voinnet, O., 2005. The complex interplay between plant viruses and host RNA-silencing pathways. Curr. Opin. Plant Biol. 8, 415-423.

Ebhardt, H.A., Thi, E.P., Wang, M.B., Unrau, P.J., 2005. Extensive 3' modification of plant small RNAs is modulated by helper component-proteinase expression. Proc Natl Acad Sci USA 102, 13398-13403.

English, J.J., Mueller, E., Baulcombe, D.C., 1996. Suppression of virus accumulation in transgenic plants exhibiting silencing of nuclear genes. Plant Cell 8, 179-188.

Fagard, M., Boutet, S., Morel, J.B., Bellini, C., Vaucheret, H., 2000. AGO1, QDE-2, and RDE-1 are related proteins required for post-transcriptional gene silencing in plants, quelling in fungi, and RNA interference in animals. Proc. Natl. Acad. Sci. USA 97, 11650-11654.

Fire, A., Xu, S., Montgomery, M., Kostas, S., Driver, S., and Mello, C. 1998. Potent and specific genetic interference by double-strandedRNA in *Caenorhabditis elegans*. Nature 391, 806-811.

Förstemann, K., Tomari, Y., Du, T., Vagin, V.V., Denli, A.M., Bratu, D.P., Klattenhoff, C., Theurkauf, W.E., Zamore, P.D., 2005. Normal microRNA maturation and germ-line stem cell maintenance requires Loquacious, a double-stranded RNA-binding domain protein. PLoS Biol. 3,e236.

Fouts, D., True, H., Celander, D., 1997. Functional recognition of fragmented operator site by R17/MS2 coat protein, a translational repressor. Nuc. Acid. Res. 25, 4464-4473.

Gardiner, W.E., Sunter, G., Brand, L., Elmer, J.S., Rogers, S.G., Bisaro, D.M., 1988. Genetic analysis of tomato golden mosaic virus: The coat protein is not required for systemic spread or symptom development. EMBO J. 7, 899-904.

Gasciolli, V., Mallory, A.C., Bartel, D. P., Vaucheret, H., 2005. Partially redundant functions of Arabidopsis DICER-like enzymes and a role for DCL4 in producing trans-acting siRNAs. Cur. Biol. 15, 1494-1500.

Ghoshroy, S., Lartey, R., Sheng, J., Citovsky, V., 1997. Transport of proteins and nuceleic acids through plasmodesmata. Annu. Rrev. Plant Physiol. Plant Mol. Biol. 48, 27-49.

Giesman-Cookmeyer, D., Silver, S., Vaewhongs, A.A., Lommel, S.A., Deom, C.M., 1995. Tobamovirus and dianthovirus movement proteins are functionally homologous. Virology 213, 38-45.

Gitlin, L., Andino,R., 2003. Nucleic acid-based immune system: the antiviral potential of mammalian RNA silencing. J Virol. 77, 7159-7165.

Golem, S., Culver, J.N., 2003. Tobacco mosaic virus induced alterations in the gene expression profile of Arabidopsis thaliana. Mol. Plant Microbe Interac. 16, 681-688.

Goodwin, J., Chapman, K., Swaney, S., Parks, T.D., Wernsman, E.A., Dougherty, W.G., 1996. Genetic and biochemical dissection of transgenic RNA-mediated virus resistance. Plant Cell 8, 95-105.

Grey, F., Antoniewicz, A., Allen, E., Saugstad, J., McShea, A., Carrington, J.C., Nelson, J., 2005. Identification and characterization of human cytomegalovirus-encoded microRNAs. J Virol. 79, 12095-12099.

Guo, H.S., Ding, S.W., 2002. A viral protein inhibits the long range signaling activity of the gene silencing signal. EMBO J. 21, 398-407.

Hacker, D.L., Petty, I.T., Wei, N., Morris, T.J., 1992. Turnip crinkle virus genes required for RNA replication and virus movement. Virology 186, 1-8.

Haley, B., Zamore, P. D., 2004. Kinetic analysis of the RNAi enzyme complex. *Nature Struct. Bol.* 11, 599-606.

Hammond, S.M., Bernstein, E., Beach, D., Hannon, G., 2000. An RNA-directed nuclease mediates post-transcriptional gene silencing in *Drosophila* cell extracts. Nature 404, 293-296.

Han, M.H., Goud, S., Song, L., Fedoroff, N., 2004. The *Arabidopsis* double-stranded RNA-binding protein HYL1 plays a role in microRNA-mediated gene regulation. Proc. Natl. Acad. Sci. USA 101, 1093-1098.

Hannon, G.J., 2002. RNA interference. Nature 418, 244-251.

Hart, C.M., Fischer, B., Neuhaus, J.M., Meins, F.J., 1992. Regulated inactivation of homologous gene expression in transgenic Nicotiana sylvestris plants containing a defense-related tobacco chitinase gene. Mol Gen Genet. 235, 179-188.

Heaton, L.A., Lee, T.C., Wei, N., Morris, T.J., 1991. Point mutations in the turnip crinkle virus capsid protein affect the symptoms expressed by *Nicotiana benthaminana*. Virology 183, 143-150.

Heinlein, M., Epel, B.L., Padgett, H.S., Beachy, R.N., 1995. Interaction of tobamovirus movement proteins with the plant cytoskeleton. Science 270, 1983-1985.

Henderson, I.R., Zhang, X., Lu, C., Johnson, L., Meyers, B.C., Green, P.J., Jacobsen, S.E., 2006. Dissecting Arabidopsis thaliana DICER function in small RNA processing, gene silencing and DNA methylation patterning. Nat Genet. 38, 721-725.

Herr, A.J., 2005. Pathways through the small RNA world of plants. FEBS Lett. 579, 5879-5888.

Herr, A.J., Jensen, M.B., Dalmay, T., Baulcombe, D.C., 2005. RNA polymerase IV directs silencing of endogenous DNA. Science 308, 118-120.

Himber, C., Dunoyer, P., Moissiard, G., Ritzenthaler, C., Voinnet, O., 2003. Transitivity-dependent and -independent cell-tocell movement of RNA silencing. EMBO J. 22, 4523-4533.

Hiraguri, A., Itoh, R., Kondo, N., Nomura, Y., Aizawa, D., Murai, Y., Koiwa, H., Seki, M., Shinozaki, K., Fukuhara, T., 2005. Specific interactions between Dicer-like proteins and HYL1/DRB-family dsRNA-binding proteins in *Arabidopsis thaliana*. Plant Mol. Biol. 57, 173-188.

Hull, R., 2002. Matthews' Plant Virology. Fourth edition. Academic Press.

Hunter, C., Sun, H., Poethig, R.S., 2003. The *Arabidopsis* heterochronic gene ZIPPY is an ARGONAUTE family member. Curr. Biol. 13, 1734-1739.

Hutvagner, G., 2005. Small RNA asymmetry in RNAi: function in RISC assembly and gene regulation. FEBS Lett. 579, 5850-5857.

Itaya, A., Folimonov, A., Matsuda, Y., Nelson, R. S., Ding, B., 2001. Potato spindle tuber viroid as inducer of RNA silencing in infected tomato. Mol. Plant Microbe Interact. 14, 1332-1334.

Iyer, L.M., Koonin, E.V., Aravind, L., 2003. Evolutionary connection between the catalytic subunits of DNA-dependent RNA polymerases and eukaryotic RNA-dependent RNA polymerases and the origin of RNA polymerases. BMC Struct Biol. 3:1.

Jacobsen, S.E., Running, M.P., Meyerowitz, E.M., 1999. Disruption of an RNA helicase/RNAse III gene in Arabidopsis causes unregulated cell division in floral meristems. Development 126, 5231-5243.

Jing, Q., Huang, S., Guth, S., Zarubin, T., Motoyama, A., Chen, J., Di Padova, F., Lin, S.-C., Gram, H., Han, J., 2005. Involvement of microRNA in AU-Rich element mediated mRNA instability. Cell 120, 623-634.

Johansen, L.K., Carrington, J.C., 2001. Silencing on the spot. Induction and suppression of RNA silencing in the Agrobacterium-mediated transient expression system. Plant Physiol. 126, 930-938.

Jones-Rhoades, M.W., Bartel, D.P., 2004. Computational identification of plant microRNAs and their targets, including a stress-induced miRNA. Mol. Cell 14, 787-799.

Jones-Rhoades, M.W., Bartel, D.P., Bartel, B., 2006. Micro-RNAs and their regulatory roles in plants. Annu. Rev. Plant Biol. 57, 19-53.

Jopling, C. L., Yi, M., Lancaster, A., Lemon, S. M., Sarnow, P., 2005. Modulation of hepatitis C virus RNA abundance by a liver-specific MicroRNA. Science 309, 1577-1581.

Kachroo, P., Yoshioka, K., Shah, J., Dooner, H. K., Klessig, D. G., 2000. Resistance to Turnip crinkle virus in Arabidopsis is regulated by two host genes and is salicylic acid dependent but *NPR1*, ethylene, and jasmonate independent. Plant Cell 12, 677-690.

Kaplan, I.B., Zhang, L., Palukaitis, P., 1998. Characterization of cucumber mosaic virus. V. Cell-to-cell movement requires capsid protein but not virions. Virology 246, 221-223.

Kasschau, K.D., Carrington, J.C., 1998. A counterdefensive strategy of plant viruses: suppression of post-transcriptional gene silencing. Cell 95, 461-470.

Kasschau, K.D., Cronin, S., Carrington, J.C., 1997. Genome amplification and long-distance movement functions associated with the central domain of tobacco etch potyvirus helper component-proteinase. Virology 228, 251-262.

Kasschau, K.D., Xie, Z., Allen, E., Llave, C., Chapman, E.J., Krizan, K.A., Carrington, J. C., 2003. P1/HC-Pro, a viral suppressor of RNA silencing, interferes with Arabidopsis development and miRNA function. Dev. Cell 4, 205-217.

Kidner, C., Martienssen, R. A., 2005. The developmental role of microRNA in plants. Curr. Opin. Plant Biol. 8, 38-44.

Kim, V.N., 2005. Small RNAs: Classification, biogenesis, and function. Mol. Cells 19, 1-15.

Kong, Q., Oh, J.W., Carpenter, C. D., Simon, A. E., 1997a. The coat protein of turnip crinkle virus is involved in subviral RNA-mediated symptom modulation and accumulation. Virology 238, 478-485.

Kong, Q., Wang, J., Simon, A. E., 1997b. Satellite RNA-mediated resistance to Turnip crinkle virus in *Arabidopsis* involves a reduction in virus movement. Plant Cell 9, 2051-2063.

Kubota, K., Tsuda, S., Tamai, A., Meshi, T.,2003. Tomato mosaic virus replication protein suppresses virus-targeted posttranscriptional gene silencing. J. Virol. 77, 11016-11026.

Kumagai, M.H., Donson, J., Dellacioppa, G., Harvey, D., Hanley, K., Grill, L.K., 1995. Cytoplasmic inhibition of carotenoid biosynthesis with virus-derived RNA. Proc. Natl. Acad. Sci. USA 92, 1679-1683.

Kurihara, Y., Watanabe, Y., 2004. Arabidopsis micro-RNA biogenesis through Dicer-like 1 protein functions. Proc. Natl. Acad. Sci. USA 101, 12753-12758.

Kushner, D.B., Lindenbach, B.D., Grdzelishvili, V.Z., Noueiry, A.O., Paul, S.M., Ahlquist, P., 2003. Proc. Natl. Acad. Sci. USA 100, 15764-15769.

Lacomme, C., Hrubikova, K., Hein, I., 2003. Enhancement of virus-induced gene silencing through viral-based production of inverted-repeats. Plant J. 34, 543-553.

Lai, M.M., 1998. Cellular factors in the transcription and replication of viral RNA genomes: a parallel to DNA-dependent RNA transcription. Virology 244:1-12.

Lakatos, L., Csorba, T., Pantaleo, V., Chapman, E.J., Carrington, J.C., Liu, Y.P., Dolja, V.V., Calvino, L.F., López-Moya, J.J., Burgyán, J., 2006. Small RNA binding is a common strategy to suppress RNA silencing by several viral suppressors. EMBO J. 25, 2768-2780.

Lakatos, L., Szittya, G., Silhavy, D., Burgyán, J., 2004. Molecular mechanism of RNA silencing suppression mediated by p19 protein of tombusviruses. EMBO J. 23, 876-84.

Lau, N.C., Lim, E.P., Weinstein, E.G., Bartel, D.P., 2001. An abundant class of tiny RNAs with probable regulatory roles in *Caenorhabditis elegans*. Science 294, 858-862.

Lazarowitz, S.G., Beachy, R.N., 1999. Viral movement proteins as probes for intracellular and intercellular trafficking in plants. Plant Cell 11, 535-548.

Lee, Y., Ahn, C., Han, J., Choi, H., Kim, J., Yim, J., Lee, J., Provost, P, Radmark,O, Kim,S., Kim, V.N., 2003. The nuclear RNase III Drosha initiates microRNA processing. Nature 425, 415-419.

Li, J., Yang, Z., Yu, B., Liu, J., Chen, X., 2005. Methylation protects miRNAs and siRNAs from a 3_-end uridylation activity in *Arabidopsis*. Curr. Biol. 15, 1501-1507.

Li, W.Z., Qu, F., Morris T.J., 1998. Cell-to-cell movement of turnip crinkle virus is controlled by two small open reading frames that function *in trans*. Virology 244, 405-416.

Li, X., Heaton,L.A., Morris, T.J., Simon, A.E., 1989. Turnip crinkle virus defective interfering RNAs intensify viral symptoms and are generated de novo. Proc. Natl. Acad. Sci. USA 86, 9173-9177.

Li, X.H., Simon, A.E., 1990. Symptom intensification on cruciferous hosts by the virulent sat-RNA of turnip crinkle virus. Phytopathology 80, 238-242.

Lim, F., Spingola, M., Peabody, D.S., 1994. Altering the RNA binding specificity of a translational repressor. J. Biol. Chem. 269, 9006-9010.

Lindbo, J.A., Dougherty, W.G., 1992. Untranslatable transcripts of the tobacco etch virus coat protein gene sequence can interfere with tobacco etch virus replication in transgenic plants and protoplasts. Virology 189, 725-733.

Liu, J., Carmell, M.A., Rivas, F.V., Marsden, C.G., Thomson, J.M., Song, J.J., Hammond, S.M., Joshua-Tor, L., Hannon, G.J., 2004a. Argonaute2 is the catalytic engine of mammalian RNAi. Science 305, 1437-1441.

Liu, L., Grainger, J., Canizares, M.C., Angell, S.M., Lomonossoff, G.P., 2004b. Cowpea mosaic virus RNA-1 acts as an amplicon whose effects can be counteracted by a RNA-2-encoded suppressor of silencing. Virology 323, 37-48.

Liu, Z.B., Ulmasov, T., Shi, X., Hagen, G., Guilfoyle, T.J. 1994. Soybean GH3 promoter contains multiple auxin-inducible elements. Plant Cell 6, 645-657.

Llave, C., Kasschau, K.D., Rector, M.A., Carrington, J.C., 2002. Endogenous and silencing-associated small RNAs in plants. Plant Cell 14, 1605-1619.

Lu, C., Fedoroff, N., 2000. A mutation in the *Arabidopsis* HYL1 gene encoding a dsRNA binding protein affects responses to abscisic acid, auxin, and cytokinin. Plant Cell 12, 2351-2366.

Lu, R., Folimonov, A., Shintaku, M., Li, W.X., Falk, B.W., Dawson, W.O., Ding, S.W., 2004. Three distinct suppressors of RNA silencing encoded by a 20-kb viral genome. Proc. Natl Acad. Sci. USA 101, 15742-15747.

Lund, E., Guttinger, S., Calado, A., Dahlberg, J.E., Kutay, U., 2004. Nuclear export of microRNA precursors. Science 303, 95-98.

Mallory, A.C., Reinhart, B.J., Bartel, D., Vance, V.B., Bowman, L.H., 2002. A viral suppressor of RNA silencing differentially regulates the accumulation of short interfering RNAs and micro-RNAs in tobacco. Proc. Natl. Acad. Sci. USA 99, 15228-15233.

Mallory, A.C., Reinhart, B.J., Jones-Rhoades, M.W., Tang, G., Zamore, P.D., Barton, M.K., Bartel, D. P., 2004. EMBO J. 24, 3356-3364.

Mayo, M.A., Taliansky, M.E., Fritsch, C., 1999. Large satelliteRNA: molecular parasitism or molecular symbiosis. Curr. Top. Microbiol. 239, 159-175.

McLean, B.G., Hempel, F.D., Zambryski, P.C., 1997. Plant intercellular communication via plasmodesmata. Plant Cell 9, 1043-1054.

Merai, Z., Kerenyi, Z., Kertesz, S., Magna, M., Lakatos, L., Sihavy, D., 2006. Double-stranded RNA binding may be a general plant RNA viral strategy to suppress RNA silencing. J Virol. 80, 5747-5756.

Mlotshwa, S., Schauer, S.E., Smith, T.H., Mallory, A.C., Herr, J.M.Jr., Roth, B., Merchant, D.S., Ray, A., Bowman, L.H., Vance, V.B., 2005. Ectopic DICER-LIKE1 expression in P1/HC-Pro Arabidopsis rescues phenotypic anomalies but not defects in microRNA and silencing pathways. Plant Cell. 17, 2873-2885.

Moissiard, G., Voinnet, O., 2004. Viral suppression of RNA silencing in plants. Mol. Plant Pathol. 5, 71-82.

Molnár, A., Csorba, T., Lakatos, L., Varllyay, E., Christophe Lacomme, C., Burgyán, J., 2005. Plant Virus-Derived Small Interfering RNAs Originate Predominantly from Highly Structured Single-Stranded Viral RNAs. J. Virol. 79, 7812-7818.

Mourrain, P., Beclin, C., Elmayan, T., Feuerbach, F., Godon, C., Morel, J.B., Jouette, D., Lacombe, A.M., Nikic, S., Picault, N., Re´moue´, K., Sanial, M., Vo, T.-A., Vaucheret, H., 2000. *Arabidopsis* SGS2 and SGS3 genes are required for posttranscriptional gene silencing and natural virus resistance. Cell 101, 533-542.

Muangsan, N., Beclin, C., Vaucheret, H., Robertson, D., 2004. Geminivirus VIGS of endogenous genes requires SGS2/SDE1 and SGS3 and defines a new branch in the genetic pathway for silencing in plants. Plant J. 38, 1004-1014.

Mueller, E., Gilbert, J.E., Davenport, G., Brigneti, G., Baulcombe, D.C., 1995. Homology-dependent resistance: Transgenic virus resistance in plants related to homology-dependent gene silencing. Plant J. 7, 1001-1013.

Napoli, C., Lemieux, C., Jorgensen, R., 1990. Introduction of a chimeric chalcone synthase gene into petunia results in reversible co-suppression of homologous genes in trans. Plant Cell 2, 279-289.

Neilson, J.R., Sharp P.A., 2005. Herpesviruses throw a curve ball: new insights into microRNA biogenesis and evolution. Nat. Methods 2, 252-254.

Oh, J.W., Kong, Q., Song, C., Carpenter, C.D., Simon, A.E., 1995. Open Reading Frames of Turnip Crinkle Virus Involved in Satellite Symptom Expression and Incompatibility with Arabidopsis thaliana Ecotype Dijon. MPMI 8, 979-987.

Palatnik, J.F., Allen, E., Wu, X., Schommer, C., Schwab, R., Carrington, J.C., Weigel, D., 2003. Control of leaf morphogenesis by microRNAs. Nature 425, 257-263.

Papaefthimiou, I., Hamilton, A., Denti, M., Baulcombe, D., Tsagris, M., Tabler, M., 2001. Replicating potato spindle tuber viroid RNA is accompanied by short RNA fragments that are characteristic of post-transcriptional gene silencing. Nucleic Acids Res. 29, 2395-2400.

Park, M.Y., Wu, G., Gonzalez-Sulser, A., Vaucheret, H., Poethig, R.S., 2005. Nuclear processing and export of micro-RNAs in *Arabidopsis*. Proc. Natl. Acad. Sci. USA 102, 3691-3696.

Park, W., Li, J., Song, R., Messing, J., Chen, X., 2002. CARPEL CARPEL FACTORY, a Dicer homolog, and HEN1, a novel protein, act in microRNA metabolism in *Arabidopsis thaliana*. Curr. Biol. 12, 1484-1495.

Pasquinelli, A.E., Ruvkun G., 2002. Control of developmental timing by micrornas and their targets. Annu Rev Cell Dev Biol. 18, 495-513.

Peragine, A., Yoshikawa, M., Wu, G., Albrecht, H.L., Poethig, R.S., 2004. SGS3 and SGS2/SDE1/RDR6 are required for juvenile development and the production of *trans*-acting siRNAs in *Arabidopsis*. Genes & Dev. 18, 2368-2379.

Pfaffl, M.W., 2001. A new mathematical model for relative quantification in real-time RT–PCR. Nucleic Acids Res. 29, 2002-2007.

Pfeffer, S., Dunoyer, P., Heim, F., Richards, K.E., Jonard, G., Ziegler-Graff, V., 2002. P0 of beet Western yellows virus is a suppressor of posttranscriptional gene silencing. J. Virol. 13, 6815-6824.

Pfeffer, S., Sewer, A., Lagos-Quintana, M., Sheridan, R., Sader, C., Grasser, F.A., van Dyk, L.F., Ho, C.K., Shuman, S., Chien, M., Russo, J.J., Ju, J., Randall, G., Linderback, B.D., Rice, C.M., Simon, V., Ho, D.D., Zavolan, M., Tushl, T., 2005. Identification of microRNAs of the herpesvirus family. Nat. Methods 2, 269-276.

Pfeffer, S., Zavolan, M., Gra¨ sser, F.A., Chien, M., Russo, J.J., Ju, J., John, B., Enright, A.J., Marks, D., Sander, C., Tuschl, T., 2004. Identification of virus-encoded microRNAs. Science 304, 734-736.

Pruss, G., Ge, X., Shi, X.M., Carrington, J.C., Vance, V.B., 1997 Plant viral synergism: The potyviral genome encodes a broad-range pathogenicity enhancer that transactivates replication of heterologous viruses. Plant Cell 9, 859-868.

Qi, Y., Denli, A.M., Hannon, G.J., 2005. Biochemical specialization within *Arabidopsis* RNA silencing pathways. Mol. Cell 19, 421-428.

Qi, Y., Hannon, G.J., 2005. Uncovering RNAi mechanisms in plants: biochemistry enters the foray. FEBS Lett. 579, 5899-5903.

Qi, Y., Zhong, X., Itaya, A., Ding, B., 2004. Dissecting RNA silencing in protoplasts uncovers novel effects of viral suppressors on the silencing pathway at the cellular level. Nucleic Acids Res. 32, e179.

Qu, F., Morris, T.J., 1997. Encapsidation of turnip crinkle virus is defined by a specific packaging signal and RNA size. J. Virol. 71, 1428-1435.

Qu, F., Ren, T., Morris, T.J., 2003. The coat protein of turnip crinkle virus suppresses posttranscriptional gene silencing at an early initiation step. J. Virol. 77, 511-522.

Ratcliff, F., Harrison, B.D., Baulcombe, D.C., 1997. A similarity between viral defense and gene silencing in plants. Science 276, 1558-1560.

Ratcliff, F.G., MacFarlane, S.A., Baulcombe, D.C., 1999. Gene silencing without DNA. RNA-mediated cross-protection between viruses. Plant Cell 11, 1207-1216.

Reed, J.C., Kasschau, K.D., Prokhnevsky, A.I., Gopinath, K., Pogue, K.P., Carrington, J.C., Dolja, V.V., 2003. Suppressor of RNA silencing encoded by Beet yellows virus. Virology 306, 203-209.

Reinhart, B.J., Weinstein, E.G., Rhoades, M.W., Bartel, B., Bartel, D.P., 2002. MicroRNAs in plants. Genes & Dev. 16, 1616-1626.

Ren, T., Qu, F., Morris, T.J., 2000. HRT gene function requires interaction between a NAC protein and viral capsid protein to confer resistance to turnip crinkle virus. Plant Cell. 12, 1917-1926.

Rhoades, M.W., Reinhart, B.J., Lim, L.P., Burge, C.B., Bartel, B., Bartel, D.P., 2002. Prediction of plant microRNA targets. Cell 110, 513-520.

Roberts, A.G., Cruz, S.S., Roberts, I.M., Prior, D., Turgeon, R., Oparka, K.J., 1997. Phloem unloading in sink leaves of *Nicotiana benthamiana*: comparison of a fluorescent solute with a fluorescent virus. Plant Cell 9, 1381-1396.

Robinson, D.J., Ryabov, E.V., Raja, S.K., Roberts, I.M., Taliansky, M.E., 1999. Satellite RNA is essential for encapsidation of groundnut rosette umbravirus RNA by groundnut rosette assistor luteovirus coat protein. Virology 254:105-114.

Robinson-Beers, K., Pruitt, R.E., Gasser, C.S., 1992. Ovule development in wild-type arabidopsis and two female-sterile mutants. Plant Cell 4, 1237-1249.

Romaniuk, P.J., Lowary, P., Wu, H.N., Stormo, G., Uhlenbeck, O.C., 1987. RNA binding site of R17 coat protein. Biochemistry 26, 1563-1568.

Roossinck, M. J., Sleat, D., Palukaitis, P., 1992. Satellite RNAs of plant viruses: structures and biological effects. Microbiol. Rev. 56, 265-279.

Rubino, L., Russo, M., 1995. Characterization of resistance to cymbidium ringspot virus in transgenic plants expressing afull-length viral replicase gene. Virology 212, 240-243.

Ruiz, M.T., Voinnet, O., Baulcombe, D.C., 1998. Initiation and maintenance of virus-induced gene silencing, Plant Cell 10, 937-946.

Russo, M., Burgyan, J., Martelli, G.P., 1994. Molecular biology of tombusviridae. Adv. Virus Res. 44, 381-428.

Saito, T., Yamanaka, K., Okada, Y., 1990. Long-distance movement and viral assembly of tobacco mosaic virus mutants. Virology 176, 329-336.

Sano, M., Kato, Y., Taira, K., 2006. Sequence-specific interference by small RNAs derived from adenovirus VAI RNA. FEBS Lett. 580, 1553-1564.

Santa Cruz, S., Chapman, S., Roberts, A.G., Roberts, I.M., Prior, D.A., Oparka, K.J., 1996. Assembly and movement of a plant virus carrying a green fluorescent protein overcoat. Proc. Natl Acad. Sci. USA 93, 6286-6290.

Scheets, K., 1998. Maize chlorotic mottle machlomovirus and Wheat streak mosaic rymovirus concentrations increase in the synergistic disease corn lethal necrosis. Virology 242, 28-38.

Schiebel, W., Haas, B., Marinkovic, S., Klanner, A., Sanger, H. L., 1993. RNA-directed RNA polymerase from tomato leaves. II. Catalytic in vitro properties. J. Biol. Chem. 268, 11858-11867.

Schmitz, I., Rao, A.L.N., 1998. Deletions in the conserved aminoterminal basic arm of cucumber mosaic virus coat protein disrupt virion assembly but do not abolish infectivity and cell-to-cell movement. Virology 248, 323-331.

Schneider, W.L., Greene, A.E., Allison, R.F., 1997. The carboxyterminal two-thirds of the cowpea chlorotic mottle bromovirus capsid is incapable of virion formation yet supports systemic movement. J. Virol. 71, 4862-4865.

Scholthof, H.B., Morris, T.J., Jackson, A.O., 1993 The capsid protein of tomato bushy stunt virus is dispensable for systemic movement and can be replaced for localized expression of foreign genes. Mol. Plant-Microbe Interact. 6, 309-322.

Scholthof, K-B.G., 1999. A synergism induced by satellite Panicum mosaic virus. Mol. Plant Microbe Interact. 12, 163-166.

Schwab, R., Palatnik, J.F., Riester, M., Schommer, C., Schmid, M., Weigel, D., 2005. Dev. Cell 8, 517-527.

Schwarz, D.S., Hutvagner, G., Du, T., Xu, Z., Aronn, N., Zamore, P.D., 2003. Asymmetry in the assembly of the RNAi enzyme complex. Cell 115, 199-208.

Seron, K., Haenni, A.L., 1996. Vascular movement of plant viruses. Mol Plant Microbe Interact. 9, 435-42.

Sijen, T., Fleenor, J., Simmer, F., Thijssen, K.L., Parrish, S., Timmons, L., Plasterk, R.H., Fire, A., 2001. On the role of RNA amplification in dsRNA-triggered gene silencing. Cell 107, 465-476.

Silhavy, D., Molnar, A., Lucioli, A., Szittya, G., Hornyik, C., Tavazza, M., Burgyan, J., 2002. A viral protein suppresses RNA silencing and binds silencing-generated, 21-to 25-nucleotide double-stranded RNAs. EMBO J. 21, 3070-3080.

Simon, A.E., Howell, S.H., 1986. The virulent satellite RNA of turnip crinkle virus has a major domain homologous to the 3'-end of the helper virus genome. EMBO J. 5, 3423-3428.

Simon, A.E., Li, X.H., Lew, J., Stange, R., Zhang, C. Polacco, M., Carpenter, C.D., 1992. Susceptibility and resistance of *Arabidopsis thaliana* to turnip crinkle virus. Mol. Plant-Microbe Interact. 5, 496-503.

Simon-Mateo, C., Garcia, J.A., 2006. MicroRNA-guided processing impairs Plum pox virus replication, but the virus readily evolves to escape this silencing mechanism. J. Virol. 80, 2429-2436.

Smith, C.J., Watson, C.F., Bird, C.R., Ray, J., Schuch, W., Grierson, D., 1990. Expression of a truncated tomato polygalacturonase gene inhibits expression of the endogenous gene in transgenic plants. Mol. Gen. Genet. 224, 477-481.

Song, C., Simon, A.E., 1994. RNA-dependent RNA polymerase from plants infected with turnip crinkle virus can transcribe plus- and minusstrands of virus-associated RNAs. Proc. Natl. Acad. Sci. USA 91, 8792-8796.

Song, J.J., Smith, S.K., Hannon, G.J., Joshua-Tor, L., 2004. Crystal structure of Argonaute and its implications for RISC slicer activity. Science 305, 1434-1437.

Souret, F.F., Kastenmayer, J.P., Green, P.J. 2004. AtXRN4 degrades mRNA in Arabidopsis and its substates include selected miRNA targets. Mol. Cell. 15, 173-183.

Stupina, V., Simon, A.E., 1997. Analysis in vivo of turnip crinkle virus satellite RNA C variants with mutations in the 3' terminal minus strand promoter. Virology 238, 470-477.

Sullivan, C.S., Ganem, D., 2005. MicroRNAs and viral infection. Mol. Cell 20, 3-7.

Sullivan, M.P., Ahlquist, P., 1999. A brome mosaic virus intergenic RNA3 replication signal functions with viral replication protein 1a to dramatically stabilize RNA in vivo. J Virol. 73, 2622-2632.

Sun, X., Simon, A.E., 2003. Fitness of a Turnip crinkle virus satellite RNA correlates with a sequence-nonspecific hairpin and flanking sequences that enhance replication and repress the accumulation of virions. J. Virol. 77, 7880-7889.

Szittya, G., Molnár, A., Silhavy, D., Hornylik, C., Burgyán, J., 2002. Short defective interfering RNAs of tombusviruses are not targeted but trigger post-transcriptional gene silencing against their helper virus. Plant Cell 14, 359-372.

Tang, G., Reinhart, B.J., Bartel, D.P., Zamore, P. D., 2002. A biochemical framework for RNA silencing in plants. Genes Dev. 17, 49-63.

Tanzer, M.M., Thompson, W.F., Law, M.D., Wernsman, E.A., Uknes, S., 1997. Characterization of post-transcriptionally suppressed transgene expression that confers resistance to tobacco etch virus infection in tobacco. Plant Cell 9, 1411-1423.

Thomas, C.L., Leh, V., Lederer, C., Maule, A.J., 2003. Turnip crinkle virus coat protein mediates suppression of RNA silencing in *Nicotiana benthamiana*. Virology 306, 33-41.

Vaistij, F.E., Jones, L., Baulcombe, D.C., 2002. Spreading of RNA targeting and DNA methylation in RNA silencing requires transcription of the target gene and a putative RNA-dependent RNA polymerase. Plant Cell 14, 857-867.

Valegard, K., Murray, J.B., Stonehouse, N.J., van den Worm, S., Stockley, P.G., Liljas, L., 1997. The three-dimensional structures of two complexes between recombinant MS2 capsids and RNA operator fragments reveal sequence-specific protein-RNA interactions. J. Mol. Biol. 270, 724-738.

van der Krol, A.R., Chua, N.H., 1991. The basic domain of plant B-ZIP proteins facilitates import of a reporter protein into plant nuclei. Plant Cell 3, 667-675.

van der Krol, A.R., Mur, L.A., Beld, M., Mol, J.N., Stuitje, A.R., 1990. Flavonoid genes in petunia: Addition of a limited number of gene copies may lead to a suppression of gene expression. Plant Cell 2, 291-299.

van Wezel, W.R., Dong, X., Liu, H., Tien, P., Stanley, J., Hong, Y., 2002. Mutation of three cysteine residues in tomato yellow leaf curl virus-China C2 protein causes dysfunction in pathogenesis and posttranscriptional gene silencing suppression. Mol. Plant Microbe Interact. 15, 203-208.

Vanitharani, R., Chellappan, P., Fauquet, C.M., 2003. Short interfering RNA-mediated interference of gene expression and viral DNA accumulation in cultured plant cells. Proc. Natl. Acad. Sci. USA 100, 9632-9636.

Vargason, J.M., Szittya, G., Burgya´n, J., Hall, T.M.T., 2003. Size selective recognition of siRNA by an RNA silencing suppressor. Cell 115, 799-811.

Vaucheret, H., Nussaume, L., Palauqui, J.C., Quillere, I., Elmayan, T., 1997. A transcriptionally active state is required for post-transcriptional silencing (cosuppression) of nitrate reductase host genes and transgenes. Plant Cell 9, 1495-1504.

Vaucheret, H., Palauqui, J.C., Elmayan, T., Moffatt, B., 1995. Molecular and genetic analysis of nitrite reductase co-suppression in transgenic tobacco plants. Mol Gen Genet. 248, 311-317.

Vaucheret, H., Vazquez, F., Crété, P., Bartel, D.P., 2004. The action of ARGONAUTE1 in the miRNA pathway and its regulation by the miRNA pathway are crucial for plant development. Genes & Dev. 18, 1187-1197.

Verdel, A., Jia, S., Gerber, S., Sugiyama, T., Gygi, S., Grewal, S.I., Moazed, D., 2004. RNAi-mediated targeting of heterochromatin by the RITS complex. Science 303, 672-676.

Verdel, A., Moazed, D., 2005. RNAi-directed assembly of heterochromatin in fission yeast. FEBS Lett. 579, 5872-5878.

Verver, J., Wellink, J., Lent, J.V., Gopinath, K., van Kammen, A., 1998. Studies on the movement of cowpea mosaic virus using green fluorescent protein. Virology 242, 22-27.

Voinnet, O., 2005. Induction and suppression of RNA silencing: insights from viral infections. Nature Rev. Genet. 6, 206-220.

Voinnet, O., Lederer, C., Baulcombe, D.C., 2000. A viral movement protein prevents systemic spread of the gene silencing signal in *Nicotiana benthamiana*. Cell 103, 157-167.

Voinnet, O., Pinto, Y.M., Baulcombe, D.C., 1999. Suppression of gene silencing: a general strategy used by diverse DNA and RNA viruses. Proc. Natl Acad. Sci. USA 96, 14147-14152.

Voinnet, O., Vain, P., Angell, S., Baulcombe, D.C., 1998. Systemic spread of sequence-specific transgene RNA degradation is initiated by localized introduction of ectopic promoterless DNA. Cell 95, 177-187.

von Arnim A.G., Deng X.W., Stacey M.G., 1998. Cloning vectors for the expression of green fluorescent protein fusion proteins in transgenic plants. Gene 221, 35-43.

Wang, J., Simon, A.E., 1999. Symptom attenuation by a satellite RNA in vivo is dependent on reduced levels of virus coat protein. Virology 259, 234-245.

Wang, J., Simon, A.E., 2000. 3'-end stem-loops of the subviral RNA associated with turnip crinkle virus are involved in symptom modulation and coat protein binding. J Virol. 74, 6528-6537.

Wang, M.B., Bian, X.Y., Wu, L.M., Liu, L.X., Smith, N.A., Isenegger, D., Wu, R.M., Masuta, C., Vanver, V.B., Watson, J.W., Rezaian, A., Dennis, E.S., Waterhouse, P.M. 2004. On the role of RNA silencing in the pathogenicity and evolution of viroids and viral satellites. Proc. Natl. Acad. Sci. USA 101, 3275-3280.

Wang, M.B., Metzlaff, M., 2005. RNA silencing and antiviral defense in plants. Curr. Opin. Plant Biol. 8, 216-222.

Wang, X., Lee, W.M., Watanabe, T., Schwartz, M., Janda, M., Ahlquist, P., 2005. Brome mosaic virus 1a nucleoside triphosphatase/helicase domain plays crucial roles in recruiting RNA replication templates. J Virol. 79, 13747-13758.

Wassenegger, M., Heimes, S., Riedel, L., Sanger, H.L., 1994. RNA-directed de novo methylation of genomic sequences in plants. Cell 76, 567-576.

Watson, J.M., Fusaro, A.F., Wang, M., Waterhouse, P.M., 2005. RNA silencing platforms in plants. FEBS Letters 579, 5982-5987.

Williamson, J.D., Hirsch-Wyncott, M.E., Larkins, B.A., Gelvin, S.B. 1989. Differential accumulation of a transcript driven by the CaMV 35S promoter in transgenic tobacco. Plant Physiol. 90, 1570-1576.

Xie, Z., Johansen, L.K., Gustafson, A.M., Kassachau, K.D., Lellis, A.D., Zilberman, D., Jacobsen, S.E., & Carrington, J.C. 2004. Genetic and functional diversification of small RNA pathways in plants. PloS Biol. 2, 642-652.

Xu, P., Roossinck, M. J., 2000. Cucumber mosaic virus D satellite RNA-induced programmed cell death in tomato. Plant Cell 12, 1079-1092.

Yang, S.J., Carter, S.A., Cole, A.B., Cheng, N.H., Nelson, R.S., 2004. A natural variant of a host RNA-dependent RNA polymerase is associated with increased susceptibility to viruses by *Nicotiana benthamiana*. Proc. Natl Acad. Sci. USA 101, 6297-6302.

Ye, K., Malinina, L., Patel, D.J., 2003. Recognition of small interfering RNA by a viral suppressor of RNA silencing. Nature 426, 874-878.

Yelina, N.E., Savenkov, E.I., Solovyev, A.G., Morozov, S.Y., Valkonen, J.P., 2002. Long-distance movement, virulence, and RNA silencing suppression controlled by a single protein in hordei- and potyviruses: complementary functions between virus families. J. Virol. 76, 12981-12991.

Yoshikawa, M., Peragine, A., Park, M.Y., Poethig, R.S., 2005. A pathway for the biogenesis of *trans*-acting siRNAs in *Arabidopsis*. Genes & Dev. 19, 2164-2175.

Yu, B., Yang, Z., Li, J., Minakhina, S., Yang, M., Padgett, R.W., Steward, R., Chen, X., 2005. Methylation as a crucial step in plant microRNA biogenesis. Science 307, 932-935.

Yu, D., Fan, B., MacFarlane, S.A., Chen, Z., 2003. Analysis of the involvement of an inducible *Arabidopsis* RNA-dependent RNA polymerase in antiviral defense. Mol. Plant Microbe Interact. 16, 206-216.

Zamore, P.D., 2001. RNA interference: listening to the sound of silence. Nat. Struct. Biol. 8, 746-750.

Zeng, Y., Yi, R., Cullen, B.R., 2005. Recognition and cleavage of primary microRNA precursors by the nuclear processing enzyme Drosha. EMBO J. 24, 138-148.

Zhang, G., Simon, A.E., 2003. A multifunctional turnip crinkle virus replication enhancer revealed by in vivo functional selex. J. Mol. Biol. 326, 35-48.

Zhang, G., Zhang, J., Simon, A.E., 2004. Repression and derepression of minus-strand synthesis in a plus-strand RNA virus replicon. J. Virol. 78, 7619-7633.

Zilberman, D., Cao, X., Jacobsen, S.E., 2003. ARGONAUTE4 control of locus-specific siRNA accumulation and DNA and histone methylation. Science 299, 716-719.

Zuker, M., 2003. Mfold web server for nucleic acid folding and hybridization prediction. Nucleic Acids Res. 31, 3406-3415.